A MULTI-DISCIPLINARY LABORATORY AND FIELD STUDY IN DRINKING WATER QUALITY: A NOVEL TECHNIQUE FOR ASSESSING SUSPENDED SOLIDS CONCENTRATIONS IN THE FLOC BLANKET, ANALYSIS OF FLOC BLANKET DYNAMICS, AND A FIELD STUDY OF SOURCES OF WATERBORNE DISEASE TRANSMISSION IN THE ETHIOPIAN HIGHLANDS

A Dissertation

Presented to the Faculty of the Graduate School

of Cornell University

In Partial Fulfillment of the Requirements for the Degree of

Doctor of Philosophy

by

Matthew William Hurst

May 2013

A MULTI-DISCIPLINARY LABORATORY AND FIELD STUDY IN DRINKING WATER QUALITY: A NOVEL TECHNIQUE FOR ASSESSING SUSPENDED SOLIDS CONCENTRATIONS IN THE FLOC BLANKET, ANALYSIS OF FLOC BLANKET DYNAMICS, AND A FIELD STUDY OF SOURCES OF WATERBORNE DISEASE TRANSMISSION IN THE ETHIOPIAN HIGHLANDS

Matthew William Hurst, Ph. D.

Cornell University 2013

ABSTRACT

This dissertation contains results of investigations related to: (1) application of floc blankets in vertical-upflow sedimentation tanks for low-cost, gravity driven water treatment plants and (2) sources of waterborne disease transmission in the Ethiopian highlands.

Floc blankets are fluidized beds of flocculated, suspended particles that can significantly enhance particle removal in vertical-upflow sedimentation tanks relative to the removals obtained in the absence of floc blankets. An experimental apparatus was built to evaluate floc blanket dynamics and mechanisms underlying floc blanket performance. Blanket dynamics are not well understood, but are important for understanding blanket formation and operational control in full-scale water treatment plants. Sequential image analysis provided suspended solids concentration and floc-water interface height (i.e., floc blanket height) through analysis of transmitted light intensity through a 1.3 cm thick section of a floc blanket.

Suspended solids concentrations were calibrated to known kaolinite and aluminum hydroxide concentrations and then turbidity measurements were employed to validate image analysis of solids concentration in the floc blanket, as well as in the floc blanket supernatant. Analysis of consecutive images revealed distinct stages in floc blanket formation: thickening (increasing suspended solids concentration) absent a floc-water interface, thickening with an interface, and steady-state. Preliminary performance data suggest blanket performance is more significantly related to blanket suspended solids concentration than blanket height. Future investigators are recommended to study: inflow and bottom geometry conditions which impact re-suspension of particles, mechanisms of particle removal in the blanket, and the impact of natural organic matter (NOM) on blanket performance, formation, and stability.

Bacterial counts and household surveys were performed in a town in the Ethiopian Highlands which experienced an acute watery diarrhea (AWD) outbreak in 2008. A multivariate regression model related to household self-reported incidence of diarrhea indicated that the incidence of diarrhea was related to sanitary disposal of feces from children under five, and locating hand washing stations near to household latrines. Significant risk factors (p-value < 0.05) associated with disease incidence varied by socio-economic status, in part, because water, sanitation and hygiene (WASH) behaviors were linked with socio-economic status. All source and household samples for fecal contamination failed World Health Organization (WHO) water quality standards. Analysis of water quality data and risk factors at the household level revealed that household water contamination was likely related to hand contact with water. Analysis of hand rinsing data (before and after hand washing) revealed a significantly higher reduction in microbial contamination when soap was utilized during hand

washing (94% reduction with soap compared to 49% for washing with only water). Analysis of these results suggest that future interventions which focus on increasing the number of people who wash their hands with soap or improving household water quality will reduce waterborne disease incidence.

BIOGRAPHICAL SKETCH

Matt Hurst was born in Tucson, Arizona in 1984. His academic interest in the environmental field began when he attended an environmental science class his senior year of high school. During his senior year of high school, he ultimately chose to study civil engineering and chemistry, and four years later graduated magna cum laude with a degree in Civil Engineering and degree in Chemistry with minors in Spanish and Environmental Engineering from Rose-Hulman Institute of Technology in Terre Haute, Indiana. In college, he was the president of the student group UNITY and worked with the Human Rights Council of Terre Haute. In September, 2007, he entered Cornell University and initiated his studies towards the M.S. Degree in Environmental Processes at the School of Civil and Environmental Engineering. He finished his M.S. degree in Environmental Processes studying steady-state floc blanket performance in 2010, and enjoyed the subject so much that he continued to study floc blankets for his Ph.D. He worked as a research assistant in the AguaClara project in the School of Civil and Environmental Engineering, and also joined as a trainee for an interdisciplinary program focused on food systems and poverty reduction. During his PhD, he spent one year living and conducting research in the Amhara Region of Ethiopia.

This dissertation is dedicated in memory of my father Robert William Hurst.

Thank you for making my dreams possible.

ACKNOWLEDGMENTS

I want to especially thank two major advisors, Dr. Weber-Shirk and Professor Lion for their support, guidance, patience, and encouragement during this process. Both have shaped and guided this dissertation with practical advice and experience. I am grateful to the fruitful discussions and hours of research with graduate and undergraduate students on the AguaClara project. I am very grateful to minor advisors: Professor Barrett, Professor Steenhius, and Professor Holst-Warhoft for their encouragement, interest in this research, and interest in me as a scholar. I give special thanks to Professor Pinstrup-Andersen serving as Professor Barrett's proxy for the oral defense.

I am very appreciative to colleagues in the NSF Food Systems and Poverty Reduction IGERT including Dr. Medvecky, Dr. Colfer, Dr. Dudley, and many, many other invaluable faculty and student collaborations along the way. I am very thankful to Mamaru Moges, Dr. Tilahun, Dr. Kaba, Fasikaw Atenaw, and many, many other Ethiopian colleagues at Bahir Dar University for their encouragement, insights, and friendship. I am very grateful to Janice Liotta for her assistance in experimental design, and Professor Bowman for his encouragement and insight.

I am indebted to Professor Pell, the Dean of International Relations, for the financial assistance, insights, and encouragement. I also thank the NSF Food Systems and Poverty Reduction IGERT program, the Sanjuan Foundation, and last, but not least, the School of Civil and Environmental Engineering at Cornell University for support of the research described in this thesis.

TABLE OF CONTENTS

LIST OF FIGURES

LIST OF TABLES

LIST OF ABBREVIATIONS

ASCE – American Society of Civil Engineers

AWD – acute watery diarrhea

AWWA – American Water Works Association

BEA – British Environmental Agency

DALY – disability adjusted life year

GO – governmental organization

NGO – non-governmental organization

NOM – natural organic matter

NTU – Nephelometric Turbidity Unit

ROI – region of interest

TIFF – tagged image file format

WTP – water treatment plant

WHO – World Health Organization

WASH – water, sanitation, and hygiene

LIST OF SYMBOLS

A light attenuation

$A_{Interface}$ cross-sectional area of the interface (L^2)

$A_{SedTank}$ upper plan view surface area above the tapered portion of the sedimentation tank (L^2)

A_s normal area of the tube settler (L^2)

$C_{Al(OH)_3}$ aluminum hydroxide suspended solids concentration (M/L^3)

C_{Clay} clay suspended solids concentration (M/L^3)

C_{Total} total suspended solids concentration (M/L^3)

d final particle diameter (L)

d_0 initial particle diameter (L)

d_{Tube} inner diameter of tubing (L)

$\frac{d(C_{Reactor}\forall_{Reactor})}{dt}$ mass rate of accumulation in the reactor (M/t)

$\frac{d(C_{FB}\forall_{FB})}{dt}$ mass rate of accumulation in the blanket (M/t)

$\frac{d(C_S\forall_S)}{dt}$ mass rate of accumulation in the supernatant (M/t)

D_{Jet} smallest dimension of jet flow (L)

f_{AlOH3} fraction of total suspended solids mass as aluminum hydroxide

f_{Clay} fraction of total mass as clay

h_{FB} height of floc blanket (L)

I light intensity measured from sample

$k_{Al(OH)3->Clay}$ ratio of extinction coefficients for the absorbance of aluminum hydroxide and clay

I_0 light intensity measured from a blank sample

L length of tubing (L)

$\dot{m}$ mass loading (M/t)

$\dot{m}_F$ mass loading from the flocculator (M/t)

$\dot{m}_{FBWaste}$ mass rate loss from floc blanket wasting (M/t)

$\dot{m}_{SWaste}$ mass rate loss from supernatant wasting (M/t)

$\dot{m}_{TSLoss}$ mass rate loss from the tube settlers (M/t)

Q flow rate (L^3/t)

V is the average axial velocity of flow (L/t)

V_C capture velocity of the tube settler (L/t)

V_{Jet} fluid velocity at the center of the jet (L/t)

V_t terminal settling velocity of a particle (L/t)

α angle of tube settler with respect to the horizontal

α_1 first order coefficient

α_2 second order coefficient

ε energy dissipation rate (L^2/t^3)

ε_{Max} maximum energy dissipation at the center of the jet (L^2/t^3)

θ fluid residence time in the flocculator (t)

ν kinematic viscosity (L^2/t)

$\rho_{Al(OH)_3}$ density of aluminum hydroxide (M/L^3)

ρ_{Clay} density of clay particle (M/L^3)

ρ_{Floc_0} initial floc particle density (M/L^3)

ρ_{H_2O} density of water (M/L^3)

Π_{Jet} contraction coefficient for 180° turnaround by jet

Φ porosity of a particle

CHAPTER 1: INTRODUCTION

Background Information

Water, sanitation, and hygiene (WASH) efforts in the past two decades (1990-2010) are reported to have enabled 2 billion people access to improved water sources and 1.8 billion people access to improved sanitation (WHO/UNICEF, 2012). Yet, as of 2013, approximately one-third of the world's population is estimated to lack access to basic sanitation and one-sixth to lack access to improved water sources (WHO, 2013). Waterborne disease burden is disproportionately placed upon low income populations, particularly in Sub-Saharan Africa and Southeast Asia (WHO, 2000). Quantified in total Disability Adjusted Life Years (DALY), diarrheal disease accounts for up to 6.4% of the total disease burden in Sub-Saharan Africa (Lopez, 2006).

Access to safe water can significantly reduce water-related disease (Kremer & Peterson-Zwane, 2010). Nonetheless, many communities must rely on surface water sources that are not treated, and therefore, not safe for consumption. In many cases, water treatment is most necessary during rainy phases when the concentration of suspended material in the water increases due to erosion and run-off from the watershed.

A central goal of surface water treatment is to remove suspended, particulate matter in the water that may be pathogenic (disease-causing). Conventional surface water treatment technology relies on electricity and complex components that may be unobtainable or difficult to maintain for resource poor communities.

An alternative to conventional forms of centralized water treatment is to utilize gravity-driven and low cost water treatment plants. AguaClara is an award-winning project in the School of Civil and Environmental Engineering at Cornell University that utilizes design, laboratory and field research, as well as extensive community outreach and working partnerships to provide cost-effective community-scale water treatment plants for resource poor communities.

AguaClara water treatment plants utilize a gravity-driven treatment process train of rapid mix, flocculation, sedimentation, filtration and disinfection. In sedimentation, AguaClara plants employ vertical-upflow clarifiers containing floc blankets. Floc blankets are concentrated, fluidized beds of particles that enhance colloidal particle removal in the sedimentation tank compared to conventional upflow clarifiers in absence of a floc blanket (Galvin, 1992). Floc blankets are also thought to reduce operation and maintenance costs in a water treatment plant by: (1) reducing solids loading to sand filter, thereby, reducing the frequency water is utilized for backwash, and (2) incorporating a floc hopper (i.e., a submerged basin with a rim at the floc-water interface that flocs spill into) that concentrates waste, and retains a portion of the clarified water in the sedimentation tank.

Floc blankets have not been well characterized in literature, and are thought to be unstable (Chen *et al*., 2006). For example, floc blankets are said to be prone to 'floc blanket carryover,' a process by which the floc blanket turns over in the sedimentation tank and a significant portion of the concentrated, suspended particles in the bed ends up leaving the sedimentation tank (AWWA/ASCE, 1990). Thus, the underlying mechanisms responsible for floc blanket instability merit additional research.

Chapters 2 and 3 of this dissertation focus on the laboratory research that simulated the process treatment train of rapid mix, flocculation, and sedimentation present in AguaClara treatment plants. Image analysis results from the experimental reactor enhance current field understanding of mass transport dynamics in floc blankets. Better understanding of mechanisms of floc blanket formation, performance, and stability are crucial in formulating better strategies for operational control in a water treatment plant (WTP).

In isolation, water treatment is not always a sufficient intervention strategy in reducing water-related disease. Waterborne pathogens are spread by the fecal-oral route which makes prevention of contamination of water after treatment difficult due to a multitude of potential exposure routes. Water-related disease can be caused by direct consumption of pathogenic material present in the water (i.e., waterborne) or from contamination of water due to poor sanitation and hygiene practices in the household (i.e., water-washed). Some of the specific exposure routes that can cause water-related disease include: fecal contamination, food contamination, water source quality, water handling practices in the household, and hygiene practices (i.e., hand washing and food washing) (Eisenberg *et al*., 2007).

Chapter 4 presents a case study of exposure routes of waterborne disease and potential intervention strategies for Agew Gimjabet, a town in the Ethiopian highlands. Analysis was undertaken with water samples that were tested for fecal coliforms supported with data from household surveys. The ultimate aim of this research was to understand prevalent sources of contamination and envision future intervention control strategies.

An Introduction to Floc Blankets and Floc Blanket Image Analysis

The following floc blanket research is described in more detail in chapters 2 and 3.

A turbidity measurement is the amount of light scattered in a water sample, and is correlated with the concentration of suspended material present in that water sample. Turbidity measurements are calibrated to a known standard which is typically Formazin, and are frequently measured in units of Nephelometric Turbidity Units (NTUs).

Colloidal particles (0.001-1.0 μm) are correlated with the presence of pathogenic organisms and are difficult to remove by gravity sedimentation owing to their low sedimentation velocities. Application of chemical coagulants such as alum ($Al_2(SO_4)_3$*$14(H_20)$) is employed in water treatment to bridge between negatively charged colloidal particles. Although aluminum can form a variety of charged species in water such as Al^{+3}, $Al(OH)^{+2}$ and $Al(OH)_2^{+}$, for typical circumneutral pH values (pH~6.5 – 8) present in water treatment, precipitation of aluminum hydroxide ($Al(OH)_3(s)$) is dominant. Aluminum hydroxide is positively charged at circumneutral pH. When aluminum hydroxide coats the surface of colloids, it aids in neutralizing colloids' negative surface charge.

The simulated unit process treatment train in laboratory experiments included: rapid mix, flocculation, floc blanket clarification, and lamellar sedimentation. Rapid mix is the unit process whereby raw water is blended with chemical coagulant. Large scale turbulent mixing can be accomplished by a flow expansion followed by small scale turbulent mixing so that molecular diffusion can finish the mixing process in a few seconds. Flocculation requires a

controlled energy dissipation rate (i.e., mixing intensity) of ~10 mW/kg and sufficient residence time to promote particle aggregation. The resulting larger, aggregated particles (i.e., flocs) exiting the flocculator can be captured by gravity sedimentation.

Vertical-upflow floc blanket clarification utilizes a bed of concentrated, fluidized particles which is purported to enhance colloid capture through increased particle-particle interactions (Miller & West, 1968; Reynolds & Richards, 1996; Tchobanoglous *et al*., 2003). The location of the floc-water interface distinguishes the position of the concentrated bed of particles below a relatively clear supernatant. The velocity immediately above the floc-water interface (i.e., the interface velocity) ($V_{Up-Interface}$) is defined as the plant flow rate (Q) divided by the plan area of the sedimentation tank submerged in the floc blanket ($A_{Interface}$) (Equation 1-1). The interface velocity controls extent of fluidization, suspended solids concentration, and performance (capture of colloids).

$$V_{Up-Interface} = \frac{Q}{A_{Interface}} \qquad (1\text{-}1)$$

Floc-water interface height, a critical operating parameter, is controlled from wasting by a floc hopper. Without stringent monitoring and wasting rate adjustments by plant operators, blankets can experience 'carryover' (Lin *et al*., 2004; Chen *et al*., 2006). Blanket height has been shown to be related with floc blanket performance (Miller & West, 1968; Hurst *et al*., 2010). Hurst *et al*. (2010) reported significant improvements in performance for blanket heights up to 45 cm.

Frequently, floc blankets reside in sedimentation tanks constructed with concrete walls 1-4 meters deep making visualization difficult. As a result, previous investigators have relied on

solids grab samples (Zhang *et al*., 2006), settling tests (Sung *et al*., 2005), and a "sonar (ORCA) bed level transducer" (Hawk, 2013) to estimate solids concentration, settling characteristics of flocs, and floc-water interface height, respectively. In combination, these tests can estimate the mass flux (mass per unit planar area per time) between the floc blanket and supernatant in the floc blanket (Su *et al*., 2004).

The focus of investigators measuring and modeling mass flux across the floc-water interface (Chen *et al*., 2003; Sung & Lee, 2005; Zhang *et al*., 2006) is likely a result of: (1) the limitations of investigator's instruments to collect more detailed temporal and spatial data in the floc blanket, and (2) the idea that floc blankets are prone to instability (AWWA/ASCE, 1990; Chen *et al*., 2006). Mass flux calculations do not elucidate underlying blanket dynamics such as the processes of blanket formation and blanket instability. Fluctuations in influent conditions such as changing interface velocity, chemical coagulant dose, or influent turbidity would likely change the floc properties inside the blanket, and ultimately, alter the blanket dynamics.

Image analysis techniques described in Chapters 2 and 3 of this dissertation permit greater temporal and spatial resolution of blanket concentration and floc-water interface height. An experimental apparatus was built to permit image analysis of floc blanket concentration and floc-water interface position (described in Figure 2-8). An LED light panel in the back provides nearly uniform light across the sedimentation tank (Appendix B), while a computer controlled camera obtains sequential photographs. The experimental apparatus mimics a cross-section of the sedimentation tank designed by Cornell's AguaClara Project and maintains full

height (1 m) and half width dimensions (0.5 m) while restricting the length to 1.3 cm to permit transmitted light to be used for measurement of typical floc blanket suspended solids concentrations (~500 – 4000 mg/L) (Hurst et al., 2010).

The experimental apparatus acts as a large sampling spectrophotometer for suspended solids concentration. Light attenuation (A) measurements were defined as the negative logarithm of the transmitted light intensity (I) normalized to the transmitted light intensity of the water blank (I_0) (aerated, temperature controlled tap water) (Equation 1-2). Although there is variability in the light intensity with respect to position in the sedimentation tank (Appendix B), each measurement is normalized with respect to transmitted light intensity, thus, variability in light intensity will not significantly impact light attenuation readings.

$$A = -\log\left(\frac{I}{I_0}\right) \qquad (1\text{-}2)$$

The experimental apparatus was calibrated with respect to suspended solids concentrations. The predominant components of suspensions in the described experiments in Chapters 2 and 3 were: (1) kaolinite clay and (2) aluminum hydroxide, which is formed from the hydrolysis of alum coagulant. Once light attenuation measurements were calibrated to known suspensions of kaolinite clay and aluminum hydroxide, subsequent light attenuation measurements could be correlated with floc blanket solids concentrations.

Prior to calibration with suspended solids, the experimental apparatus was calibrated with red dye #40 to confirm the expectation of linearity of the light attenuation in a light absorbing solution and solution concentration (described in greater detail in Appendix C). Next, the

experimental apparatus calibration curves were built from suspensions of kaolinite clay and aluminum hydroxide discussed in greater detail in Appendix D and Appendix E, respectively. Briefly, a second order polynomial provided a reasonable fit to account for the non-linearity in light attenuation response observed at higher suspension concentrations. Then, a "combined" calibration curve was built using combined suspensions of clay and aluminum hydroxide. The calibration method is described in greater detail in the Materials and Methods section (Figure 2-5) and Supplementary Information in Chapter 2. Predicted concentration from imaging results were compared with grab sample total suspended solids (TSS) concentration tests (Appendix F) and shown in (Figure 2-6). Post experiment data analysis was conducted to elucidate floc blanket concentration and floc-water interface height. Program user instructions and methodology pertaining to analysis of experimental data are described in detail in Appendices G, H, and I. The effluent stream from the floc blanket enters a series of inclined lamellar (i.e., plate or tube) settlers after passing through the floc blanket and supernatant. Performance was quantified by the effluent turbidity from the lamellar settlers. Experiments benefited from use of process control software developed by Weber-Shirk (2008) to automate operation of the laboratory-scale treatment process train as well as to monitor and record influent and effluent turbidity readings.

Captured particles settle onto the surfaces of inclined plates, and then return to the supernatant of the sedimentation tank. The critical capture sedimentation velocity (i.e., capture velocity) (V_C) is correlated with the lowest terminal particle sedimentation velocity (V_T) where 100% capture efficiency is achieved. Capture velocity for tube settlers utilized in laboratory experiments is described by the following relationship (Schulz & Okum, 1984):

$$V_C = \frac{V_\alpha}{\frac{L}{d}\cos(\alpha) + \sin(\alpha)} \qquad (1\text{-}3)$$

Where: d is the inner diameter of the tube, L is the length of the tube, α is the angle of orientation, and V_α is the average fluid velocity in the tube.

Flocs are fractal and porous in nature, and the fractal nature of a floc is typically characterized by the floc fractal dimension. The fractal dimension of a floc characterizes the volume of solids per total occupied floc volume and accounts for floc porosity (Bellout *et al*., 1997). Higher fractal dimensions indicate a more compact floc structure (Jarvis *et al*. 2005). Increases in the size of flocs with fractal properties will result in decreasing floc density. The terminal settling velocity (V_T) of a floc as a function of their size, density, and fractal dimension is given by Weber-Shirk & Lion (2010) and is shown in equation (1-4). Although larger flocs are less dense, they settle more rapidly because of their increased size when their fractal dimension is greater than 1.

$$V_T = \frac{g d_0^{(3-D_{Fractal})} d^{(D_{Fractal}-1)}}{18\Phi\nu}\left(\frac{\rho_{Floc_0}}{\rho_{H_2O}} - 1\right) \qquad (1\text{-}4)$$

Where: d_0 (= 1 μm) is the size of a primary clay particle, d is the floc size, $D_{Fractal}$ is the fractal dimension of the floc, ν (= 10^{-6} m^2/s)is the kinematic viscosity, Φ (= 24/45) is the shape factor of the floc, ρ_{Floc_0} (= 2.62 kg/m^3) is the initial density of the floc, and ρ_{H_2O} is the density of water.

Overview of Floc Blanket Research

The laboratory studies in Chapters 2 and 3 focus on the use of image analysis as a tool to

elucidate mass transport dynamics that occur in vertical-upflow floc blanket clarification. Analysis of concentration and blanket height data illustrate three stages of floc blanket formation and underscores the importance of blanket thickening and mass return from the supernatant during the interval of time where floc blanket height increases. Performance is measured as the removal of turbidity (correlating to concentration of colloidal particles). A preliminary result is that concentration impacts performance more significantly than floc blanket height. Enhanced understanding of blanket dynamics can provide better design guidelines to be utilized in the operational control of vertical-upflow floc blanket clarifiers.

Overview of WASH Field Study

A town, Agew Gimjabet, in the Ethiopian highlands experienced AWD outbreak in 2008 linked with unsafe water source supplies. The study aim was to identify prevalent factors influencing spread of water-related disease and suggest means to reduce household water contamination. Water contamination was quantified by membrane filter enumeration of fecal coliform bacteria using lauryl sulfate broth as described by the British Environmental Agency (BEA, 2009) and described in greater detail in Materials and Methods of Chapter 4. Household surveys were utilized to identify risk factors associated with diarrheal disease incidence. From household survey responses, a multivariate regression model associated with self-reported incidence of diarrhea revealed that diarrheal disease incidence was related to sanitary disposal of children's feces under five, and to the presence of a hand washing station located near to the latrine. Analysis conducted from pooling household survey and water quality data highlight the significant contamination that occurs in the transport, storage, and handling of water, and underscores that hand contact with water is a major potential source of household water contamination. Results suggest that future interventions which prevent

household water contamination such as increasing the number of people who wash their hands with soap will reduce waterborne disease incidence.

CHAPTER 2: AN APPARATUS FOR OBSERVATION AND ANALYSIS OF FLOC BLANKET FORMATION AND PERFORMANCE[1]

[1] The contents of this chapter have been submitted to *Journal of Environmental Engineering* for publication with co-authors: Dr. M. Weber-Shirk, P. Charles, and Prof. L. Lion.

An Apparatus for Observation and Analysis of Floc Blanket Formation and Performance

Matt Hurst[1], Monroe Weber-Shirk*[2], Paul Charles[3], and Leonard W. Lion[4]

Cornell University

School of Civil and Environmental Engineering

Hollister Hall

Ithaca, NY 14853-3501

Phone: (607) 216-8445

Fax: (607) 255-9004

* Corresponding author

Email: mw24@cornell.edu

[1] Graduate Student, Civil and Environmental Engineering, Cornell University Hollister Hall

Ithaca, NY 14853-3501 mwh65@cornell.edu

[2] Senior Lecturer, Civil and Environmental Engineering, Cornell University Hollister Hall

Ithaca, NY 14853-3501 mw24@cornell.edu

[3] Facilities Manager, Civil and Environmental Engineering, Cornell University Hollister Hall

Ithaca, NY 14853-3501 pjc32@cornell.edu

[4] Professor, Civil and Environmental Engineering, Cornell University Hollister Hall

Ithaca, NY 14853-3501 LWL3@cornell.edu

Abstract

Floc blankets are fluidized beds of aggregated suspended particles utilized in some upflow sedimentation tanks for drinking water treatment. Floc blankets can significantly enhance particle removal and may reduce operation and maintenance costs. An experimental apparatus was built with the goal of developing an understanding of floc blanket physics and to establish a mechanistic basis for optimizing floc blanket performance. Visual insights into floc blanket mechanics are obtained by analyzing transmitted light intensity through a 1.3 cm thick section of a floc blanket. Floc blankets were formed under simulated raw water conditions of 100 Nephelometric Turbidity Units (NTU), an alum coagulant dose of 45 mg/L (4.1 mg/L as Al), and at sedimentation tank upflow velocities ranging from 0.4 to 1.8 mm/s. This study presents: (1) non-destructive methods for measuring floc blanket concentration and position of the floc-water interface, (2) steady-state performance data from the experimental apparatus, and (3) the effect of upflow velocity on solids concentration in a floc blanket.

Keywords: floc blanket, image analysis, floc-water interface, debris flow, suspended solids concentration, hindered sedimentation

CE Subject Headings: Sedimentation Tanks, Suspended Solids, Settling Velocity, Fluid Velocity, Concentration, Graphic Methods

Introduction

A central goal in water treatment plants (WTPs) is the removal of particulate matter from source water. Suspended sediment (typically measured as turbidity) is associated with the presence of pathogenic organisms that are capable of transmitting waterborne diseases. Fine, suspended particles, which normally do not settle, will agglomerate with the addition of chemical coagulants, form larger particles, and then can be removed by sedimentation. Floc particles are fractal in nature; as the flocs grow, they become less dense and more porous (Jarvis et al., 2005).

The presence of a floc blanket is an alternative configuration for upflow clarifiers. A floc blanket is a bed of concentrated, fluidized of flocculated particles with relatively uniform concentration throughout (Gould, 1969). Enhanced particle removal can be achieved in a combined floc blanket-lamellar sedimentation system compared to conventional sedimentation tanks with plate or tube settlers (Hurst et al., 2010). The high concentration of flocculated particles in the floc blanket increases particle-particle interactions with influent particles from the flocculator, promoting aggregation and enhancing particle removal (Miller & West, 1968; Reynolds & Richards, 1996; Tchobanoglous, Burton, & Stensel, 2003).

The interface upflow velocity ($V_{Up-Interface}$), a design variable that influences solids concentration in a floc blanket, is defined as the volumetric flow rate (Q) divided by the area of the floc-water interface, $A_{FlocInterface}$ (Equation 1). In a floc blanket, a distinct floc-water

interface exists between the concentrated suspension of particles and an overlying region of much lower solids concentration. A balance of hindered sedimentation velocity of the concentrated suspension below the floc water interface and the upflow velocity immediately above the floc water interface is required to create a distinct steady-state floc-water interface, (Gould, 1974).

$$V_{Up-Interface} = \frac{Q}{A_{FlocInterface}} \qquad (2\text{-}1)$$

In tanks with tapered bottom geometry, $A_{FlocInterface}$ varies as the floc blanket height changes. The sedimentation tank vertical-upflow velocity ($V_{Up-Sed\ Tank}$) typically reported in the literature (Sung et al., 2005; Head et al., 1997) is defined as the volumetric flow rate divided by the upper plan view surface area ($A_{SedTank}$) above the tapered portion of the sedimentation tank (Equation 2).

$$V_{Up-Sed\ Tank} = \frac{Q}{A_{SedTank}} \qquad (2\text{-}2)$$

$V_{Up-Sed\ Tank}$ is a property of tank geometry and flow rate and is independent of floc blanket height.

Combined floc blanket-lamellar systems make use of a series of inclined plates or tubes situated slightly below the surface of the sedimentation tank. Particles settle onto the surfaces of the plates or tubes and then slide back down the incline into the sedimentation tank. The separation distance between plates (or tube diameter), the angle of incline and upflow velocity determine the capture velocity (also referred to as the critical velocity) in the lamellar settlers.

The relevant governing equation is given below in Materials and Methods. The sedimentation capture velocity dictates the size of the smallest particle to be captured.

Another advantage of the floc blanket system is the reduction of volume of waste through consolidation and removal of solids via a "floc hopper" (i.e., a submerged basin with a rim at the floc-water interface that flocs spill into) (Edzwald et al., 1999). The "floc hopper" concentrates floc blanket waste, allows removal of the concentrated solids, and retains a portion of clarified water in the sedimentation tank.

Floc blanket systems offer substantial opportunities to build less expensive and more effective water treatment plants (as in developing countries with limited financial resources). However, floc blanket systems can be destabilized. One such disturbance referred to as "floc blanket carryover," results in blurring of the floc-water interface and high levels of turbidity in the effluent (AWWA/ASCE, 1990; Chen et al., 2006). Insight gained from visualization of the transport of suspended material in a floc blanket coupled with improved performance data is expected to enhance the ability of treatment plant operators to sustain floc blankets.

At field scale, upflow sedimentation tanks are typically 1-4 m deep (Kawamura, 2000) obscuring direct visual observation from above. Floc blanket visualization has not been a focus of previous pilot and laboratory scale studies of floc blanket growth, stability and performance (Chen et al., 2002; Chen et al., 2006; Gregory, 1979; Head et al., 1997; Hurst et al., 2010; Lin et al., 2004; Miller & West, 1968; Purushothaman and Damodara, 1986; Su et al., 2004; Sung et al., 2005; Zhang et al., 2006). However, interactions between suspended solids, fluid, and

the geometry of the reactor are critical in understanding: (1) how floc blankets form including the effect of inflow jet conditions and bottom geometry, and (2) causes of instability such as perturbations in influent conditions.

One consequence of the lack of visual observation below the floc water interface (i.e. within the floc blanket) is disagreement in the literature over the hydraulic characteristics of the reactor which has been modeled as plug flow (Sung et al. 2005), arbitrary flow (Chen et al. 2002), and completely mixed flow (Gregory 1979).

Advances in imaging technology now permit direct observation of floc blanket systems. The ability to visually observe an experimental floc blanket system provides access to regions and processes that were previously inaccessible such as the bottom boundary conditions where settled flocs either leave the suspension or may be re-suspended. The goal of this research was to develop a reactor system and methods suitable for imaging solid concentrations within the floc blanket. This paper presents:

- non-destructive methods for measuring: floc blanket concentration, position of the floc-water interface, and concentration profile of the debris flow
- exemplary steady-state performance data obtained from the experimental apparatus
- application of the apparatus to evaluate effect of upflow velocity on solids concentration in a floc blanket

Materials and Methods

The experimental reactor represents a 1.3 cm thick slice of an upflow sedimentation tank and has height of 1 m and width of 0.5 m. The glass-walled apparatus (Figure 2-1) acts as a large

sampling cell for suspended solids. The 1.3 cm thickness provides an appropriate optical path length for analyzing a wide range of floc blanket suspended solids concentrations.

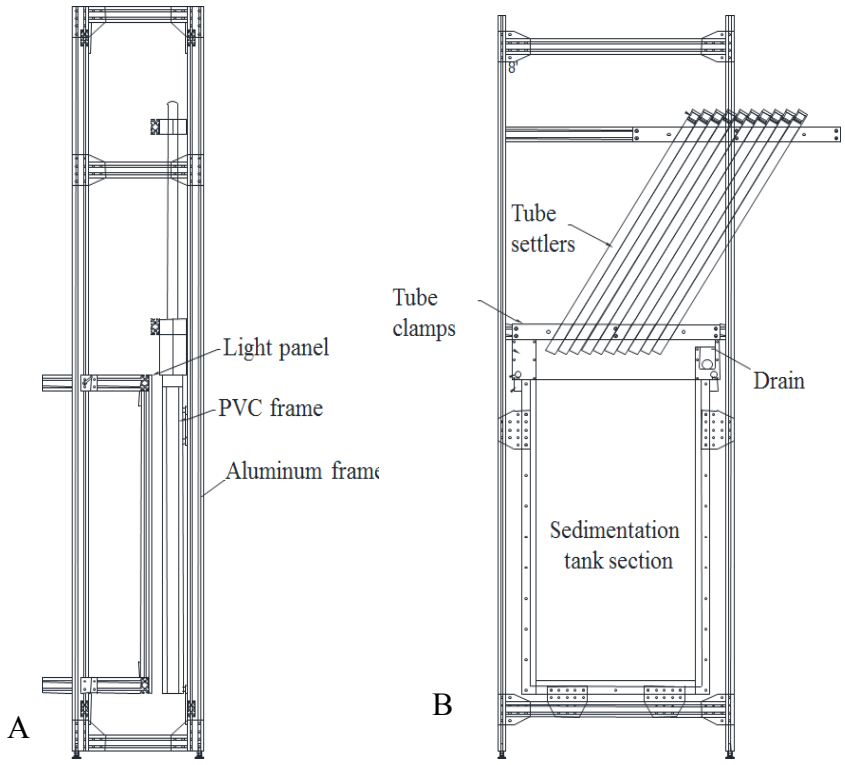

Figure 2–1. AutoCAD renderings of the side view (A) and front view (B) of the experimental apparatus (not to scale).

Raw Water Conditions and Reactor Hydraulics

The procedure described by Hurst et al. (2010) was used to produce a uniform influent for floc blanket formation. Process control software developed by Weber-Shirk (2008) was used in conjunction with inline turbidimeters to regulate dilution of a concentrated kaolinite clay suspension in temperature controlled, aerated tap water to produce conditions of constant input turbidity. Cornell University tap water has an average pH of 8.05, total alkalinity of 108 mg/L

as $CaCO_3$, total hardness of 150 mg/L as $CaCO_3$, and dissolved organic carbon (DOC) of 2.0 mg/L. (City of Ithaca, 2011).

The raw water and coagulant were blended and then entered a laminar flow coiled tube flocculator (inner diameter, d = 9.5 mm, coil diameter, D = 13 cm, and length 20 m) (Figure 2-3). The average energy dissipation rate (ε) can calculated from the product of head loss through the flocculator and acceleration due to gravity (g) per unit residence time in the flocculator and was approximately 9 mW/kg at the flow rate of 7.7 mL/s. The flow rate of 7.7 mL/s corresponds to a sedimentation tank upflow velocity of 1.2 mm/s (4.3 m/hr). For experiments with variable upflow velocities the flow rate through the flocculator was held constant and excess water was sent to waste to vary the flow rate into the sedimentation tank. For higher flow rates, two flocculators in parallel were used and excess water was sent to waste.

After tube flocculation, the flow was released near the bottom of the sedimentation reactor. The floc blanket elevation in the apparatus was controlled by removing a portion of the flow at a desired height within the reactor. The remaining effluent flowed through a cluster of 10 tube settlers. Portions of the effluent and influent flow were continuously sampled by inline turbidimeters (Figure 2-2).

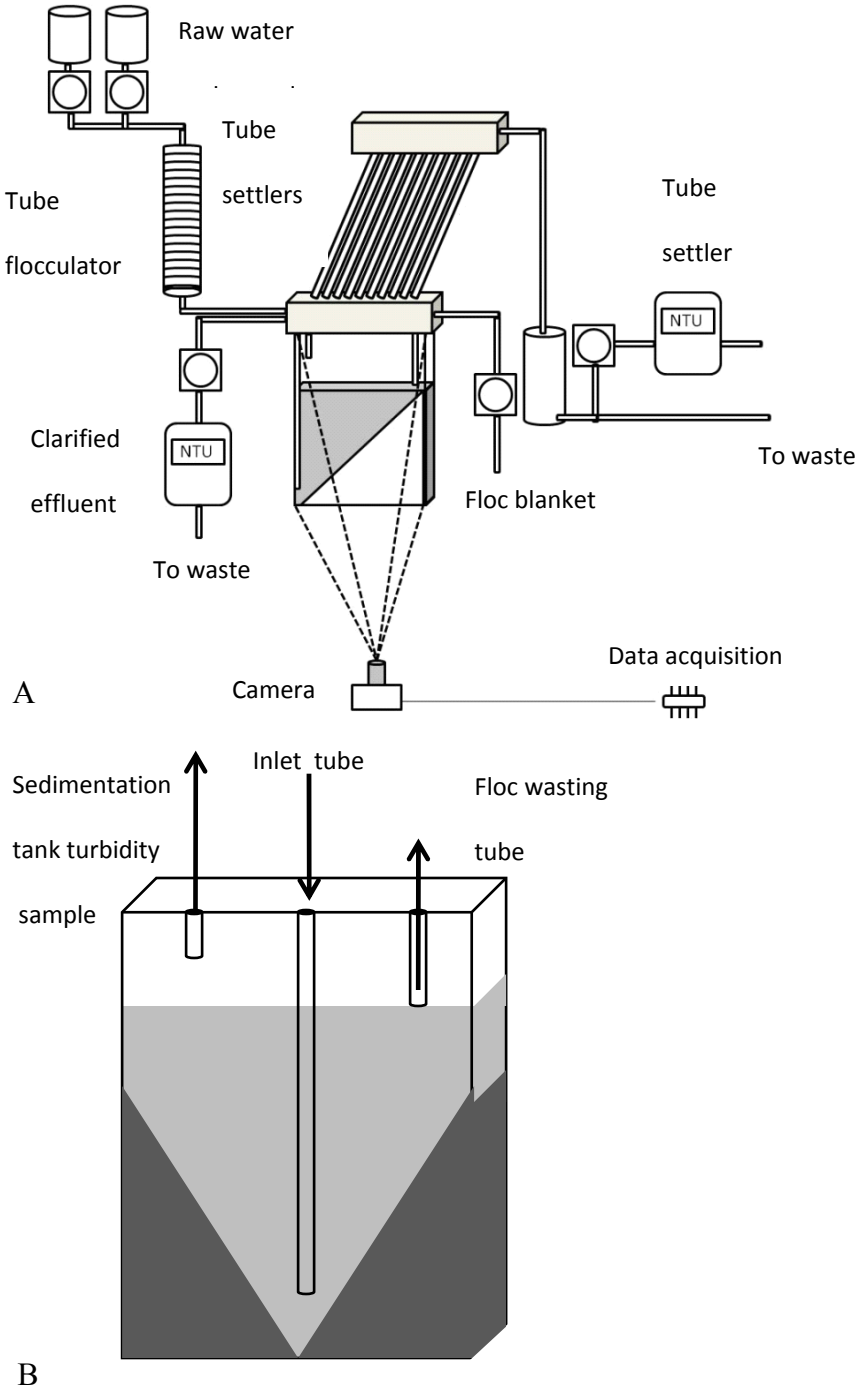

Figure 2–2. A. Schematic of water and data flow for the entire experimental system. B. Inlet and outlets for the sedimentation tank excluding tube settlers.

Apparatus Design

Figure 2-3 details the sedimentation tank and component dimensions. Removable inserts were constructed from paper foam board to create different bottom geometries. For these experiments, the bottom inserts had an angle of inclination of 60 degrees. The "jet reverser" at the center position in the bottom was milled from a 10 cm X 10 cm (1.3 cm thick) block of PVC (Figure 3B) and served to redirect the incoming downward flow from the flocculator upward into the floc blanket. The floc blanket height was defined as the distance from the bottommost point of the jet reverser to the floc-water interface (Figure 2-3A).

The inlet tubing was ellipsoidal with an inner major axis diameter of 1.27 cm and a minor axis diameter of 0.46 cm. and was placed in the center of the sedimentation tank. This shape was formed from 1.3 cm OD brass tubing to allow flocs to flow across the center region occupied by the inlet tube. The jet velocity (V_{Jet}) coming out of the inlet is the flocculator flow rate divided by the cross sectional area of the inlet (A_{Inlet}). At the flow rate of 7.7 mL/s, the jet velocity was 0.18 m/s.

A 1 m x 0.5 m 30 W panel (e-Lumanation) of light-emitting diodes served as the light source. The light panel was mounted on the back side of the reactor. Images were acquired with a Basler color SCA640-70FC IEEE-1394B (658x490 pixels) camera with an 8 mm lens. The camera was interfaced with LabVIEW image acquisition software. The software controlled the rate of image capture and shutter speed. Unless otherwise specified, the camera was mounted

at a distance of 1.75 m from the reactor, creating a field of view of 94 cm x 71 cm. At this configuration, each pixel corresponded to a 1.5 mm x 1.5 mm section of the reactor.

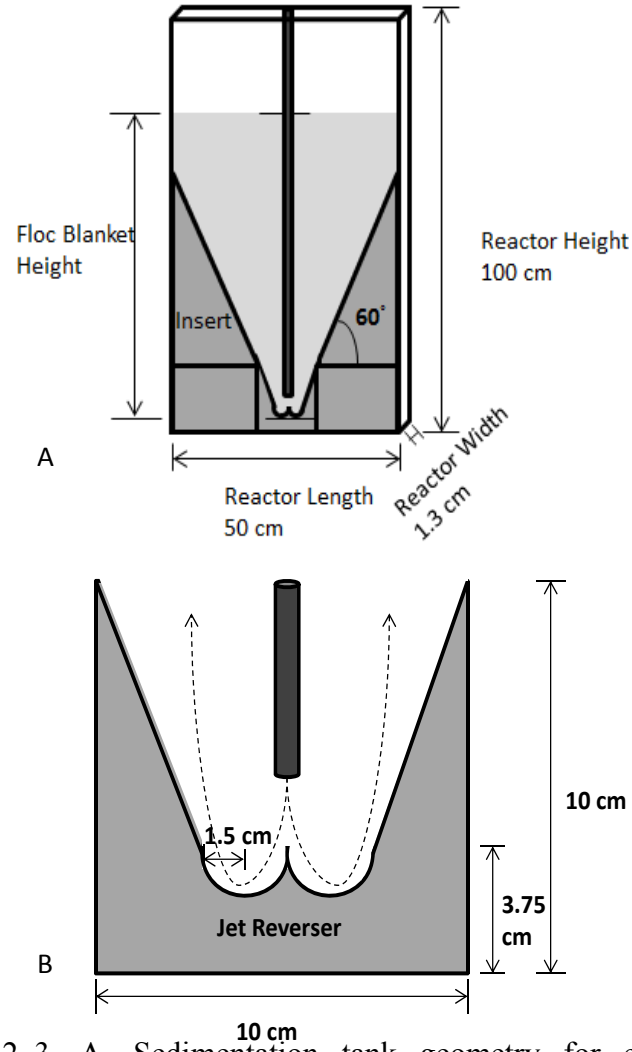

Figure 2–3. A. Sedimentation tank geometry for experiments detailed in this paper. B. Dimensions for jet reverser (approximate flow path indicated by dashed line).

The glass plate tank walls were 1.3 cm thick to withstand the hydrostatic pressure of a 1-m water column. A PVC spacer with O-ring seals set the spacing between the glass walls. A PVC reservoir was placed above the top of the glass reactor with sufficient space to hold an

overflow weir to maintain a constant water level and ten 2.6 cm I.D. tube settlers.

Tube settler length and average fluid velocity set the capture velocity (often referred to as the critical velocity) of the tube settlers. The capture velocity (V_C) is the terminal settling velocity corresponding to the smallest particle size that can be captured with 100% efficiency by the tube settlers. The capture velocity for tube settlers is described by the following relationship (Schulz and Okum, 1984):

$$V_C = \frac{V_\alpha}{\frac{L}{d}\cos(\alpha) + \sin(\alpha)} \qquad (2\text{-}3)$$

Where: d is the inner diameter of the tube (d = 2.6 cm), L is the length of the tube (L = 85 cm), α is the angle of orientation (α = 60°), and V_α is the average fluid velocity in the tube.

Performance Analysis

Exemplary steady-state performance results for the combined floc blanket-lamellar sedimentation system are shown in Figure 2-4. This floc blanket was formed under conditions of 100 NTU influent, with a coagulant dose of 45 mg/L alum (4.1 mg/L as Al), and a sedimentation tank upflow velocity of 1.2 mm/s. The floc blanket height was set at 56 cm. Capture velocity of the tube settlers was set at 0.07 mm/s. Average effluent turbidity was 0.56 Nephelometric Turbidity Units (NTU) ±14% and average influent turbidity was 100.8 NTU ±1.4%.

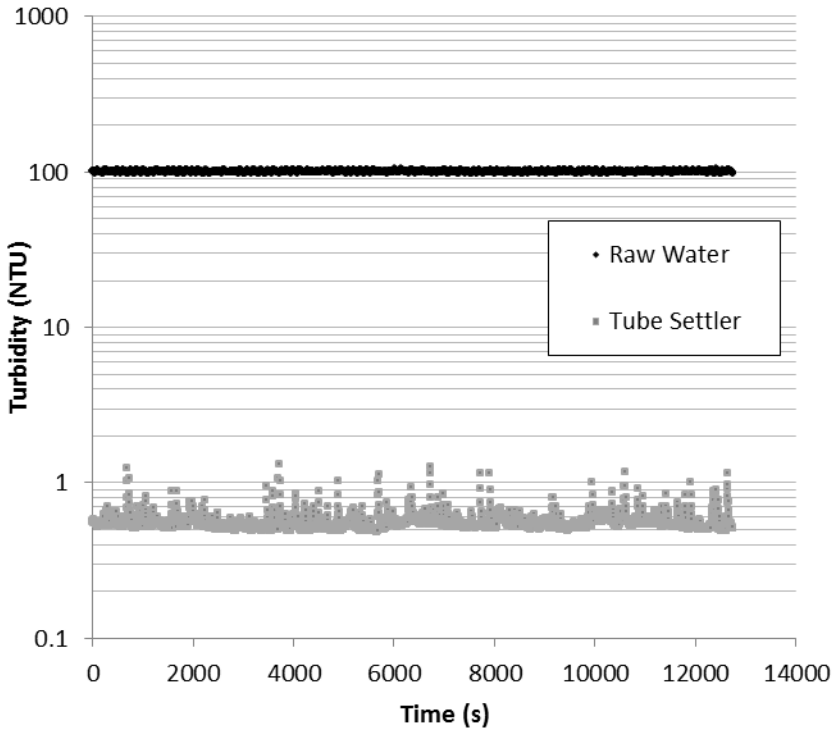

Figure 2–4. Steady-state performance data for raw water and tube settler effluent.

Quantitative Image Analysis

Data analysis procedures were developed for obtaining floc blanket concentration from a digital camera image. Light attenuation (A) by the particle suspension was measured by taking the negative logarithm of the transmitted light intensity (I) normalized by the transmitted light intensity through a clean water blank (I_0) (Equation 2-4). Light attenuation was shown to be linearly related to concentration of a red dye solution. Light attenuation by a suspension is due to scattering and surface absorbance and was expected to be well correlated with particle concentration in the light path. Light attenuation was calibrated to known suspension concentrations to allow in situ measurement of solids concentrations.

$$A = -\log\left(\frac{I}{I_0}\right) \qquad (2\text{-}4)$$

Calibration for Aluminum Hydroxide-Kaolinite Flocs

Calibration curves for (1) aluminum hydroxide, (2) clay and (3) combined aluminum hydroxide-kaolinite clay were obtained. The combined aluminum hydroxide-kaolinite clay calibration curve is shown in Figure 2-5. A second-order polynomial ($r^2 \geq 0.991$) was used to fit the light attenuation curves (see Equation 2-5). Mathematical development of the two-component calibration curve for the suspension of clay and aluminum hydroxide is detailed in the supplementary information provided for this article.

$$A_\lambda = \alpha_{2-Clay}(C_{Total} f_{Clay} + k_{AlOH3->Clay} f_{AlOH3} C_{Total})^2 + \alpha_{1-Clay}(C_{Total} f_{Clay} + k_{AlOH3->Clay} f_{AlOH3} C_{Total}) \quad (2\text{-}5)$$

Where: A_λ is light attenuation at the selected wavelength, f_{Clay} is the fraction of total mass as clay, f_{AlOH3} is the fraction of total mass as aluminum hydroxide, C_{Total} is the total concentration of clay and aluminum hydroxide, $k_{Al(OH)3->Clay}$ is the ratio of extinction coefficients for the absorbance of aluminum hydroxide and clay, α_{2-Clay} is the scattering coefficient for clay, and α_{1-Clay} is the extinction coefficient for absorbance for clay.

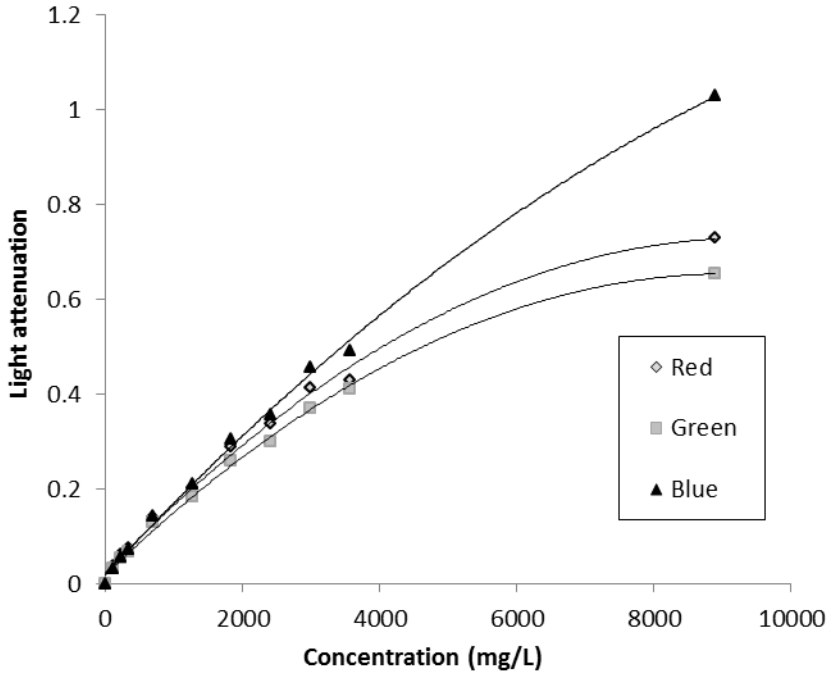

Figure 2–5. Calibration curve of a combined kaolinite-aluminum hydroxide system with a clay to alum dosing ratio of 2.7:1.

The non-linear relationship between light attenuation and solids concentration in Figure 2-5 is due to the scattering behavior of the floc suspension. Light that is scattered away from the detector by one particle can then be scattered back towards the detector by a second particle (Mohammadi, 2002). Increasing the particle concentration increases the fraction of scattered light that interacts with multiple particles and yet makes it to the detector. This multiple scattering causes the light attenuation at high solids concentrations to be less than would be expected based on linear extrapolation.

Although floc aggregation dramatically changes the visual appearance of turbid suspensions, it does not significantly change the average light attenuation. The average light attenuation is unaffected by aggregation because the distances between the clay particles in a floc are

typically larger than the wavelength of light, thus, the scattering properties of clay particles in a floc are similar to the scattering properties of dispersed clay particles in suspension. Reported observations confirm that turbidity does not change significantly as flocculation proceeds (Tse et al., 2011). Particle aggregation does cause a large increase in the standard deviation of light attenuation and changes in the standard deviation of light attenuation have been used to measure the extent of floc aggregation (Gregory, 1985; Jarvis et al., 2005).

The standard curve for a two component aluminum hydroxide-kaolinite clay mixture was validated experimentally. TSS (Total Suspended Solids) were measured by Method 2540D procedures outlined in Standard Methods (Clesceri et al., 1998). For this TSS test, a peristaltic pump withdrew a sample from a 4.8 mm ID tube for three minutes at a flow rate of 0.83 mL/s. Based upon visual observation, the withdrawal impacted solids ~2.4 cm above and ~2.4 cm below the withdrawal center, thus, 48 mm x 48 mm image interrogation areas were chosen. After each withdrawal, the floc blanket was allowed to re-equilibrate for ten minutes before the next sample was obtained.

Images were obtained at a shutter speed of 400 μs at the following positions: (A) 7 cm above the floc-water interface, (B) 3 cm above the floc water interface, (C) 3 cm below the floc-water interface, and (D) 7 cm below the floc-water interface (Figure 6). The interrogation areas overlapped a vertical distance of 0.4 cm each, but were obtained for separate solid samples and images.

TSS test results for typical floc blanket concentration ranges of analysis were compared to the concentrations predicted with the combined calibration curve (Figure 5). The predicted TSS agreed with measured TSS sample (average values) within ±13% over a 10-fold range of concentrations. A ±13% error was deemed acceptable as it is close to the typical ±10% measurement error in TSS tests.

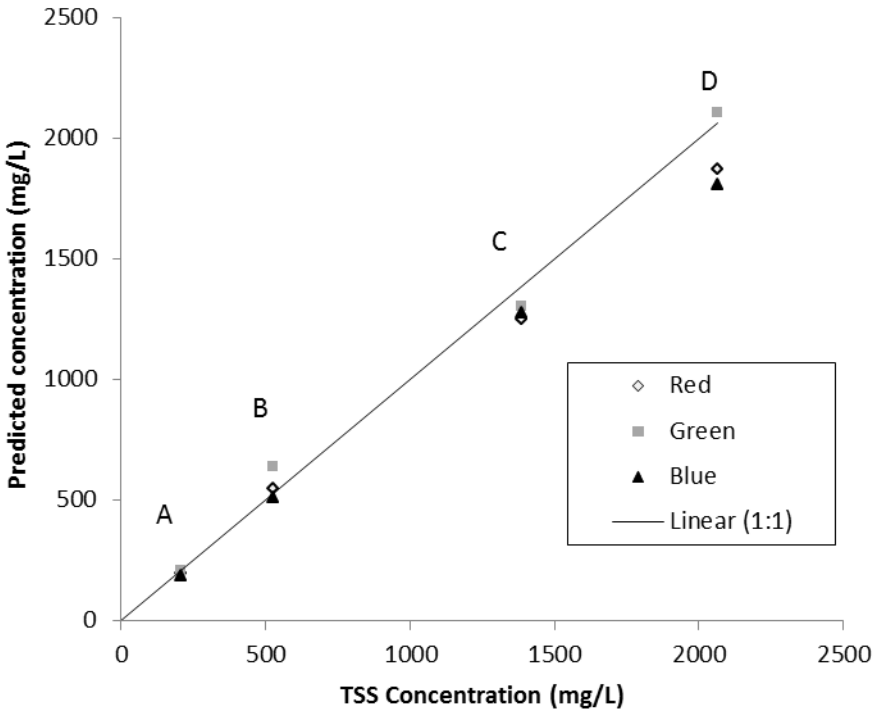

Figure 2–6. Predicted concentration from image analysis and concentrations from TSS grab samples for. Slopes from red, green, blue wavelengths are: 0.89, 0.98, and 0.86, respectively.

Imaging of Floc Blanket Solids Concentrations

Figure 2-7 presents an example of conversion of an image into a mapping of suspended solids concentration within a floc blanket. The figure was obtained from an 8 bit floc blanket image at a single time point by converting the red wavelength absorbance readings (Equation 2-4) to

suspended solids concentration readings (see Supplementary Information). The resulting matrix of concentration values was then converted to the 8 bit grey-scale values shown in Figure 2-7. The high concentrations along the sloped bottom of the reactor are expected because a debris flow of higher concentration created by settled solids is observed along the sloped bottom wall.

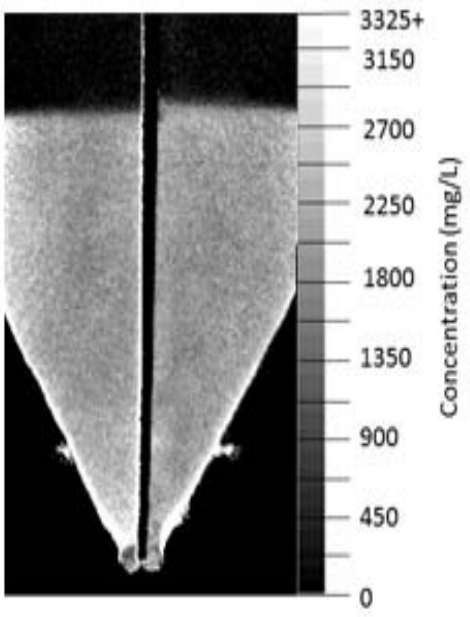

Figure 2–7. Plot of solids concentration (not pixel intensity) for a single image of a floc blanket built under conditions of 45 mg/L alum dosing and 100 NTU.

Method for Measurement of the Position of the Floc-Water Interface

Image analysis software developed in LabVIEW was used to locate the position of the floc-water interface (analysis steps are illustrated in Figure 2-8). An interrogation area was chosen that would include the floc-water interface as the floc blanket grew in height (Figure 2-8A).

Then the average light attenuation for each pixel row in the interrogation area was calculated. The average attenuation was calculated from equation (2-4) and solids concentration was predicted utilizing the combined solids calibration curve (see supplementary information). The solids concentration was an average of that predicted from the blue, green, and red wavelengths. The floc-water interface was located at the largest difference in positive and negative values for the second derivative of solids concentration (Figure 2-8C). Results from this method for the case that is illustrated in Figure 2-8C indicate the floc water interface was located at 56 cm. Visual inspection (Figure 2-8A) confirmed a floc-water interface at 56 cm.

Results and Discussion

Unless otherwise specified, the floc blankets used for analysis were formed under the conditions of: 100 NTU influent, 45 mg/L alum dose with a sedimentation tank upflow velocity of 1.2 mm/s. Images were taken every three seconds. The floc blanket waste outlet was positioned at a floc blanket height of 56 cm. The fluid above the floc blanket was not clarified by lamellar sedimentation for these experiments. Characterization of overall turbidity removal in a combined floc blanket-lamellar sedimentation system is a goal of planned future research.

Floc Blanket Concentration Analysis

The variability in floc blanket concentration was characterized with respect to: measurement length scale, height, time, and upflow velocity. In prior research, floc blanket solids concentration has been assayed utilizing TSS tests on samples from different points within the floc blanket (Hurst et al., 2010). The advantages of image analysis are that floc blanket concentration may be non-destructively measured as a function of position and time over the

entire floc blanket, and image analysis can provide higher resolution spatial and temporal data compared to TSS solids tests.

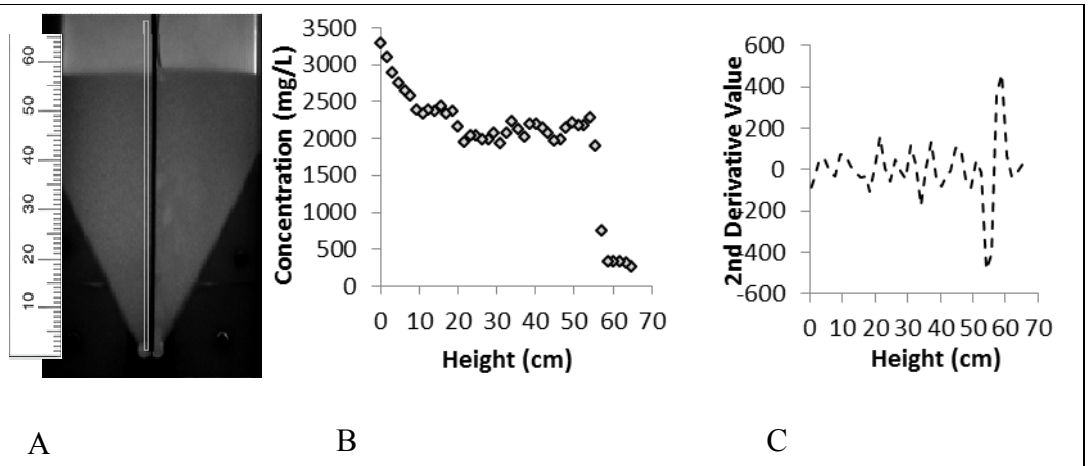

A B C

Figure 2–8. A. Grayscale intensity image with the selected interrogation area (shown as a light box in the image). B. Plot of solids concentration with respect to distance. C. Second derivative of solids concentration with respect to distance.

Variation in floc blanket concentration with respect to measurement length scale

Variability in solids concentration was evaluated over a range of length scales (Figure 9). The interrogation area was 150 mm wide x 270 mm high (100x180 pixels) with the top of the area located 4 cm below the floc-water interface. The image was taken when the floc blanket height reached the floc waste inlet (Figure 2-9A).

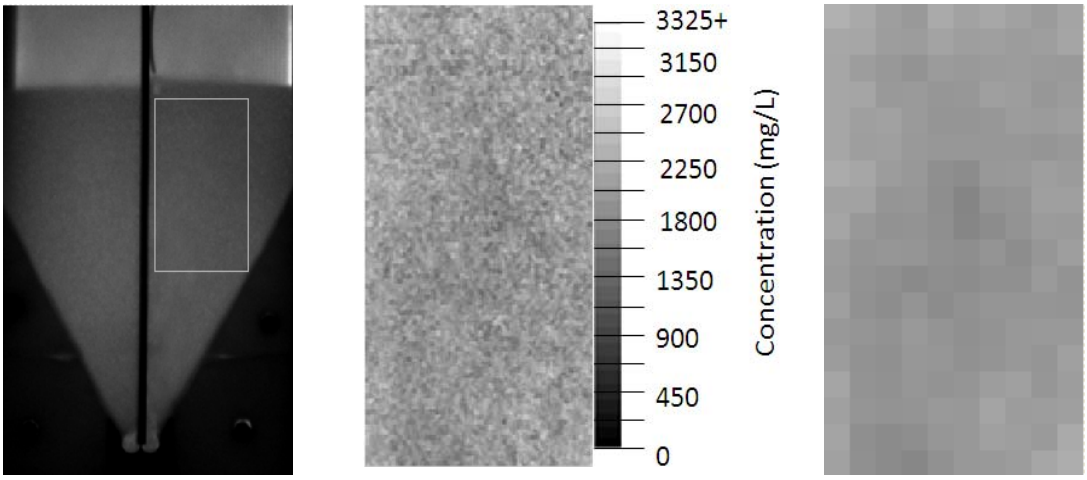

Figure 2–9. A. Image and interrogation area (150 mm wide x 270 mm high) selected for analysis (starting four centimeters below the floc-water interface). B. Concentration map based on analysis of 1.5 mm squares. C. Concentration map based on analysis of 15 mm squares.

In Figure 2-9B, each pixel corresponds to a 1.5 mm x 1.5 mm section of the reactor. At this spatial scale there is a large variation of solids concentration (1990 mg/L ± 10.6%) with a maximum concentration reading above 3325 mg/L and a minimum of 225 mg/L. This large range demonstrates that the number of flocs in a 1.3 cm long light path is highly variable. As expected at a spatial scale of 15 mm x 15 mm the variability caused by the presence or absence of individual flocs in the light path is reduced (average concentration = 1990 mg/L ± 5.2%).

Local variability in solids concentration is expected to be related to the mean floc separation distance normalized by the optical path length of 1.3 cm. Floc separation distance depends upon floc blanket concentration and floc size. Influent floc size was estimated to be 1 mm based on the fractal floc model of Weber-Shirk and Lion (2010) and the measured

sedimentation velocity of flocs as a function of energy dissipation rate (Tse et al., 2011). The low energy dissipation rate of the floc blanket (2-3 orders of magnitude lower than the energy dissipation rate in the tube flocculator) coupled with large solids residence time in the floc blanket (Hurst et al., 2010) leads to the expectation that flocs have the potential to substantially grow in size in the floc blanket.

The volume of fluid occupied per floc was calculated using the fractal floc model of Weber-Shirk & Lion (2010). Assuming a 2 mm diameter floc with a fractal dimension of 2.3 and a floc blanket concentration of 2000 mg/L (with clay to alum ratio of 2.7:1) gives a floc volume fraction of ~0.2 and a fluid volume occupied per floc of 21 mm^3. Given the optical path of 13 mm the area occupied by one floc was 1.6 mm^2. Small interrogation areas have a small number of flocs and a corresponding high variability in light attenuation. The minimum interrogation area of 225 mm^2 used for subsequent measurements was based upon a plot of the coefficient of variation obtained for five different interrogation areas in range 2.25 mm^2 to 900 mm^2 (Figure 2-10). The variation in measured concentration grows as the number of flocs in the interrogation area decreases.

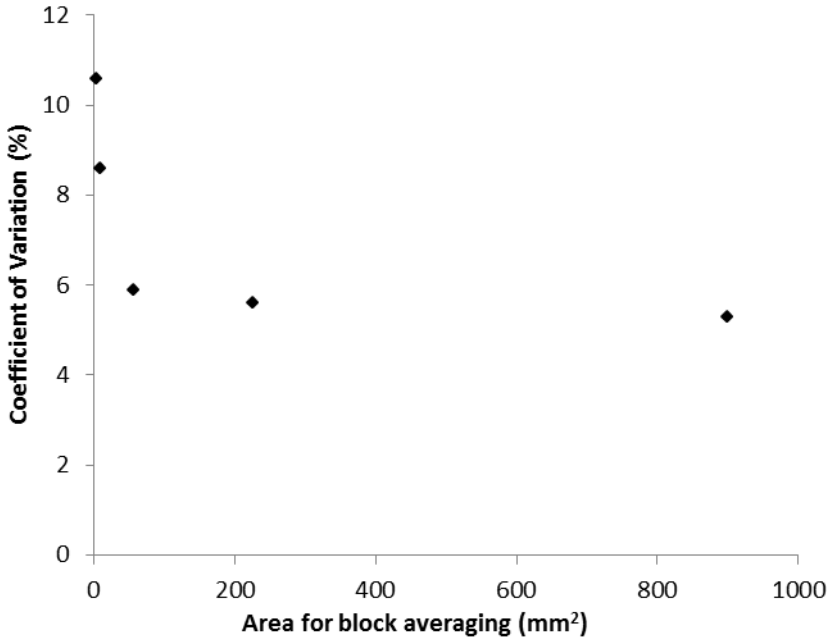

Figure 2–10. Coefficient of variation compared to the interrogation area.

Variation in floc blanket concentration with respect to height

The variability in concentration with respect to floc blanket height is shown in Figure 8B. Suspended solids concentration is relatively uniform (±10%) with respect to height, but higher concentrations exist at the bottom of the reactor and near the floc-water interface. Above the sloped bottom where there are optical edge effects and a debris flow, there exists a relatively uniform concentration of 2100 mg/L ±10% (averaged across all concentration values below the floc-water interface and above the debris flow). However, the bulk solids concentration increases up to 10% above the average near the floc-water interface (i.e. between 47 cm to 54 cm).

Variability with respect to time

The average concentration for a 15 mm x 15 mm region (centered at a height of 35 cm from the bottom of the jet reverser and 12 cm from the left edge) was measured over the course of floc blanket formation and growth (Figure 2-11A and B). Images were taken at intervals of 3 seconds between 0 to 10,000 seconds. Solids concentration remained low (below 500 mg/L) between 0 and 3000 seconds because the interrogation area was above the floc-water interface. Between 3000-4000 seconds, the floc-water interface passed through the region. After the floc water interface passed this position, the solids concentration was relatively stable between 1800 mg/L and 2000 mg/L. Blanket concentration is related to the discrete floc terminal sedimentation velocity. An increase in blanket concentration therefore reflects an increase in floc sedimentation velocity. The observed gradual increase in blanket concentration could be the result of an increase in floc size or an increase in floc density.

A 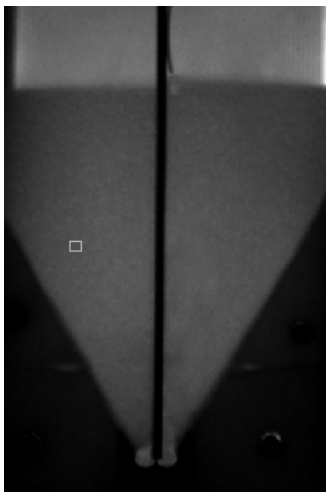

B 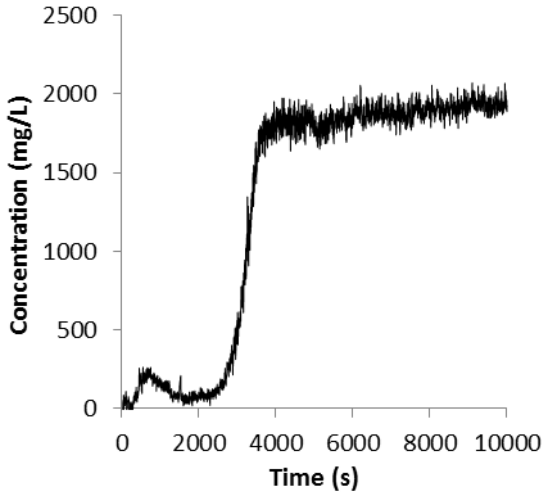

Figure 2–11. A. Selection of 15 mm square interrogation area. B. Average solids concentration at a fixed interrogation area during floc blanket growth.

Variation in concentration with respect to upflow velocity

The interface upflow velocity is related to hindered sedimentation velocity and hindered sedimentation velocity is related to solids concentration (Gould, 1974; Head et al., 1997). In hindered sedimentation, the upflow velocity in the suspension is significantly higher than the upflow velocity above the suspension due to the volume occupied by the particles. Settled water turbidity is a function of the floc blanket suspended solids concentration (Gregory, 1979), thus, understanding the impact of the interface upflow velocity on solids concentration is important in predicting particle removal capabilities of the floc blanket.

Gould (1974) hypothesized that the hindered sedimentation velocity of the floc blanket must match the average upflow velocity ($V_{Up-Interface}$) immediately above the floc-water interface. Gould's hypothesis is supported by the following logic:

1. The net vertical velocity of the flocs at the interface is negligible relative to the fluid velocity above the interface because the influent solids concentration is small relative to the floc blanket solids concentration.
2. Therefore, the floc blanket position remains relatively stationary compared to the interface upflow velocity. As a result, the hindered sedimentation velocity of the flocs below the interface must be almost equal to the upflow velocity immediately above the interface.
3. The solids in the floc blanket are well mixed so that the concentration in the floc blanket is relatively uniform and evenly distributed (an observation made by Gould, 1969, and confirmed here when the interrogation area was much larger than the area occupied by one floc (Figure 2-10)). Thus, the hindered sedimentation velocity and the solids concentration are relatively constant within the floc blanket.

Floc blanket concentration was assessed with respect to varying sedimentation tank upflow velocities (Figure 2-12). A series of floc blankets were built with a floc-water interface at 56 cm, with upflow velocities of 0.4 mm/s, 0.6 mm/s, 0.9 mm/s, 1.2 mm/s, 1.5 mm/s, 1.8 mm/s (Figure 2-12). The resulting solids concentrations provide a relationship between upflow velocity and bulk solids concentration in this floc blanket system. Each floc blanket was created and then maintained at steady height for three hydraulic residence times before the solids concentration was measured. Each data point represents three hydraulic residence time's average of data points collected at 3 second intervals for a 225 mm^2 interrogation area centered at a height of 35 cm from the bottom of the jet reverser and 12 cm from the left edge. The results confirm that higher suspended solids concentrations occur at lower interface upflow velocities.

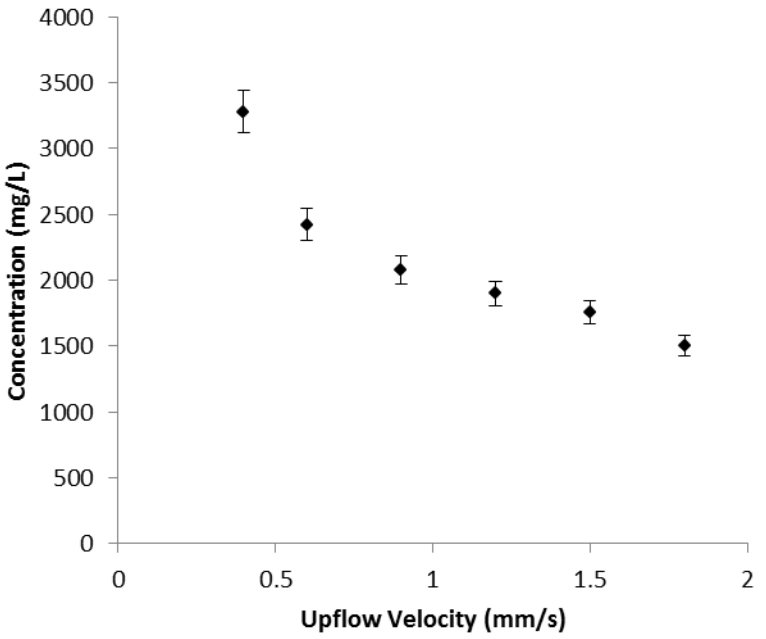

Figure 2–12. Concentration of floc blanket and associated upflow velocity immediately above the floc-water interface.

Floc Blanket Thickening

Increase in floc blanket height over time is shown in Figure 2-13A and increase in concentration over time is shown in Figure 2-13B. The floc water interface was not detected by the floc-water interface program before 3300 seconds. The solids concentrations were measured using a series of interrogation areas located 4 cm below the floc water interface. The upflow velocity immediately above the floc-water interface varied as the floc blanket grew in height due to the tapered bottom geometry up to a floc blanket height of 43 cm (Figure 2-13B).

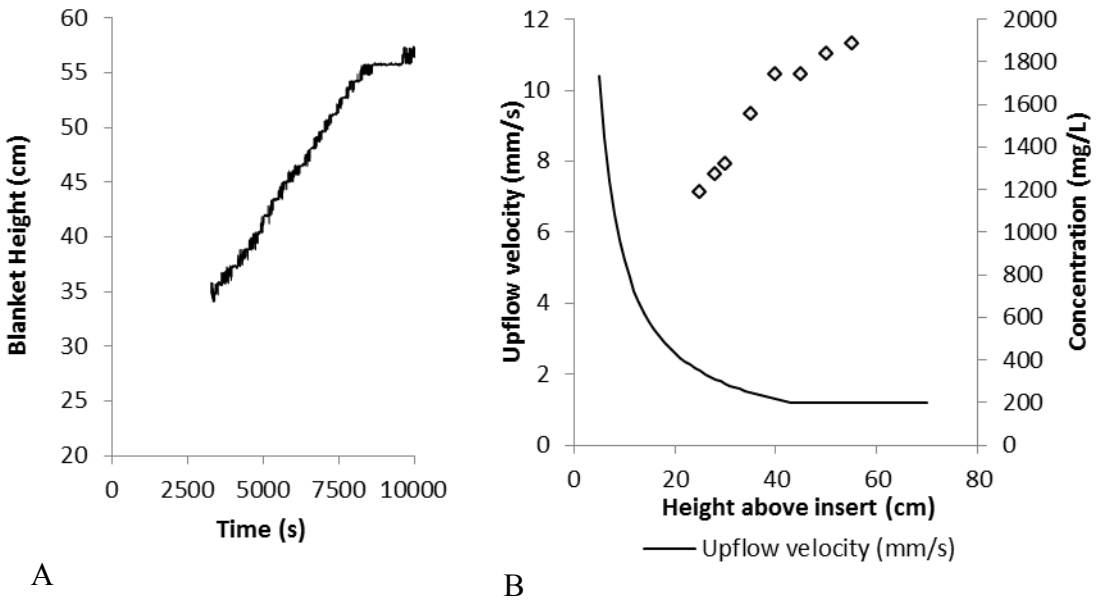

A B

Figure 2–13. A. Floc blanket height during floc blanket formation. B. Interface upflow velocity and floc blanket solids concentration during floc blanket formation.

The interface upflow velocity became constant in the experimental apparatus at a floc blanket height above 43 cm (Figure 2-13B). It was originally hypothesized that the floc blanket concentration would remain uniform. However, the blanket concentration continued to increase up to a height of 56 cm. This observation demonstrates that floc blanket concentration and the corresponding discrete floc sedimentation velocity can increase over time even at a constant interface upflow velocity. The observed increase must result from either an increase in floc size or increase in floc density over time. As solids concentration increases, the head loss through the floc blanket and subsequently energy dissipation rate through the floc blanket also increase. It is possible that the increase in energy dissipation rate coupled with large solids residence times leads to the formation of flocs with an increased sedimentation velocity.

Conclusions

The experimental apparatus and methods of non-destructive analysis of solids concentration provide a system for an improved understanding of floc blanket formation and behavior. Preliminary data presented in this paper confirm prior observations that floc blanket concentration is relatively uniform with respect to height (Figure 2-11B) (Gould, 1969) and that concentration in a floc blanket is influenced by the interface upflow velocity (Figure 2-12) (Gregory, 1979; Letterman, 1999; Hurst et. al., 2010).

However, the data presented in this paper demonstrate that a more nuanced view of Gould's hypothesis is possible. The data obtained here indicate that the floc blanket solids concentration increases over time even when upflow velocity immediately above the floc water interface remains constant (Figure 2-13B). While the postulated cause is an increase in floc terminal settling velocity over time (which is either a result of a change in floc size or density), more study is required to fully understand what physical changes flocs undergo that cause an increase in solids concentration.

The solid, liquid, and bottom geometry interactions in the floc blanket are critical components in ensuring that settled flocs are returned to the inlet jet to be re-suspended. The preliminary results of this research reveal debris flow along the inclines of the reactor wall (Figure 2-7). Future research is needed to identify physical mechanisms and geometric bottom conditions required for re-suspension of settled solids. Future research with the experimental apparatus is expected to: (1) evaluate particle removal efficiency as a function of interface upflow velocity,

floc blanket height, tube settler capture velocity, and (2) determine the effect of jet and bottom geometry on the ability to re-suspend returning debris flow.

References

AWWA/ASCE. (1990). *Water Treatment Plant Design*. McGraw-Hill, New York.

Chen, L., Lee, D.-J., and Chou, S.-S. (2006). Charge reversal effect on blanket in full-scale floc blanket clarifier. *J. Env. Eng. ASCE.* **132**(11), 1523-1526.

Chen, L., Sung, S., Lin, W., Lee, D.-J., Huang, C., Juang, R., et al. (2002). Observations of blanket characteristics in full-scale floc blanket clarifiers. *Water Sci. and Tech.* **47**(1), 197-204.

Clesceri, L, Greenberg, A.E., & Eaton, A.D. (1998). *Standard Methods for the Examination of Water and Wastewater.* American Public Health Association, Baltimore.

City of Ithaca. (2011). *Drinking Water Quality Report.* City of Ithaca: Ithaca, NY.

Edzwald, J.K., Ives, K.J., Janssens, J. G., McEwen, J.B., and Wiesner, M. R. (1999). *Treatment process selection for particle removal,* Chapter 5, AWWRF/IWSA, New York.

Gould, B. (1969). Sediment Distribution in Upflow. *Australian Civ. Eng.* **10**(9), 27-29.

Gregory, R. (1979). *Floc Blanket Clarification*. Water Research Centre TR 111, Swindon, U.K.

Gregory, J. (1985). Turbidity Fluctuations in Flowing Suspensions. *J. Col. Inter. Sci.* **105**, 676-684.

Head, R., Hart, J., and Graham, N. (1997). Simulating the effect of blanket characteristics on the floc blanket clarification process. *Water Sci. and Tech.* **36**(4), 77-82.

Hurst, M., Weber-Shirk, M.L., Lion, LW. (2010). Parameters affecting steady-state floc blanket performance. *J. of Water Supply Res. Technol. Aqua.* **59**(5), 312-323.

Jarvis, P., Jefferson, B. and Parsons, S.A. (2005). Measuring floc structural characteristics. *Rev in Env. Sci. & Bio. Tech.* **4**, 1-18.

Kawamura, S. (2000). *Integrated design and operation of water treatment facilities,* Chapter 3, John Wiley and Sons, New York.

Letterman, R. 1999 *Water Quality and Treatment: A Handbook of Community Water Supplies.* McGraw-Hill, New York.

Lin, W., Sung, S., Chen, L., Chung, H., Wang, C., Wu, R., et al. (2004). Treating high-turbidity water using full-scale floc blanket clarifiers. *J. Env. Eng. ASCE.* **130**(12), 1481-1487.

Mohammadi, M.S. (2002). A Generalized Refractive Index Equation for Estimating the

Average Particle Size in Colloidal Suspensions. *J. Dispersion Sci. and Tech.* **23**(5), 689-697.

Miller, D.G., and West, J.T. Pilot Plant Studies of Floc Blanket Clarification. (1968). *AWWA Journ.* **60**(2), 154-164.

Purushothaman, M. and Damodara, T. (1986). Defluoridation for rural areas-alum floc sludge blanket technique. *J. of Indian Water Works Assoc.* **18**(1), 91-97.

Schulz, C.R., and Okun, D.A. (1984). *Surface Water Treatment for Communities in Developing Countries.* John Wiley and Sons, New York.

Su, S., Wu, R., and Lee, D. (2004). Blanket dynamics in upflow suspended bed. *Water Res.* **38**(1), 89-96.

Sung, S., Lee, J., and Wu, R. (2005). Steady-state Solid Flux Plot of Blanket in Upflow Suspended Bed. *J Chinese Inst. Chem. Eng.* **36**(4), 385-391.

Tchobanoglous, G., Burton, F. L., and Stensel, D. H. (2003). *Wastewater Engineering Treatment and Reuse.* McGraw-Hill, New York.

Tse, I.C., Swetland, K., Weber-Shirk, M.L., and Lion, L.W. (2011) Fluid shear influences on the performance of hydraulic flocculation systems. *Water Res.* **45**(17), 5412-5418.

Weber-Shirk, M. L. (2008). *An Automated Method for Testing Process Parameters.* Retrieved April 5, 2009, from AguaClara Wiki: http://confluence.cornell.edu/display/AGUACLARA/Process+Controller+Background

Weber-Shirk, M. L., Lion, L. W. (2010). Flocculation model and collision potential for reactors with flows characterized by high Peclet numbers. *Water Res.* **44**(18), 5180-5187.

Zhang, Z., Chen, Z., Li, Y., Fan, J., Fan, B., Luan, Z., and Lu, D. (2006). Performance of a novel vertical-flow settler: a comparative study. *J. Enviro. Sci*. **18**(5), 858-863.

Supplementary Information

Analysis of floc blanket concentration for aluminum hydroxide-kaolinite flocs was accomplished by combining separate experimentally obtained calibration curves for clay and aluminum hydroxide. The advantage of combining two separate calibration curves into a single calibration curve is that the concentration of any mixture of clay and aluminum hydroxide may be analyzed.

For a two component mixture of component 1 and component 2, Beer's Law maintains that absorbance is additive permitting a single expression:

$$A_\lambda = \varepsilon_1 b C_1 + \varepsilon_2 b C_2 \qquad (2\text{-}6)$$

Equation 2-6 can be re-written so that only one extinction coefficient is utilized. The use of one molar extinction coefficient is accomplished when the second component concentration (C_2) is converted to a concentration (C_{2k}) that would have the same absorbance as the first component (Equation 2-7). The conversion factor (k) is the ratio of the extinction coefficients (Equation 2-8).

$$k = \frac{\varepsilon_1}{\varepsilon_2} \qquad (2\text{-}7)$$

$$C_{2k} = kC_2 \qquad (2\text{-}8)$$

The resulting expression for a two component system with one extinction coefficient is Equation 2-9:

$$A_\lambda = \varepsilon_1 b(C_1 + C_{2k}) \qquad (2\text{-}9)$$

A second-order polynomial gave a better fit than its linear counterpart for both the clay and aluminum hydroxide suspensions and took the general form shown in Equation 2-10 (where

α_1 is analogous to an extinction coefficient and α_2 is analogous to a scattering coefficient). The intercepts are neglected as the values are small and their absence introduces little error (±1%) into the final calculations.

$$A_\lambda = \alpha_2 C^2 + \alpha_1 C \qquad (2\text{-}10)$$

Akin to the progression leading up to equation 2-10, a second component (i.e. aluminum hydroxide) may be fit to the first component curve (i.e. clay) utilizing one fitting parameter for second order polynomial expressions. The conversion factor chosen ($k_{Al(OH)3->Clay}$) was expressed as a ratio of their first order terms (α_{1-Clay}, α_{1-AlOH_3}) in Equation 2-11. The first order term was chosen because it was more sensitive to changes in concentration at typical floc blanket concentration ranges (1500-4000 mg/L). The aluminum hydroxide concentration was converted to an equivalent clay concentration because each floc was predominantly composed of clay (89.5% at the alum dosing of 45 mg/L for the 100 NTU clay suspension).

$$k_{Al(OH)3->Clay} = \frac{\alpha_{1-AlOH_3}}{\alpha_{1-Clay}} \qquad (2\text{-}11)$$

The expression for aluminum hydroxide could be converted to an equivalent clay calibration curve utilizing the fitting parameter from equation 9 resulting

in: $\alpha_{2-AlOH3}(C_{AlOH3}{}^2) + \alpha_{1-AlOH3}(C_{AlOH3}) = \alpha_{2-Clay}(k_{AlOH3->Clay}C_{AlOH3})^2 + \alpha_{1-Clay}(k_{AlOH3->Clay}C_{AlOH3})$ (2-12)

Where: C_{Clay} is the concentration of clay in the raw water and C_{AlOH3} is the concentration of aluminum hydroxide from alum dosing assuming all aluminum in solution precipitates as aluminum hydroxide.

The resulting equation for a two component mixture utilizing the first and second order coefficients from the clay calibration curve is as follows (Equation 2-13): $A_\lambda = \alpha_{2-Clay}(C_{clay} + k_{AlOH3->Clay}C_{AlOH3})^2 + \alpha_{1-Clay}(C_{Clay} + k_{AlOH3->Clay}C_{AlOH3})$ (2-13)

The fraction of total mass as clay (f_{Clay}) and aluminum hydroxide (f_{AlOH3}) are given by:

$$f_{Clay} = \frac{C_{Clay}}{C_{Clay} + C_{AlOH3}} \quad (2\text{-}14)$$

$$f_{AlOH3} = 1 - f_{Clay} \quad (2\text{-}15)$$

Knowing the fraction of total mass as clay and aluminum hydroxide, allows for light attenuation to be calculated based on the total solids concentration of the sample (Equation 2-16):

$$A_\lambda = \alpha_{2-Clay}(C_{Total}f_{Clay} + k_{AlOH3->Clay}f_{AlOH3}C_{Total})^2 + \alpha_{1-Clay}(C_{Total}f_{Clay} + k_{AlOH3->Clay}f_{AlOH3}C_{Total}) \quad (2\text{-}16)$$

Where: C_{Total} is the total concentration of clay and aluminum hydroxide.

CHAPTER 3: IMAGE ANALYSIS OF FLOC BLANKET DYNAMICS: INVESTIGATION OF FLOC BLANKET THICKENING, GROWTH, AND STEADY-STATE[1]

[1] The contents of this chapter have been submitted to *Journal of Environmental Engineering* for publication with co-authors: Dr. M. Weber-Shirk and Prof. L. Lion.

Image Analysis of Floc Blanket Dynamics: Investigation of Floc Blanket Thickening, Growth, and Steady-State

Matt Hurst[1], Monroe Weber-Shirk[2]*, and Leonard W. Lion[3]

Cornell University

Ithaca, NY 14853-3501

Phone: (607) 216-8445

Fax: (607) 255-9004

* Corresponding author

Email: mw24@cornell.edu

[1] Graduate Student, Civil and Environmental Engineering, Cornell University Hollister Hall Ithaca, NY 14853-3501 mwh65@cornell.edu

[2] Senior Lecturer, Civil and Environmental Engineering, Cornell University Hollister Hall Ithaca, NY 14853-3501 mw24@cornell.edu

[3] Professor, Civil and Environmental Engineering, Cornell University Hollister Hall Ithaca, NY 14853-3501 LWL3@cornell.edu

Image Analysis of Floc Blanket Dynamics: Investigation of Floc Blanket Thickening, Growth, and Steady-State

Abstract

Floc blankets are fluidized, concentrated beds of particles utilized in some upflow sedimentation tank reactor configurations in water treatment. The presence of a floc blanket can significantly enhance removal of turbidity when coupled with lamellar sedimentation. Blanket dynamics have not been extensively studied, but are important for understanding blanket formation and operational control in full-scale water treatment plants. This research employed image analysis to reveal the temporal dynamics of floc blanket suspended solids concentration and floc-water interface height. Turbidity measurements were used to corroborate image analysis as a valid method for measuring solids concentration in the floc blanket and in the floc blanket supernatant. Observations from image analysis reveal relatively distinct stages in the creation of a floc blanket: thickening (increasing suspended solids concentration) in the absence of a floc-water interface, thickening with an interface, and steady-state. Preliminary performance results suggest that turbidity removal is more significantly impacted by blanket concentration than blanket height. Two important factors were found to impact blanket dynamics during the interval when the height of the floc-water interface was increasing: (1) thickening and (2) mass transfer between the supernatant above the floc water interface and the floc blanket. Floc blanket thickening during formation has been confirmed to occur at both variable and constant interface upflow velocity. This observation suggests that floc properties (size and density) change during floc blanket formation.

Keywords: floc blanket, image analysis, growth rate, mass balance, suspended solids concentration, hindered sedimentation

Introduction

An explicit goal of water treatment plants (WTPs) is to remove turbidity from the influent source water. Floc blankets are relatively uniformly concentrated fluidized beds of particles formed in some upflow sedimentation tanks (Gould, 1969), and are an alternative reactor configuration for removal of influent turbidity. Floc blankets are characterized by the presence of a floc-water interface between a concentrated bed of suspended particles and a relatively clear supernatant. The upflow velocity immediately above the interface ($V_{Up-Interface}$) is defined as the volumetric flow rate (Q) divided by the area of the floc-water interface, $A_{FlocInterface}$ (Equation 3-1) and controls the extent of fluidization, solids concentration, and performance (solids capture) in floc blankets.

$$V_{Up-Interface} = \frac{Q}{A_{FlocInterface}} \qquad (3\text{-}1)$$

The presence of a floc blanket can be useful in WTPs for reducing solids loading to filters, especially for highly turbid waters (Lin *et al*., 2004). Blanket concentration and blanket height are correlated with a reduction in settled water turbidity (Hurst *et al*., 2010). In conjunction with lamellar sedimentation, floc blankets enhance particle removal by providing: (1) an increased likelihood of particle-particle interaction that can result in further flocculation of particles and (2) filtration-like removal of small particles (Miller & West, 1968; Reynolds & Richards, 1996; Tchobanoglous, Burton, & Stensel, 2003; Hurst *et al*., 2010).

Several gaps exist in the literature related to floc blanket dynamics:

(1) the guidance given to plant operators is vague and/or not generalizable. Exemplary empirical guidelines for operation of a floc blanket include: (1) the volume of sludge from a 100 mL grab sample should be 18-25 mL after five minutes of settling, and (2) to flood the effluent weirs when floc break-up is suspected to occur during conveyance of sedimentation tank effluent to sand filters (Kelly, 1998). These guidelines are anecdotally based on one sedimentation basin and have no direct relationship with underlying blanket dynamics.

(2) there is an existing perception that blankets are prone to 'anomalous' and unstable behavior (AWWA/ASCE, 1990; Chen *et al*., 2003), and testable hypotheses have not been given to explain this behavior. The notion that floc blankets are prone to instability (i.e. relatively rapid increases in floc blanket height resulting in particle carry-over and high supernatant solids concentrations) has prompted some prior investigators to consider mass flux with respect to blanket formation and stability (Chen *et al*., 2006, Su *et al*., 2004, and Sung *et al*., 2003). Floc blanket mass flux models have focused on the flux across the floc-water interface (Sung *et al*., 2005; Chen *et al*., 2002; Gregory, 1979). However, instability in the floc blanket likely results from changes in inflow conditions (solids concentration, coagulant dose, volumetric flow rate, etc.) which change the floc properties and dynamics inside the floc blanket.

The objective of this research was to employ image analysis to achieve an improved understanding of the spatial and temporal dynamics of suspended solids in floc blankets. This research presents results that: (1) validate real-time concentration measurements by image analysis with continuously sampled turbidity measurements, and (2) characterize changes in

floc blanket concentration and height during formation of the floc blanket. Experimental results in this study were obtained using a novel apparatus equipped to permit image analysis of floc blanket suspended solids concentration and the position of the floc-water interface (Hurst *et al*. 2013). Image analysis constitutes a non-destructive technique for measuring suspended solids concentration with much greater spatial and temporal resolution over the entirety of the reactor compared to episodic observation of Total Suspended Solids (TSS) in grab samples.

Materials and Methods

All experiments were performed utilizing the reactor apparatus described in Hurst *et al*. (2013). Briefly, the experimental reactor acts as a large sampling cell for imaging of suspended solids. The optical path length ($L_{Reactor}$ = 1.3 cm) is suitable for use of transmitted light to analyze the range of suspended solids concentrations present in the reactor.

Uniform influent turbidity was produced via process control software (developed by Weber-Shirk, 2008) as described by Hurst *et al*. (2010). The software in conjunction with inline turbidimeters regulates the dilution of a concentrated clay stock of kaolin in temperature controlled, aerated Cornell University tap water (Temperature ≈ 20° C, pH ≈ 8.05, total alkalinity ≈ 110 mg/L as $CaCO_3$, total hardness ≈ 150 mg/L as $CaCO_3$, and dissolved organic carbon (DOC) concentration ≈ 2.0 mg/L (City of Ithaca, 2011)) to produce a simulated raw water with constant turbidity (typically ± 3%).

Reactor hydraulics are diagrammed in Figure 3-1. Coagulant and raw water are combined and enter a laminar flow, coiled tube flocculator (inner diameter, d = 9.5 mm, coil diameter, D = 13 cm, and length 20 m). The hydraulic residence time for the tube flocculator used in experiments was 3 minutes. The average energy dissipation rate in the tube flocculator was approximately 9 mW/kg. After tube flocculation, the flow was introduced near the bottom of an upflow sedimentation reactor. The total experimental flow rate (Q_{Inflow}) of 7.7 mL/s corresponded to a sedimentation tank upflow velocity of 1.2 mm/s above the sloped bottom.

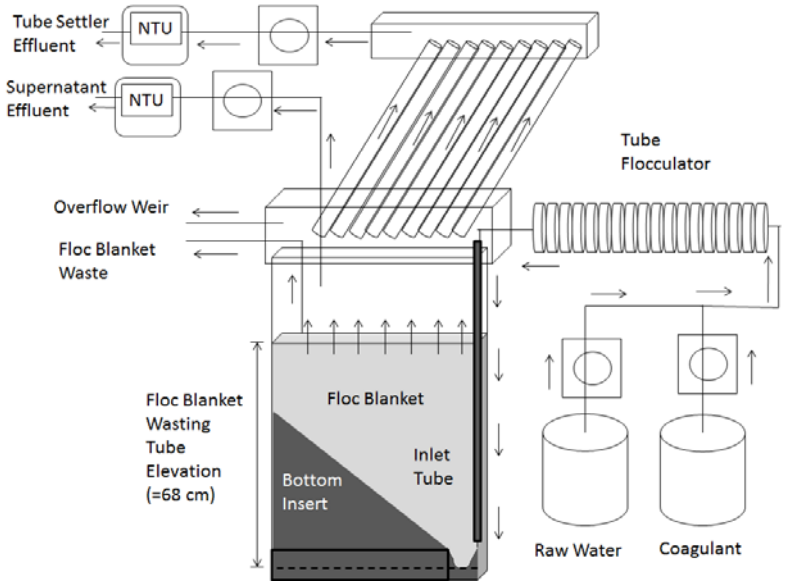

Figure 3–1. Diagram of apparatus and sampling points.

Figure 3-2 details the sedimentation tank and component dimensions. The removable bottom insert shown in Figure 3-2A was fabricated from foam board. For these experiments, the bottom insert (with a height of 45 cm) had an angle of inclination of 48 degrees. The "jet reverser" at the bottom-right position was milled from a 10 cm X 10 cm (1.3 cm thick) block of PVC (Figure 3-2B). Floc blanket height was defined as the distance from the bottom-most point of the "jet reverser" to the floc-water interface between the floc blanket and supernatant

(Figure 3-2A). A "jet reverser" (see Figure 3-2B) at the bottom of the reactor changes the direction of the incoming flocculated suspension to an upward flow that resuspends settled flocs that slide down the slope of the inclined side of the reactor (bottom insert shown in Figure 3-1). The "jet reverser" width ($W_{JetReverser}$) was 10 cm. A typical floc blanket image is displayed in the sedimentation tank in Figure 3-2A. The floc blanket is the more concentrated (i.e. the darker shaded) region which is below the relatively clearer (i.e. the lighter shaded) supernatant.

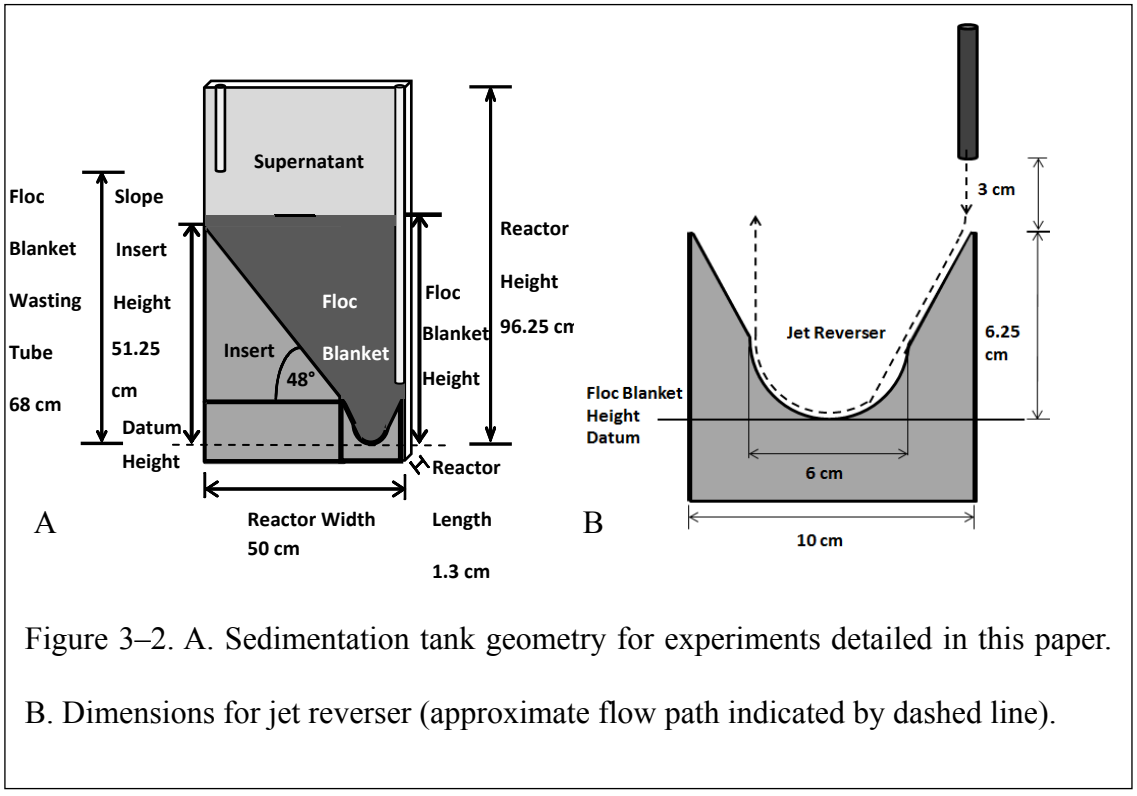

Figure 3–2. A. Sedimentation tank geometry for experiments detailed in this paper. B. Dimensions for jet reverser (approximate flow path indicated by dashed line).

The inlet tubing for the sedimentation tank was ellipsoidal with an inner major axis diameter of 1.27 cm and a minor axis diameter of 0.46 cm, and was placed along one edge of the sedimentation tank. At the experimental flow rate of 7.7 mL/s, the average jet velocity leaving the inlet tube was 0.18 m/s. The maximum energy dissipation rate at the center of the jet was calculated to be ~80 mW/kg (Equation 3-2).

$$\varepsilon_{Max} \cong \frac{\left(\Pi_{Jet} V_{Jet}\right)^3}{D_{Jet}} \qquad (3\text{-}2)$$

Where: Π_{Jet} is a constant ($\cong 0.4$), V_{Jet} is 0.18 m/s, and D_{Jet} is the smallest dimension of flow, 0.46 cm. Equation 3-2 was adapted from Baldyga et al. (1995).

Tube settler and floc blanket supernatant effluent performance were measured via continuous sampling through inline turbidimeters. Floc blanket supernatant was sampled 15 cm above the final height of the floc-water interface. Floc blanket height was controlled by wasting flocs at the target height. The remaining effluent flowed upward through a cluster of 10 tube settlers. The flow through each tube settler was controlled by a peristaltic pump. Excess flow in the reactor exited through an overflow weir which had a water level 1.5 cm above the entrance elevation of the tube setters.

A flow balance for the reactor is shown in equation 3-3. The inflow rate (Q_{Inflow}) and total outgoing flow rate ($Q_{Outflow}$) are equal to a combination of the floc blanket wasting flow rate ($Q_{FBWaste}$, 2.0 mL/s), the floc blanket supernatant sampling flow rate ($Q_{S-Sample}$, 0.1 mL/s), the tube settler effluent flow rate (Q_{TS}, 5.4 mL/s), and the overflow weir flow rate ($Q_{OverflowWeir}$, 0.2 mL/s).

$$Q_{Inflow} = Q_{Outflow} = Q_{FBWaste} + Q_{S-Sample} + Q_{TS} + Q_{OverflowWeir} \qquad (3\text{-}3)$$

Tube settler length and average fluid velocity determine the capture velocity (also referred to as critical velocity) of the tube settlers. The capture velocity (V_C) is the terminal settling velocity of the smallest particle size that can be captured with 100% efficiency by the tube

settlers. The capture velocity is defined by the following equation (Schulz & Okum, 1984) and was set to 0.09 mm/s:

$$V_C = \frac{V_\alpha}{\frac{L}{d}\cos(\alpha) + \sin(\alpha)} \qquad (3\text{-}4)$$

Where: d is the inner diameter of the tube (d = 2.6 cm), L is the length of the tube (L = 85 cm), α is the angle with respect to horizontal (α = 60°), and V_α is the average fluid velocity in the tube (4.0 mm/s).

Mounted on the backside of the reactor was a 1 m x 0.5 m 30 W panel (e-Lumanation) of light-emitting diodes that provided a relatively uniform light source. Images were taken with a Basler color SCA640-70FC IEEE-1394B (658x490 pixels) camera. The camera had an 8 mm lens and interfaced with LabVIEW image acquisition software. The software controlled the rate of image capture and shutter speed. The camera was mounted at a distance of 1.75 m from the reactor, generating a field of view of 94 cm x 71 cm. With this positioning, each pixel corresponded to a 1.5 mm x 1.5 mm section of the reactor.

Light attenuation (A) of the particle suspension is the negative logarithm of the transmitted light through the sample suspension (I) divided by the transmitted light through a blank water sample (I_0) (Equation 3-5).

$$A = -\log\left(\frac{I}{I_0}\right) \qquad (3\text{-}5)$$

Suspended solid floc blanket concentration measurements were calibrated to light attenuation measurements of known standards as described by Hurst *et al*. (2013). A concentration measurement can be attained for each pixel based on the light attenuation reading and the solid mass fraction that is clay. The calibration method is fully described in Hurst *et al*. (2013). Briefly, the total light attenuation is calculated from a second order polynomial based on the combined solids concentration of the sample (Equation 3-6):

$$A_\lambda = \alpha_2 C_{Total}^2 \left[f_{Clay} + k\left(1 - f_{Clay}\right) \right]^2 + \alpha_1 C_{Total} \left[f_{Clay} + k\left(1 - f_{Clay}\right) \right] \qquad (3\text{-}6)$$

Where: C_{Total} is the total concentration of clay and aluminum hydroxide, f_{Clay} is the solid mass fraction that is clay, k is the ratio of light attenuation from aluminum hydroxide to light attenuation from clay given the same concentration of both, α_1 is the first order coefficient and α_2 is the second order coefficient.

The non-linear relationship between light attenuation and solids concentration in equation (6) is caused by the scattering behavior of light in the suspension. While one particle can scatter light away from the detector, a second particle can then scatter that light back towards the detector (Mohammadi, 2002). As particle concentration increases, the fraction of scattered light that interacts with multiple particles on its way to the detector increases. This multiple scattering effect causes light attenuation at high solids concentrations to be less than would be expected based on first order decay.

Flocculation of suspended particles changes the visual appearance of the original suspension, however, does not significantly change the average light attenuation. The distance between the clay particles in a floc are typically larger than the wavelength of light, thus, the scattering properties of clay particles in a floc are similar to the scattering properties of dispersed clay particles in suspension. Experimental observations reported by Tse *et a*l. (2011) confirm that average turbidity does not change significantly as flocculation proceeds.

Results and Discussion

Validation of image analysis

As a means of validating image analysis, continuously logged turbidity measurements and image analysis were compared in evaluating suspended solids mass accumulation in the experimental reactor system. The total mass rate of accumulation may be obtained from the difference between the mass input from influent and mass loss from effluent streams. Given the low solids concentration in the effluent from the tube settlers relative to the supernatant and floc blanket, the rate of mass accumulation in the lamella was considered negligible, and the mass rate of accumulation in the reactor $\frac{d(C_{Reactor}\forall_{Reactor})}{dt}$ can be expressed as the summation of the mass rate of accumulation in the floc blanket $\frac{d(C_{\mathrm{FB}}\forall_{\mathrm{FB}})}{dt}$ and mass rate of accumulation in the supernatant above the floc-water interface $\frac{d(C_{\mathrm{S}}\forall_{\mathrm{S}})}{dt}$.

Mass balance analysis of the reactor (Figure 3-3) requires tracking of: (1) mass influent rate from the flocculator ($\dot{m}_F$), (2) rate of mass loss from floc blanket wasting ($\dot{m}_{FBWaste}$), (3) rate

of mass loss from the supernatant ($\dot{m}_{SWaste}$), and (4) rate of mass loss from the tube settlers ($\dot{m}_{TSLoss}$). The continuously logged inline turbidities of the effluent and influent streams were converted to solids concentrations based on a measured turbidity of 1 NTU from 1.2 mg/L of kaolin clay.

The mass loading rate for a given reactor flow ($\dot{m}$) is a product of the concentration (C) and flow rate (Q) (Equation 3-7).

$$\dot{m} = QC \tag{3-7}$$

The rate of suspended solids mass accumulation in the reactor must be equal to the difference of the influent and effluent streams (3-8).

$$\frac{d(C_{\text{Reactor}} \forall_{\text{Reactor}})}{dt} = \frac{d(C_{FB} \forall_{FB})}{dt} + \frac{d(C_S \forall_S)}{dt} = \dot{m}_F - \dot{m}_{FBWaste} - \dot{m}_{SWaste} - \dot{m}_{TSLoss} \tag{3-8}$$

Each term was calculated from turbidity data and the known volumetric flow rate (Equation 3-3). Results for continuously sampled turbidity observations are shown in Figure 3-4 for the experiment corresponding to the image analysis shown below in Figure 3-7. The floc blanket used for this analysis was formed under conditions of 100 NTU turbidity influent, a coagulant dose of 45 mg/L alum (4.1 mg/L as Al), and a sedimentation tank upflow velocity of 1.2 mm/s. Capture velocity of the tube settlers was set at 0.09 mm/s.

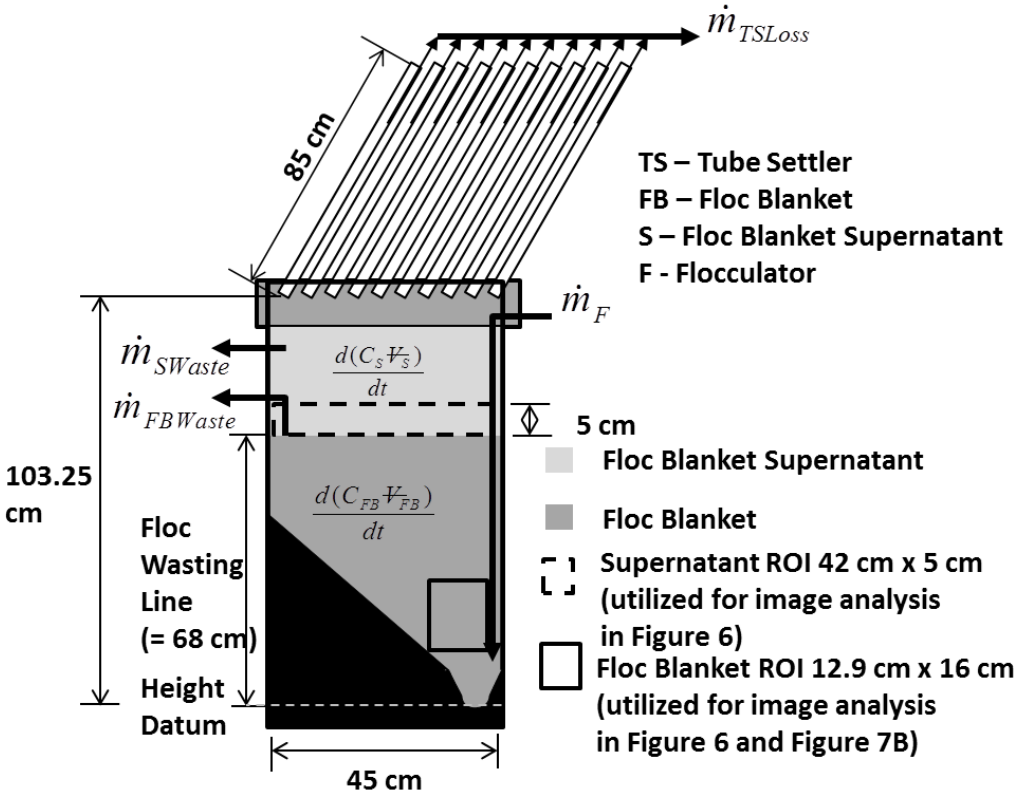

Figure 3–3. Mass input and loss in the sedimentation tank. Regions of interest (ROI) used for image analysis are indicated.

As seen in Figure 3-4, after 6800 seconds corresponding to a blanket height of 68 cm (see also Figure 7D), the performance for the clarifier and tube settler remained relatively constant. Between 6800 - 20000 seconds, average tube settler turbidity was 0.53 Nephelometric Turbidity Units (NTU) ±9.8%, average floc blanket supernatant turbidity was 23.9 NTU ±7.8%, and average influent turbidity was 99.7 NTU ±1.2%. Although the blanket reached the floc blanket wasting tube after 6800 seconds, the turbidity in the floc blanket wasting continued to increase until about 8000 seconds because the solids concentration near the floc-water interface continued to increase.

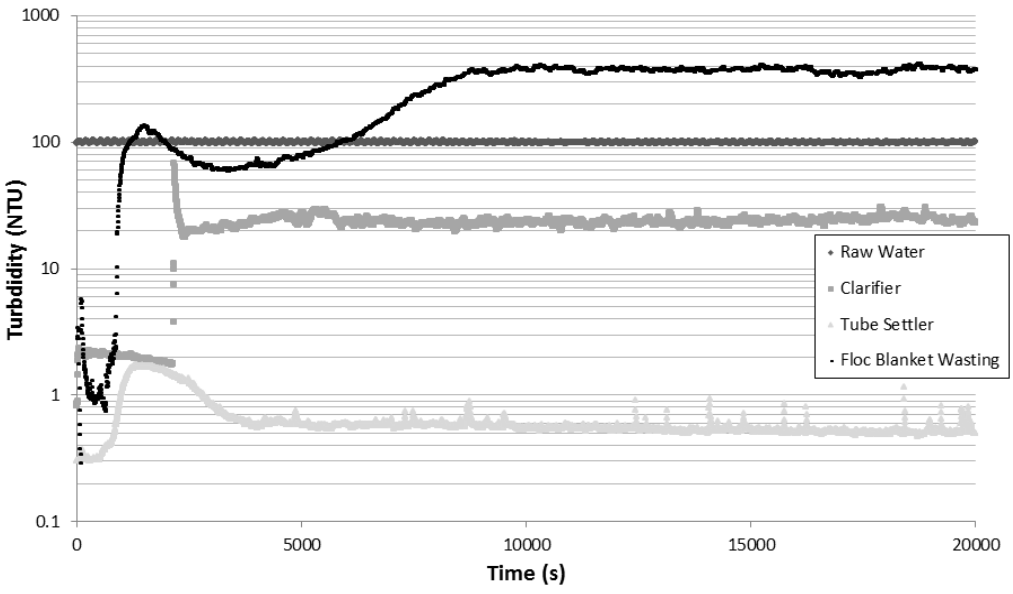

F

Figure 3–4. Raw water, clarifier, tube settler and floc blanket wasting turbidity for a floc blanket formed under an upflow velocity of 1.2 mm/s, coagulant dose of 45 mg/L and 100 NTU influent.

The tube settler effluent turbidity decreased dramatically between 2160 seconds to 4000 seconds from ~1.8 NTU to ~0.6 NTU. During this same time interval the floc blanket height only increased from 39 cm to 46 cm, and the floc blanket concentration increased from 800 mg/L to 1800 mg/L. Effluent turbidity remained relatively constant during the subsequent increase in floc blanket height from 46 cm to 68 cm. Previous investigators (Hurst et al., 2010; Miller & West, 1968) have indicated that floc blanket performance was influenced by both concentration and blanket height. However, these performance results (Figure 3-4) suggest that floc blanket concentration impacts turbidity removal more significantly than blanket height.

The turbidity readings in Figure 3-4 were related to the rate of mass accumulation in the reactor by equation (8). The result of each mass rate expression is calculated from the turbidity data in Figure 3-4 and respective flow rate, and is shown in Figure 3-5A. The resulting mass accumulation over the experimental time period of 20,000 seconds for the entire reactor is shown in Figure 3-5B. The largest contributor to mass loss in the reactor was the effluent from the floc blanket wasting tube (Figure 3-5A). The mass rate of accumulation sharply decreases as the floc blanket approached the wasting tube in the reactor (Figure 3-5B). The area under the curve up to 9000 seconds in Figure 3-5B is 5.2 grams and represents the total mass of solids in the floc blanket and supernatant at steady state.

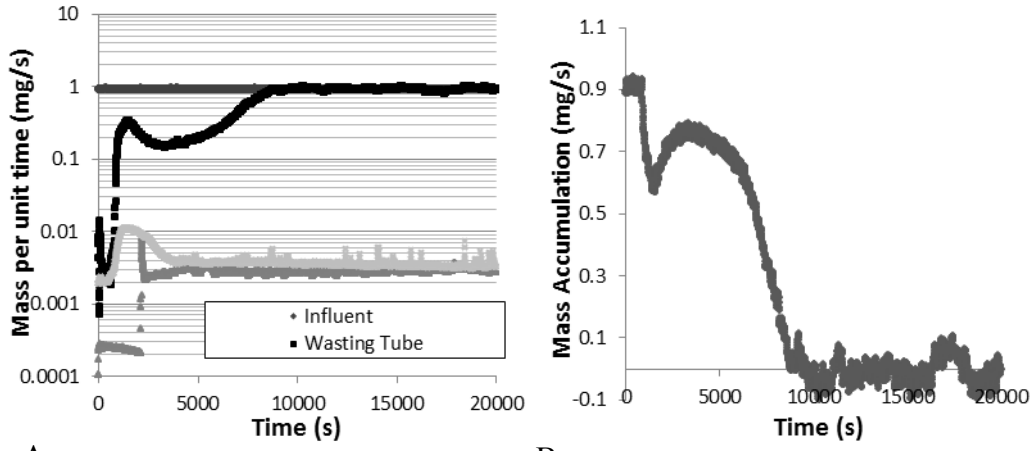

A B

Figure 3–5. A. Mass per unit time inflows and outflows to the reactor control volume. B. The resulting mass rate of accumulation in the reactor.

Sequential imaging was also used to estimate mass accumulation in the reactor. The total reactor concentration reading for suspended solids accounted for solids in the floc blanket and above the floc-water interface. The floc blanket mass was found by computing floc blanket volume (computed from floc blanket height data in Figure 3-7D shown below) and multiplying this floc blanket volume by the corresponding concentration (found by image

analysis and shown in Figure 3-7B). One limitation of measuring total suspended solids in the reactor was that the maximum height imaged by the camera was 76 cm above the bottom of the jet reverser. Since the imaged area did not include the entire supernatant, the average concentration in the supernatant from the region 71 to 76 cm (ROI shown in Figure 3-3) was used to estimate supernatant suspended solid concentration that was between 76 cm and 96.25 cm. The suspended solids concentration in the supernatant was one order of magnitude less than the blanket concentration, thus, small errors resulting from estimation of supernatant concentration did not significantly impact overall mass balance results. The area over which image analysis was not used to directly measure or estimate reactor mass was ~26% of the reactor volume.

A comparison of measurement of mass in the reactor based on influent and waste flow turbidity and control volume analysis with image analysis (Figure 3-6) validates the use of image analysis technique for measuring concentration in the reactor.

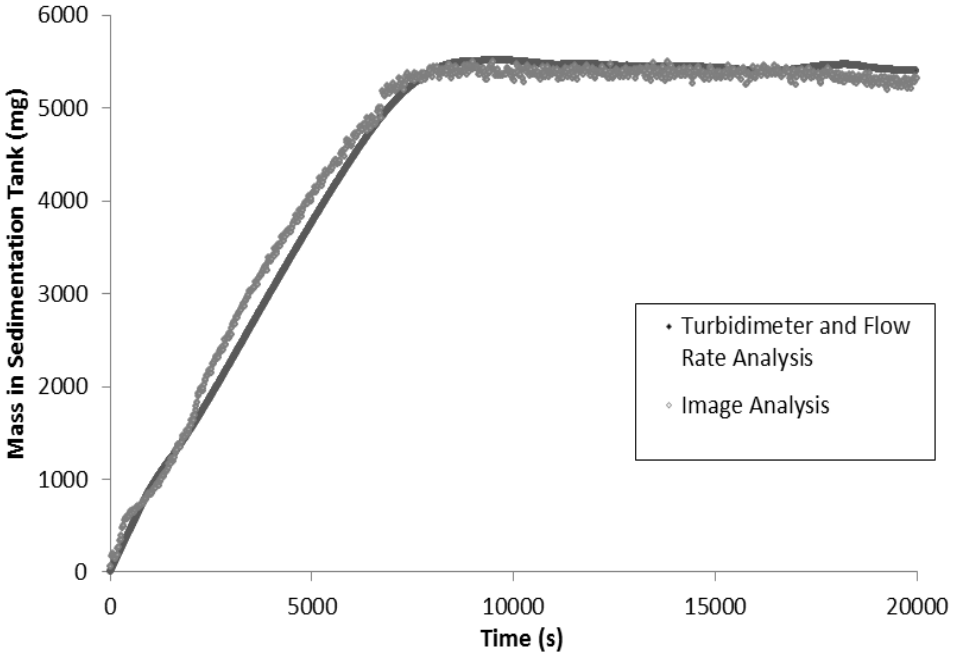

Figure 3–6. Mass accumulation in the reactor from: (1) turbidity analysis and (2) image analysis for an alum dose of 45 mg/L and influent turbidity of 100 NTU.

Observations from Image Analysis

The suspended solids concentration in a representative area within the fluidized bed (Figure 3-7A) is shown in Figure 3-7B for a blanket formed to a height of 68 cm under conditions of 45 mg/L alum (4.1 mg/L as Al) coagulant dose and 100 NTU influent turbidity. The area of image interrogation to assess floc blanket concentration was 12.9 cm X 16.2 cm (corresponding to a width of 98 pixels X height of 123 pixels) and was centered 10 cm from the right edge and 25.25 cm from the bottom of the jet reverser (Figure 3-7A).

Evolution of floc blanket height over time is shown in Figure 3-7D. Floc blanket height was determined by locating the position of the floc-water interface for each image. The zero point between the greatest difference in positive and negative values of the second derivative of solids concentration with respect to height was used to determine the position of the floc-water interface as described by Hurst *et al*. (2013). The area of interrogation to assess floc blanket height was 9.4 cm X 71 cm (corresponding to a width of 65 pixels X height of 492 pixels) and was centered 9 cm from the right edge and 51.25 cm from the bottom of the jet reverser (Figure 3-7C).

Three distinct stages in the formation of a floc blanket were observed: (1) thickening (increasing suspended solids concentration) in the absence of an observable floc-water interface, (2) thickening with an interface, and (3) steady-state. The division of floc blanket formation into these stages was based upon significant changes observed in either floc blanket concentration or height. The sequential process for floc blanket formation for a blanket created from 100 NTU influent with an alum dose of 45 mg/L is described below.

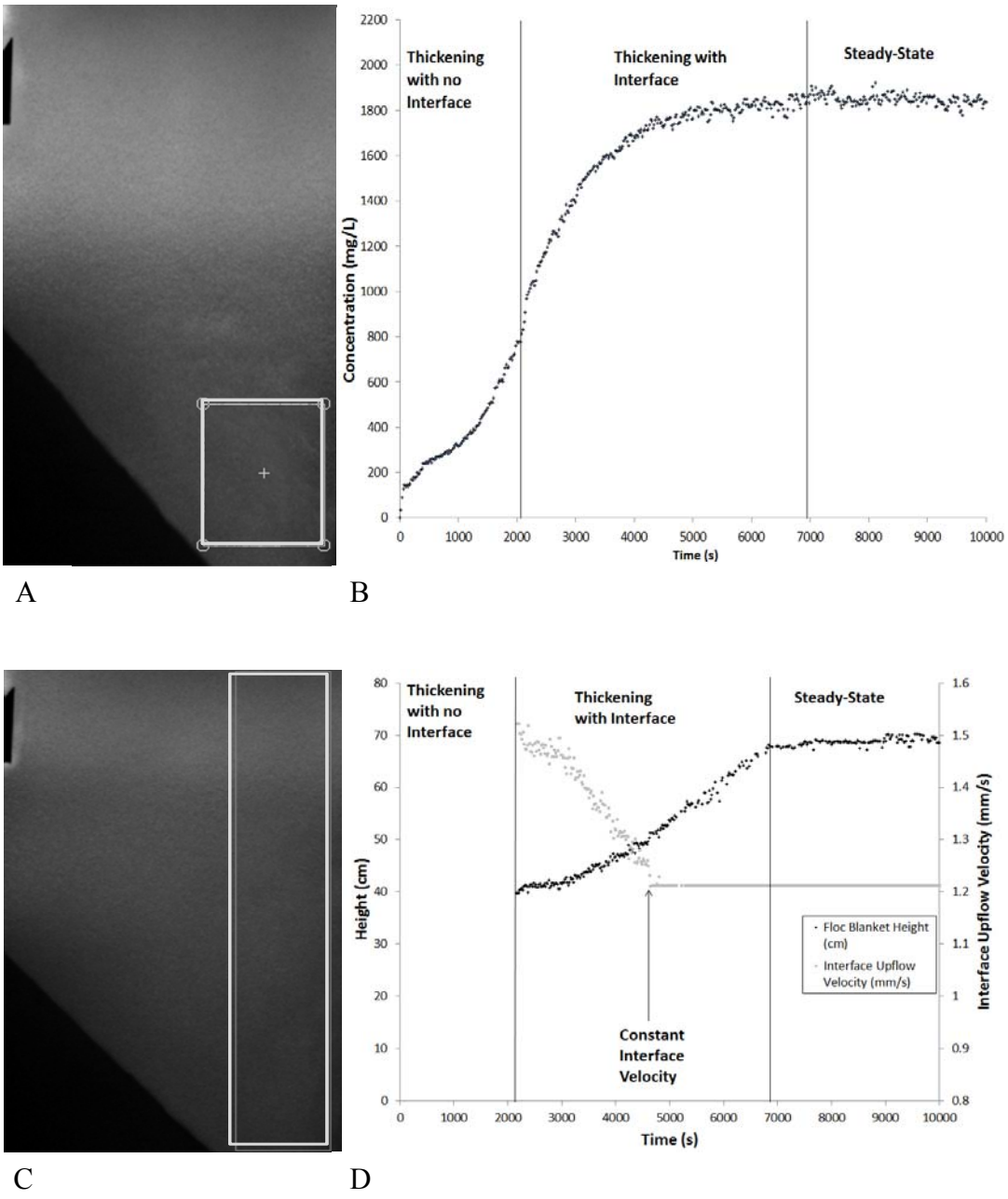

Figure 3–7. A. Area of interrogation for the concentration analysis. B. The time varying suspended solids concentration in the imaged area indicated in A for the floc blanket formed at an upflow velocity of 1.2 mm/s, alum coagulant dose of 45 mg/L, and 100 NTU influent. C. Area of interrogation for the floc blanket height analysis. D. Floc blanket height over time for the corresponding concentration in B.

Initially (from 0-2160 s), flocculated particles entered the reactor and formed a dilute particle suspension without a distinct floc-water interface (Figure 3-7A). The concentration of the dilute suspension increased over time as a result of: (1) continued influent loading of solids into the reactor, (2) retention of solids that settled at a velocity greater than the upflow velocity, (3) resuspension of settled solids by the influent jet, and (4) return of captured solids from the tube settlers. The average particle size of the dilute suspension was not quantified but visual observation indicated it was increasing over time before a distinct floc-water interface formed. An increase in particle size may be a result of particle-particle interactions in the sedimentation tank reactor and return of solids from lamellar sedimentation.

Due to the fractal nature of flocs, as floc size increases the floc density decreases (Weber-Shirk & Lion, 2010). The terminal settling velocity (V_t) of a floc as a function of their size, density, and fractal dimension is given by Weber-Shirk & Lion (2010) and is shown in equation 3-9. Although larger flocs are less dense they settle more rapidly because of their increased size as long as their fractal dimension is greater than 1.

$$V_t = \frac{g d_0^{(3-D_{Fractal})} d^{(D_{Fractal}-1)}}{18\Phi\nu}\left(\frac{\rho_{Floc_0}}{\rho_{H_2O}} - 1\right) \qquad (3\text{-}9)$$

Where: d_0 (= 1 μm) is the size of a primary clay particle, d is the floc size, $D_{Fractal}$ is the fractal dimension of the floc, ν (= 10^{-6} m^2/s)is the kinematic viscosity, Φ (= 24/45) is the shape factor of the floc, ρ_{Floc_0} (= 2.62 kg/m^3) is the initial density of the floc, and ρ_{H_2O} is the density of water.

At 2160 seconds, a significant decrease in suspended solids concentration was detected at heights above 39 cm indicating the presence of a floc blanket (Figure 3-7D). The existence of low and high solids concentration zones requires two distinct modes of settling: (1) a hindered sedimentation settling zone in the blanket and (2) a zone of settling in the supernatant that is either flocculent or discrete. The floc volume fraction, i.e., the fraction of the reactor volume occupied by flocs, in the floc blanket, is high enough such that the interstitial water velocity between flocs is greater than the interface upflow velocity, and therefore, the terminal settling velocity of an individual floc is significantly greater than the average upflow velocity. Flocs with high sedimentation velocities settle to the bottom of the floc blanket, slide down the incline and are resuspended by the incoming jet of flocculated water. Flocs with low sedimentation velocities are carried upward into the transition region between the floc blanket and the supernatant.

In the supernatant (low solids concentration) region, the floc solids concentration is significantly lower than the concentration in the blanket (i.e., an order of magnitude less than the concentration in the blanket), and thus the vertical velocity between flocs approaches the flow rate divided by the plan view area of the reactor. Flocs with sedimentation velocities greater than the upflow velocity settle back to the floc blanket and flocs with low sedimentation velocities are carried into the tube settlers. Results reported in this paper for analysis of floc blanket height begin once a distinguishable floc-water interface was detected (Figure 3-7C and Figure 3-7D).

Thickening is defined here as the process by which aggregate floc blanket solids

concentration increases after a blanket has been formed. Thickening of the experimental floc blanket occurred over the time interval from 2160 – 6800 seconds (Figure 3-7B). For the blanket formed at an alum dose of 45 mg/L, the majority of thickening occurred in conjunction with decreasing floc-water interface velocity. The floc-water interface velocity decreased because the cross sectional area of the reactor increased with increasing floc blanket height. However, some thickening also occurred at constant interface velocity (position shown in Figure 3-2A).

Once the floc blanket reached the reactor wasting tube, mass conservation requires a rate of mass accumulation equal zero to maintain a steady-state floc blanket. Steady-state was defined to exist for a blanket that had a relatively constant height and solids concentration (±5%). After thickening and with the blanket at the same elevation as the wasting tube, the experimental floc blanket solids concentration reached steady-state (time interval 6800 – 10000 s in Figure 3-7B). The floc blanket formed with 45 mg/L alum dose had a steady-state concentration of 1870 mg/L ±1.7% and a height of 68 cm ±1.0% (Figure 3-7B and Figure 3-7D).

A floc blanket was also formed at an alum dose of 25 mg/L and 100 NTU influent turbidity (Figure 8A and 8B) to evaluate the effect of alum dose compared to 45 mg/L.

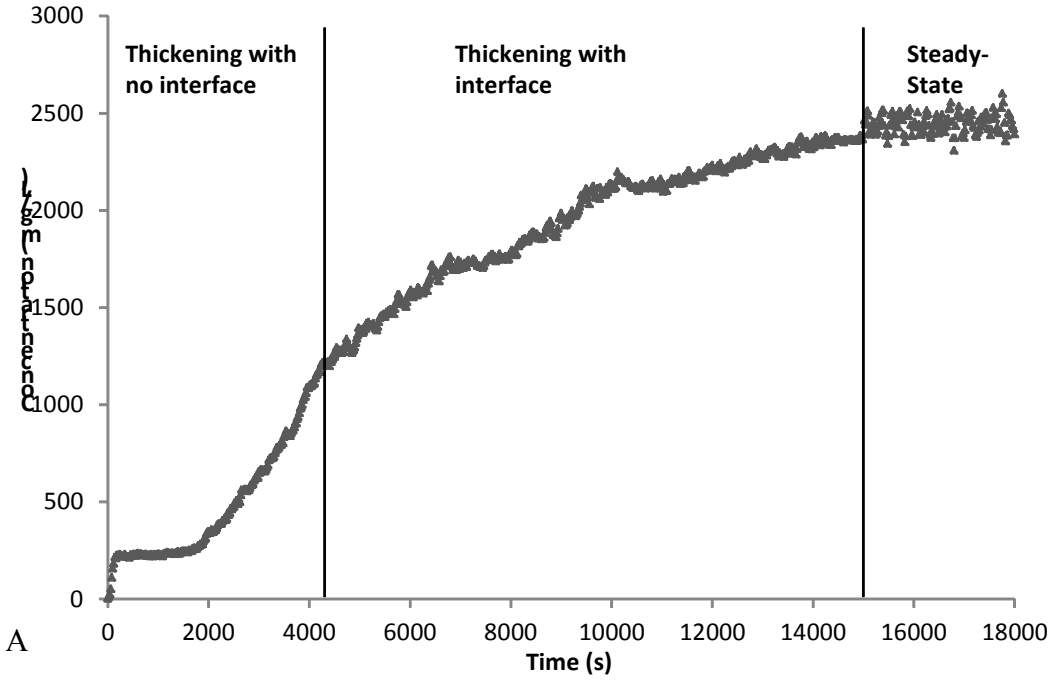

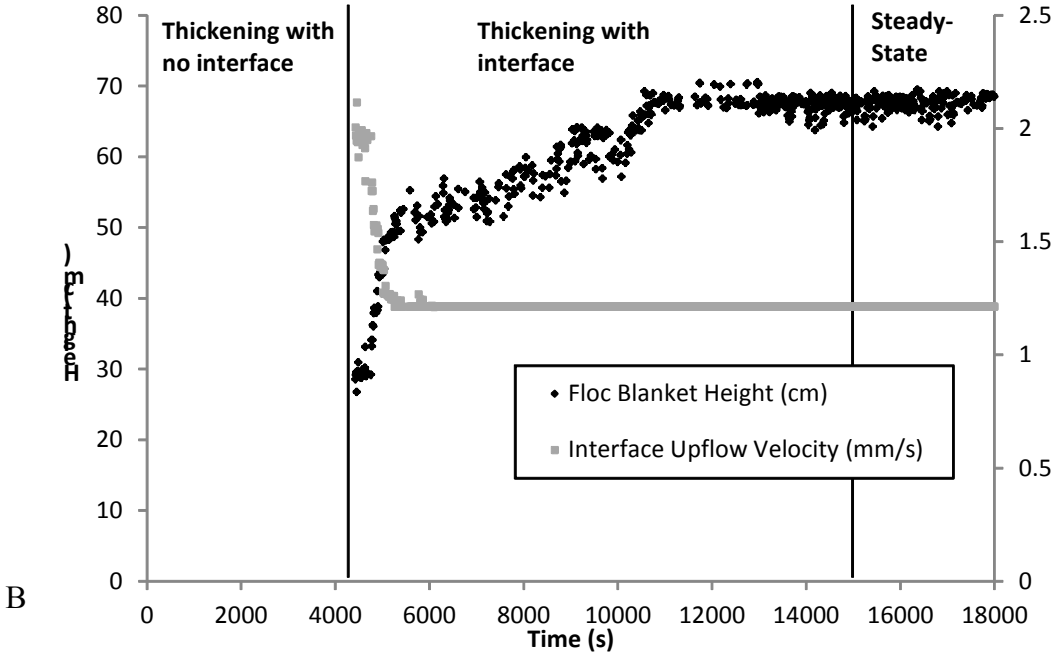

Figure 3–8. A. The concentration profile over time for the floc blanket formed under an upflow velocity of 1.2 mm/s, alum coagulant dose of 25 mg/L and 100 NTU influent. B. The floc blanket height over time for the corresponding floc blanket.

At the lower coagulant dose, significant thickening continued after the floc blanket was higher than the inclined section of the reactor. Thus, thickening occurred while interface velocity remained constant. These results in combination with those obtained for the 45 mg/L alum dose demonstrate that thickening can occur during either constant or changing floc blanket interface velocity. A change in floc blanket concentration at a constant interface upflow velocity is postulated to be the result of a change in floc size and/or density.

An additional image analysis was performed to account for the changing mass rate of accumulation in the blanket during blanket thickening. The mass rate of accumulation in the floc blanket is 1.4 mg/s when the blanket is thickening between 5800 – 6800 seconds. The mass rate of accumulation of the blanket during this time period cannot be fully accounted for by the influent stream which is contributing 0.924 mg/s [(7.7 mL/s)(100 NTU)(1.2 mg/(L NTU)]. Thus, a portion of the mass accumulating in the floc blanket is from mass in the supernatant returning to the blanket which includes solids captured and returned by the tube settlers. On average, the tube settlers return ~15% (0.151 mg/s) of the influent stream representing a significant contribution.

Mass balances can be made for suspended solids in: (1) the floc blanket and (2) the supernatant above the floc-water interface. Image analysis enables high resolution spatial and temporal mass analysis in these two regions (Figures 3-9A and 3-9B). The mass in the floc blanket can be determined as the product of floc blanket concentration and volume (converted from blanket height and corresponding cross-sectional area).

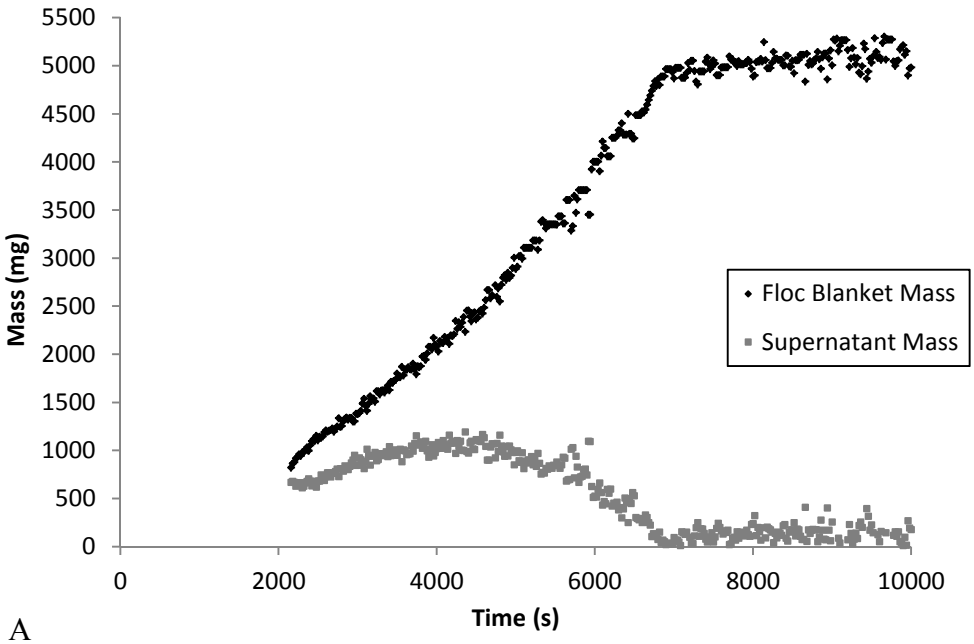

A

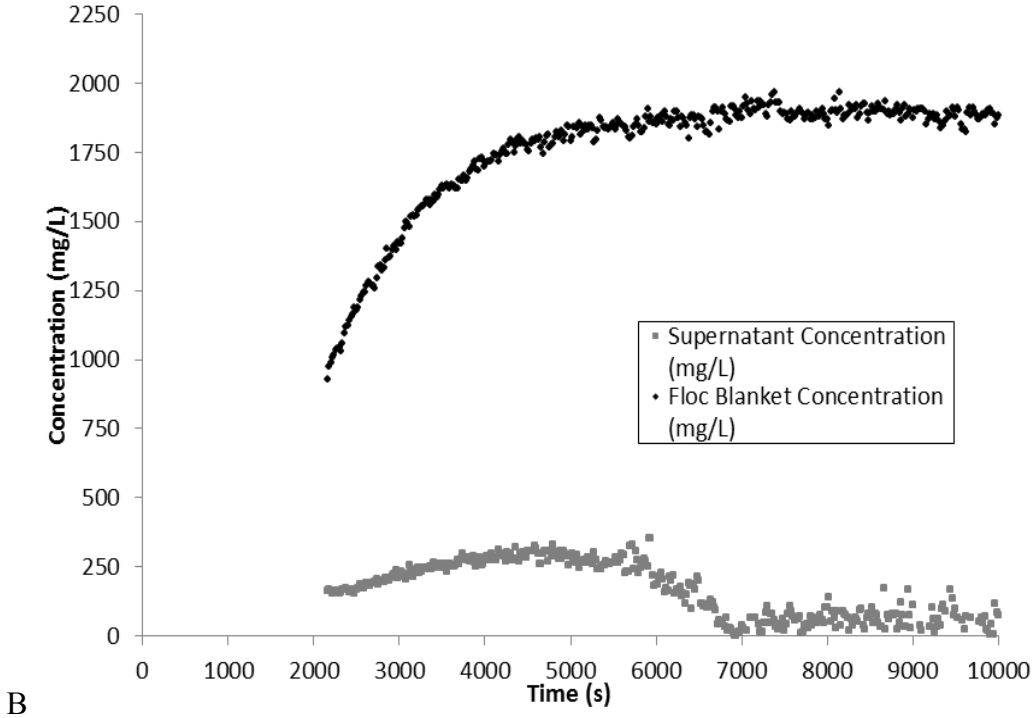

B

Figure 3–9. A. Total mass in the floc blanket and the total mass in the supernatant volume above the floc-water interface. B. Floc blanket and supernatant suspended solids concentrations.

The mass in the supernatant can be calculated as the average concentration in the supernatant multiplied by the volume. Figure 3-9 shows the total mass in the floc blanket and the total mass in the supernatant above the floc-water interface as well as floc blanket and supernatant concentrations (from image analysis) for the floc blanket with an alum dose of 45 mg/L.

The supernatant will contain flocs with: (1) sedimentation velocities lower than the interface upflow velocity and (2) flocs with sedimentation velocities higher than the interface velocity that have escaped from the floc blanket due to turbulence and will return to it by settling. Flocs with high settling velocity may also originate from the material captured in the tube settlers. In addition, it is anticipated that some flocs with lower settling velocities than the interface upflow velocity will aggregate with other flocs in the supernatant and then return to the blanket.

A significant portion of the suspended solids mass (between 40-25% of the total) resided in the supernatant between 2160-4000 seconds, and it is apparent that a significant portion of the supernatant solids were returned to the blanket between 5800 – 6800 seconds (Figure 3-9B). Therefore, the measurement of blanket concentration above the floc-water interface was an important component of mass balance analysis during blanket formation.

When the floc-water interface was first detected, concentration in the floc blanket was 1000 mg/L while the supernatant concentration was 250 mg/L. However, as the blanket grew in height and thickened, the supernatant concentration decreased (Figure 3-9B).

The interstitial water velocity is a function of floc volume fraction (the fraction of the total volume occupied by flocs) and the interface upflow velocity immediately above the floc-water interface. Initially, the blanket solids concentration was dilute (Figure 3-9B), and close to the solids concentration in the supernatant. In turn, the terminal sedimentation velocities of particles in the floc blanket were likely to be closer to the upflow velocity above the floc-water interface. As a result, a larger portion of floc particles that transitioned to the supernatant stayed in the supernatant. As the blanket thickened between 2160 to 6800 seconds, the interstitial water velocity increased (and, ultimately, the terminal sedimentation velocity of flocs in the blanket increased). While the blanket thickened, more particles in the blanket had sedimentation velocities higher than the interface velocity and more particles entering the supernatant from the floc blanket would be likely to return to the blanket.

Image analysis results of supernatant suspended solids concentration at a time of 2300 seconds for the blanket formed at 45 mg/L are shown in Figures 3-10A, 3-10B, and 3-10C. Figure 3-10A shows a suspended solids concentration profile. The region of interest for concentration analysis was positioned immediately above the floc-water interface (Figure 3-10B). The average concentration above the floc-water interface declines from 500 mg/L to 220 mg/L between 0-10 cm above the floc-water interface (Figure 3-10C). Although, the floc-water interface has been treated in the literature as a discontinuous transition in solids concentration (Sung *et al*., 2005), the results in Figure 10C show that the transition between floc blanket and supernatant is a gradient. As a result, solids concentration in the blanket near the floc-water interface is more dilute than the blanket concentration as a whole, and the

supernatant solids concentration above the floc-water interface (~10 cm) is greater than the supernatant as a whole.

The image analysis also shows that as the blanket suspended solids concentration increased, the concentration in the supernatant decreased and the concentration gradient at the floc water interface became sharper. The sedimentation velocity of flocs in blankets with a higher solids concentration and a higher floc volume fraction must be significantly higher than the sedimentation velocity of flocs in blankets with lower floc volume fraction given the same interface upflow velocity. Thus, floc blankets with higher solids concentration than the supernatant (as observed in Figure 9) contain flocs with higher sedimentation velocities than the interface velocity. When flocs with higher terminal sedimentation velocity are carried upward into the supernatant by turbulence, they will readily settle back to the floc blanket

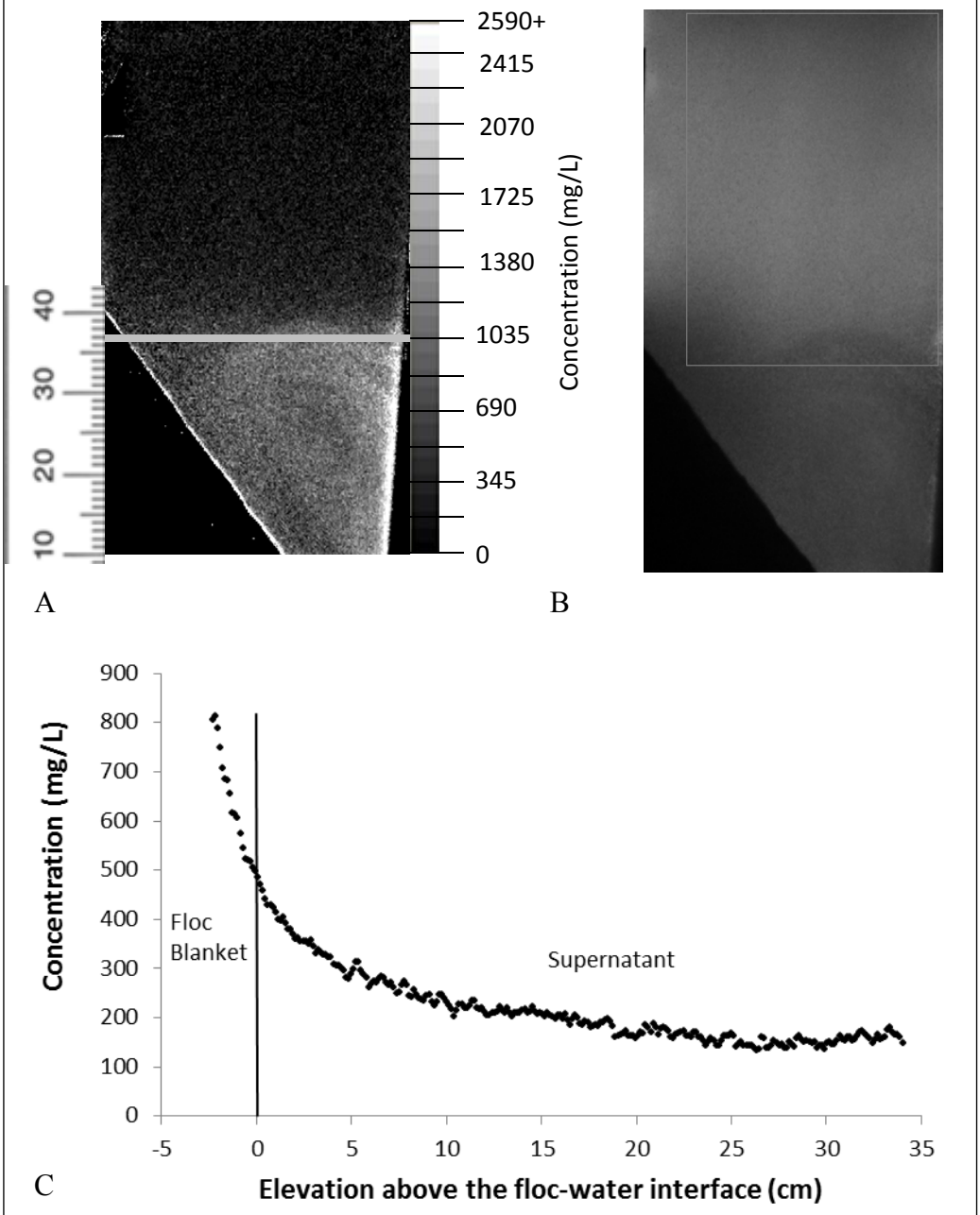

Figure 3–10. Suspended solids concentration profile for the floc blanket formed at a 45 mg/L alum dose at 2300 seconds. B. Region of interest of supernatant that was analyzed. C. Concentration profile of the supernatant above the floc-water interface.

Conclusions

There are several new insights with respect to floc blanket dynamics provided in this paper:

- Image analysis has revealed three stages of floc blanket formation: thickening (increasing suspended solids concentration) in the absence of an observable floc-water interface, thickening with an interface, and steady-state.

- Floc blanket thickening during blanket formation has been confirmed to occur at both variable and constant interface upflow velocity. This suggests that floc properties change during floc blanket formation.

- Preliminary floc blanket performance (Figure 3-4), concentration (Figure 3-7B), and height (Figure 3-7D) data from an alum dosing of 45 mg/L and influent turbidity of 100 NTU suggest that solids concentration has a more direct relation to turbidity removal than does blanket height.

- Continuously sampled turbidity measurements validate image analysis as an experimental method for measuring real-time solids concentration in a floc blanket.

- Mass transfer of suspended solids from the floc blanket supernatant to the floc blanket may be an important consideration for blanket formation dynamics. As blanket solids concentration increases, floc volume fraction in the floc blanket increases and the supernatant concentration decreases. Floc blankets with higher solids concentration than the supernatant (as observed in Figure 3-9) contain flocs with higher sedimentation velocities than the interface velocity. When flocs with greater sedimentation velocities than the interface

velocity are carried upward into the supernatant by turbulence, they will readily settle back to the floc blanket.

References

AWWA/ASCE (1990). *Water Treatment Plant Design*. McGraw-Hill, New York.

Baldyga, J., Bourne, J.R., and Gholap, R.V. (1995). The Influence of Viscosity on Mixing in Jet Reactors. *Chemical Engineering Science.* **50**(12), 1877-1880.

Chen, L., Lee, D.-J., and Chou, S.-S. (2006). Charge reversal effect on blanket in full-scale floc blanket clarifier. *J. Env. Eng. ASCE.* **132**(11), 1523-1526.

Chen, L., Sung, S., Lin, W., Lee, D.-J., Huang, C., Juang, R., *et al*. (2002). Observations of blanket characteristics in full-scale floc blanket clarifiers. *Water Sci. and Tech.* **47**(1), 197-204.

City of Ithaca. (2011). *Drinking Water Quality Report.* City of Ithaca: Ithaca, NY.

Gould, B. (1969). Sediment Distribution in Upflow. *Australian Civ. Eng.* **10**(9), 27-29.

Gregory, R. (1979). *Floc Blanket Clarification*. Water Research Centre TR 111, Swindon, U.K.

Hurst, M.W., Weber-Shirk, M.L., and Lion, L.W. (2010). Parameters affecting steady-state floc blanket performance. *J. of Water Supply Res. Technol. Aqua.* **59**(5), 312-323.

Hurst, M.W., Weber-Shirk, M.L., Charles, P., and Lion, L.W. (2013). An Apparatus for Observation and Analysis of Floc Blanket Formation and Performance. Submitted: *J. Env. Eng. ASCE.*

Kelly, M. L (ed). (1998). *Optimizing Water Treatment Plant Performance Using the Composite Correction Program Handbook*. USEPA, Cincinnati, Ohio.

Lin, W., Sung, S., Chen, L., Chung, H., Wang, C., Wu, R., *et al*. (2004). Treating high-turbidity water using full-scale floc blanket clarifiers. *J. Env. Eng. ASCE.* **130**(12), 1481-1487.

Miller, D.G., and West, J.T. Pilot Plant Studies of Floc Blanket Clarification. (1968). *AWWA Journ.* **60**(2), 154-164.

Mohammadi, M.S. (2002). A Generalized Refractive Index Equation for Estimating the Average Particle Size in Colloidal Suspensions. *J. Dispersion Sci. and Tech.* **23**(5), 689-697.

Schulz, C. R., and Okun, D. A. (1984). *Surface Water Treatment for Communities in Developing Countries.* John Wiley and Sons, New York.

Su, S., Wu, R., and Lee, D. (2004). Blanket dynamics in upflow suspended bed. *Water Res.* **38**(1), 89-96.

Sung, S., Lin, W., Chen, L., and Lee, J. (2003). Spatially Stability of Floc Blanket in Full-Scale Blanket Clarifiers . *J Chinese Inst. Chem. Eng.* **34**(6), 447-456.

Sung, S., Lee, J., and Wu, R. (2005). Steady-state Solid Flux Plot of Blanket in Upflow Suspended Bed. *J Chinese Inst. Chem. Eng.* **36**(4), 385-391.

Tchobanoglous, G., Burton, F. L., and Stensel, D. H. (2003). *Wastewater Engineering Treatment and Reuse.* McGraw-Hill, New York.

Tse, I.C., Swetland, K., Weber-Shirk, M.L., and Lion, L.W. (2011) Fluid shear influences on the performance of hydraulic flocculation systems. *Water Res.* **45**(17), 5412-5418.

Weber-Shirk, M. L. (2008). *An Automated Method for Testing Process Parameters.* Retrieved April 5, 2009, from AguaClara Wiki: http://confluence.cornell.edu/display/AGUACLARA/Process+Controller+Background

Weber-Shirk, M. L., Lion, L. W. (2010). Flocculation model and collision potential for reactors with flows characterized by high Peclet numbers. *Water Res.* **44**(18), 5180-518

CHAPTER 4: HANDS OR WATER? SOURCES OF CONTAMINATION: A FIELD STUDY IN AGEW GIMJABET, A TOWN IN THE ETHIOPAN HIGHLANDS [1]

[1] The contents of this chapter have been submitted to *Journal of Water and Health* for publication with co-authors: M. Moges, Prof. C. B. Barrett, Prof. T. Steenhius, Prof. G. Holst-Warhaft, Dr. M. Weber-Shirk and Prof. L. Lion.

Hands or Water? Sources of Contamination: A Field Study in Agew Gimjabet, a Town in the Ethiopian Highlands

Matthew W. Hurst*, Mamaru Moges, Christopher B. Barrett, Tammo Steenhuis, Gail Holst-Warhaft, Monroe Weber-Shirk, and Leonard W. Lion

Cornell University

School of Civil and Environmental Engineering

Hollister Hall

Ithaca, NY 14853-3501

Phone: (607) 216-8445

* Corresponding author

Email: mwh65@cornell.edu

Hands or Water? Sources of Contamination: A Field Study in Agew Gimjabet, a Town in the Ethiopian Highlands

Abstract

A household survey and water quality study was conducted in a town in the Ethiopian highlands that experienced an outbreak of AWD (acute watery diarrhea) in 2008. A multivariate regression model related to self-reported incidence of diarrhea created from household survey responses revealed that incidence was related to sanitary disposal of children's feces under five, and to a hand washing station located near to the latrine. Risk factors varied by socio-economic status, in part, because hygiene behaviors were associated with socio-economic status. Analysis of water contamination via fecal coliform counting indicated household water contamination was significant and likely related to hand contact with water. Analysis of hand rinsing data indicated higher reduction in microbial contamination when soap is utilized during hand washing. Results suggest future interventions which emphasize improving household water quality by increasing the number of people who wash their hands with soap will reduce waterborne disease incidence.

Keywords: waterborne illness, diarrheal disease incidence, outbreak, hand washing, sanitation, hygiene, risk factors

Introduction

Unsafe water, hygiene, and sanitation are associated with the spread of waterborne and foodborne illness. According to the WHO (2004), two million people perish each year due to unsafe water, poor hygiene and inadequate sanitation. The cause of poor sanitation, hygiene and water is ranked eleventh of the most preventable mortalities worldwide and principally impacts low income peoples (WHO, 2004).

In this study, we focus on diarrheal diseases. Diarrheal illness remains one of the most prevalent health problems in developing countries and the cause of approximately 1.6 million deaths worldwide (WHO, 2008). Quantified in total Disability Adjusted Life Years (DALY), diarrheal disease accounts for up to 6.4% of the total disease burden in Sub-Saharan Africa (Lopez, 2006).

Diarrhea is infection of the intestinal tract that can be caused by a variety of pathogenic organisms (i.e., viruses, bacteria, or protozoa). Unsafe water containing pathogenic organisms is the result of contamination of fecal matter (WHO, 2008). Transmission of pathogenic organisms occurs through a fecal-oral transmission pathway.

The fecal-oral transmission of waterborne disease makes prevention complex as there are many potential exposure pathways. Prevention of waterborne (i.e., direct transmission of disease when water containing pathogenic organisms is consumed) and water-washed (i.e., transfer of pathogens to otherwise safe water due to poor personal hygiene) diseases ultimately requires a multi-disciplinary approach to address multiple exposure factors (Figure

4-1). These exposure factors can be categorized in terms of hygiene practices (i.e., hand washing and food washing), fecal contamination, food contamination, water source quality, and water handling practices in the household (Eisenberg *et al*., 2007).

While access to safe water is reported to be more cost-effective than vaccination efforts in reducing diarrheal disease (Montgomery & Elimelech, 2007), the water-washed route of transmission presents significant and confounding exposure pathways which can compromise an otherwise safe water source. Infection can occur through incidental ingestion of pathogens through the course of other daily activities such as food consumption (Kremer & Peterson-Zwane, 2010). Poor water quality could significantly impact exposure along with sanitary conditions of fingers, transfer or drinking vessels, and potential vectors of transmission (i.e., flies) (Figure 4-1). One area of further exploration is to understand the routes by which water becomes contaminated, and how this can be prevented in the future.

Figure 4-1 explicitly draws fecal-oral transmission pathways that relate sanitary conditions and hygiene practices to health outcome. Sanitary conditions include fingers, fomites, water source, and flies. These sanitary conditions are impacted by hygiene practices such as handling and treatment household water, and food preparation. Finally, the health status is impacted by the user behavior and the sanitary conditions. For example, an uncontaminated water source can become contaminated through poor hygiene practices such as placing contaminated fingers into the water.

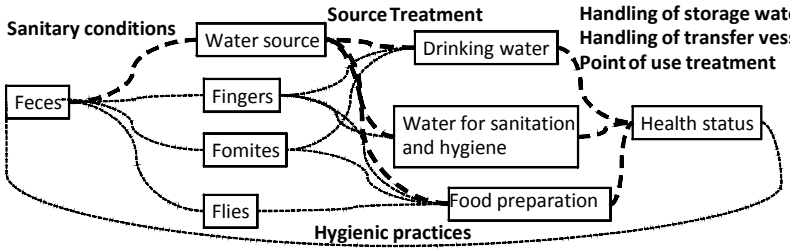

Figure 4–1. Linkages of sanitary conditions, unsafe water, and hygiene practices as exposure factors for communities (adapted and modified from: Waddington & Snilstveit, 2009). **Bold lines indicate where contamination of water can act as potential exposure factor for diarrheal illness.**

One important mechanism for water contamination is via hand contact with the household water supply (Jensen *et al*., 2002; Lindskog & Lindskog, 1988). Hand washing is reported to reduce ~~self-reported~~ diarrheal disease incidence by up to 48 percent (Cairncross *et al*., 2010). Hand washing with soap works by interrupting and preventing the transmission of fecal matter in the environment, and is considered one of the most effective interventions when and if behavioral change is achieved (Luby *et al*., 2005).

Hand washing is effective at critical times such as before or after eating, preparing food, or after defecation (Waddington & Snilstveit, 2009; Luby *et al*., 2011). It is not clear the impact that hand washing has on specific transmission routes of disease or where it is more effective in preventing transmission (i.e., preventing foodborne pathogen spread, or preventing waterborne disease).

The ultimate goal of future interventions either through building WASH infrastructure or behavioral change at the household level is to reduce pathogen loading to each household member. Reducing pathogen loading should improve household health by decreasing the number of sick days each member experiences. Effective preventative interventions identified in this study were reported to households and town officials. The objective of this study was to identify how water became contaminated and factors which influence the spread of diarrheal disease in a town in Ethiopia's Amhara highlands. This was assessed through direct observation of household practices with follow-up through water quality testing, focus groups, and household survey instruments.

Materials and Methods

The area selected for this study was the town of Agew Gimjabet. Agew Gimjabet has a population of approximately 14,000 people (2,800 households) located in the western part of the Amhara region in Ethiopia. Agew Gimjabet has a history of waterborne disease incidence. Local officials desire to learn beneficial intervention strategies that could reduce disease burden. The most recent health reports obtained from the Woreda (administrative division of Ethiopia) health office as of 2008 indicated that there were 33 cases of acute watery diarrhea (AWD) brought into the hospital that year. It is likely that there were additional unreported cases either of: (1) AWD or (2) less acute diarrhea.

First, household observations were conducted to identify key sanitary conditions or hygienic behaviors for focus in prevention of waterborne disease. Based upon these observations, household interviews and water quality sampling were performed to identify sources of

disease transmission. Finally, hand washing samples were carried out to confirm contamination of household water sources through hand contact.

Household Observations

Household observations were informally conducted from February 15 through March 12, 2012, between the hours of 9 AM and 2 PM. The purpose of these observations was to identify key mechanisms of transmission of diarrheal disease.

Water Quality Assessment

Turbidity was measured in-situ or within 6 hours of sampling with a Hach Portable Turbidimeter (2100P) (Hach Company, USA) and is expressed in this paper as NTU (Nephelometric Turbidity Units). The pH of water samples was determined by pH strip. Water quality parameters such as hardness and residual chlorine were measured using chemical test kits purchased from Wagtech (Wagtech, Ethiopia) and were analyzed within 6 hours of sampling. The appropriate test kit procedures for each parameter of interest were followed and a Wagtech Spectrophotometer 5000 was employed for colorimetric analysis. Transmittance readings were compared to a calibration curve using standards for each parameter within the range of linear instrumental response. The concentration results were compared to the anticipated concentration readings producing a maximum standard error in concentration readings of 10%.

Enumeration of presumptive fecal coliform was performed by a membrane filter method using membrane lauryl sulfate broth as described by the British Environmental Agency (BEA, 2009) Water samples were incubated within 6 hours of sampling. A 100 mL sample

was filtered utilizing a vacuum filter pump on a 0.45 μm membrane filter paper. Dilution of the sample by distilled water by a factor of 1:10 and 1:100 was utilized for samples with turbidity above 5 NTU or samples suspected to be highly contaminated with fecal coliforms. The filter paper was placed on an absorbent pad in a petri dish that was saturated with 2 mL of membrane lauryl sulfate broth (producing a red color). The petri dish was labeled and sealed, and placed in an incubator set at 44°C (±0.5°C). After 18 hours of incubation, the sample was removed and the colony forming units (CFU) were enumerated using a colony counter. Presumptive E. *coli* CFUs were distinguished under 5-10x magnification unit as those with a yellowish color, indicating presence of anaerobic respiration typical of *E. coli* bacteria.

Household Interviews

Household interview questions covered seven topics: (1) socio-economic conditions, (2) water supply, (3) transport, handling and storage of water, (4) hand washing behavior, (5) latrine use, (6) other sanitation and hygiene behaviors, and (7) health. Questions for the survey were largely adapted from baseline health and sanitation surveys from (1) Health Environments for Children Survey Instrument (WHO/CEHA, 2008), (2) WHO/UNICEF Joint Monitoring Survey (WHO/UNICEF, 2004), and (3) Demographic and Health Survey (USAID, 2011). Additional questions were added after household observations took place. The interviews occurred in the interviewee's household and took approximately 45 minutes to complete. The 235 households in the survey were chosen by convenience in sampling and household availability. Sample size calculations (Equation 4-2) revealed a minimum of 93 households were required (Supplementary Information 1). Household interviews were

conducted by convenience sampling, and generally the female head of the household would report the information, but this was not the case in all samples. The participating household member was asked to assess diarrheal disease incidence in the past year to account for potential variation in disease incidence as a result of weather.

Water Use Assessment

Water use was estimated utilizing two methods: (1) from the average number of trips users would take to fill up transport vessels with water, and (2) by estimating daily demand self-reported from the household. Water use was measured for the following activities: drinking water, making local drinks, cleaning children, washing hands, preparing food, washing dishes, washing clothes, taking a bath/shower, and washing other household items. There were very few homestead gardens and livestock did not generally drink water from water gathered from transport vessels or from the tap so these items could be excluded from analysis.

People used transport vessels (i.e., clay pot or *jerikan* (plastic container)), transfer vessels (metal can for transfer from a clay pot or plastic jug), and drinking vessels (i.e., drinking glass) of well-known volumes: 0.5 L corresponded to a *taza* (metal can for transfer from a clay pot) or drinking glass, 4 L corresponded to a jug, and 10 or 20 L corresponded to a *jerikan* (plastic container) or clay pot. Fairly accurate volumes could be obtained using these volumetric estimates.

Hand Washing Sampling

The water source sample used for hand washing was first collected. Water was then poured over the respondent's hands and collected in a wash basin that had been sterilized with 70% denatured alcohol. Then the respondent washed their hands by their custom (with or without soap). Finally, rinse water was poured over the respondent's hands after hand washing. The rinse water sample was also collected in a wash basin that was previously sterilized with 70% denatured alcohol. All hand washing samples were collected in volumes of 500 mL and then analyzed for both turbidity and fecal coliform contamination (enumerated in number of coliforms per 500 mL sample).

Results and Discussion

Water Quality

Water quality was assessed on the basis of turbidity and fecal coliform count at the source and household level. Water quality at each source is summarized for the dry and wet season in Table 4-1. Residual chlorine was not detected in any of the samples taken and pH of all water samples varied between 6.5-7.0 pH units. The unprotected water quality source is more contaminated measured in both turbidity and fecal coliform count compared to the protected source for the *bono* and piped network. Contamination increased for the unprotected spring during the wet season by an average of 41% and 33% for fecal coliform count and turbidity, respectively (Table 4-1).

Table 4-1. Summary of chemical and biological water quality parameters for water sources

Source	Season	# samples	Hardness (mg/L as CaCO3)	*E. coli* CFU count (CFU/100 mL)	Turbidity (NTU)
Unprotected Spring	Dry	4	50±5	50±89	3.4±5.2
	Wet	10	Not measured	86±67	5.1±1.2
Bono	Dry	4	62±5	9±12	1.7±1.2
	Wet	6	Not Measured	21±11	2.6±0.6
Pipe	Dry	5	50±5	7±5	1.9±1.8
	Wet	8	Not Measured	15±8	2.2±1.4

The average CFU count per 100 mL at each stage of transport, collection, and consumption of water are shown in Figures 4-2A and 4-2B. The results compare household transfer vessel use of a clay pot (Figure 4-2A) compared to a *jerikan* (Figure 4-2B). Significant increases in overall contamination occur between source and transport; however, there is no significant difference in contamination noted between clay pot and *jerikan* users. Increase in contamination between source and household consumption is a common occurrence in systems that do not disinfect the water (Rufener *et al*. 2009).

Figures 4-2A and 4-2B illustrate that contamination increases as water is transferred in vessels in the household. The greatest increase in contamination for users of clay pot occurs between use of the clay pot and use of the *taza* (drawing out container). The large neck opening of clay pots enables users to dip a *taza* into the clay pot to withdraw water. Nevertheless, dipping a *taza* also facilitates hand-water contact and contamination.

Indeed, the use of a *taza* to draw water from clay pots is likely the first time that hands make direct contact with the water. In contrast, the greatest increase in contamination for *jerikan* users occurs between transfer from *jerikan* to glass. One possible explanation is that solids that have settled to the bottom of the *jerikan* become re-suspended when the *jerikan* is flipped over to be poured. These suspended solids could contain pathogenic materials. The method to withdraw water from the clay pot with a *taza* minimizes the possibility of re-suspension of solids, and therefore, it is reasonable to expect and seen from the results that the resulting contamination is less.

A focus of public health officials in this region has been to reduce household use of clay pots as transfer and storage vessels in favor of use of a *jerikan*. One study that compared narrow-neck clay pots to large clay pots found that contamination significantly decreased when narrow-neck pots were used due to less frequent hand contact (Jensen *et al*., 2002). However, in light of these results, it does not appear that switching over to a *jerikan* significantly reduces contamination, possibly as a result of re-suspension of solids as a result of the method for pouring water from the *jerikan*. Yet another behavior that could be corrected by health officials is the method by which glasses are cleaned. It was observed that that many glasses in the household could be contaminated through the method by which they are cleaned (rapidly wiping the inside of the glass by hand).

There is also an increase in contamination of fecal coliforms between the source and water transport vessels (i.e., clay pots and *jerikans*). Observation at water gathering sites indicated that *jerikans* and clay pots are almost always covered with plastic bags. The user will pull off

the plastic covering and then fill the transport vessel to the brim. After the transport vessel is filled, the plastic covering is placed back into the vessel. It is possible that the plastic bag is contaminated by some users' hands before the plastic bag makes contact with the water when it is placed back into the transfer vessel.

All users in Agew Gimjabet rely on the unprotected spring or previously stored household water when the water supply system has insufficient water pressure. In this case, an additional source of contamination results from users mixing different quality water sources in transport, transfer and storage vessels.

A small proportion of fecal coliform count readings for water in the drinking vessels exceeded 1000 CFU/100 mL. Such a count may seem extraordinary when one considers that in one particular case, this is a 100 fold increase in contamination from the source water that was measured at 10 CFU/100 mL. However, other studies have also found one to two order of magnitude increases (as well as high variability) in coliform counts between source and household (Lindskog & Lindskog, 1988; Wright *et al*., 2004). Household drinking water coliform counts in Eastern Africa have been previously recorded to be up to 1800 CFU/100 mL (McGuigan *et al*., 1996).

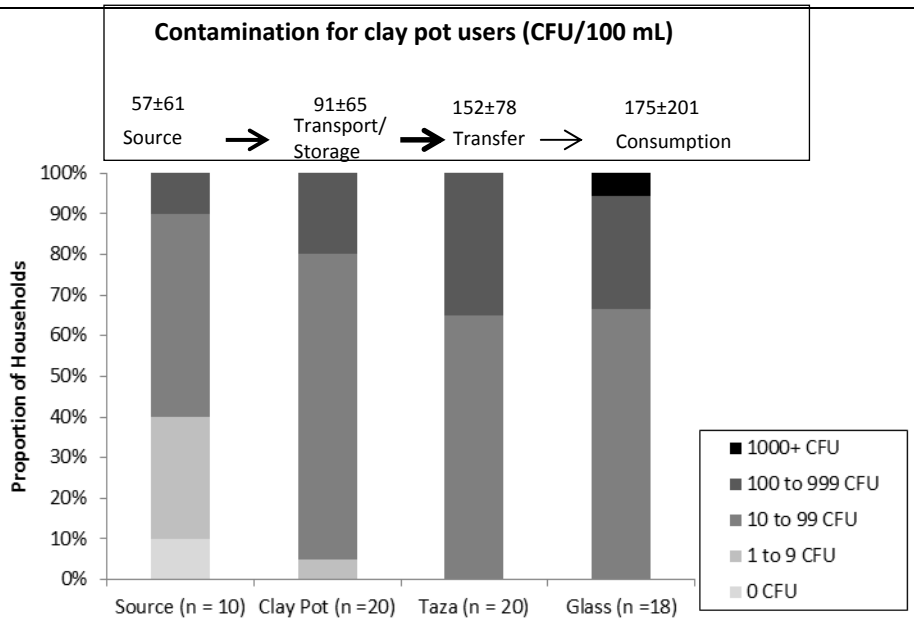

A

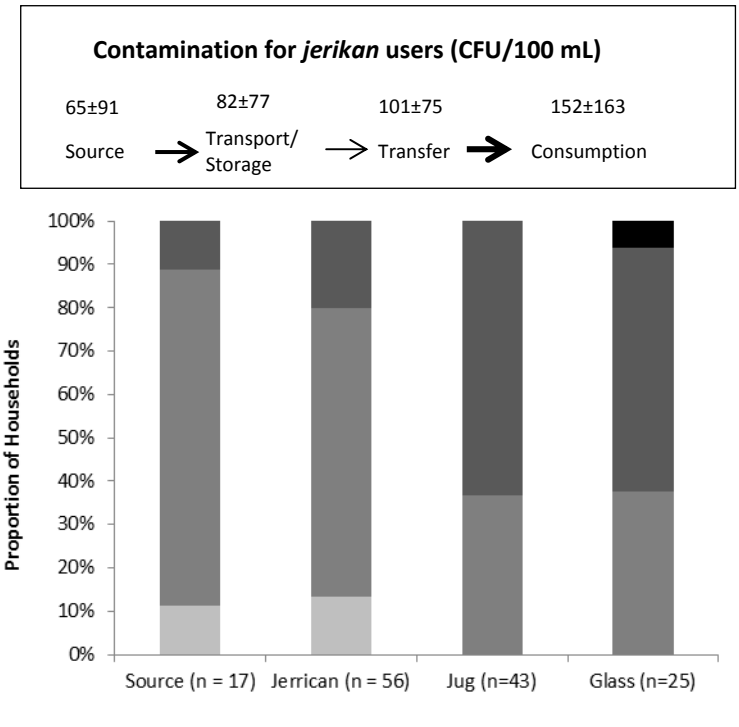

B

Figure 4–2. A. Results of *E. coli* CFUs for source, transport, storage, transfer and drinking vessels for clay pot users (15 households) for 100 mL samples. B. Results of *E. coli* CFUs for *jerikan* users (45 households) for 100 mL samples.

Socio-economic Status of Households

The socio-economic status of the households impacts the type of water source available, resources available in individual households that could be utilized to implement future WASH infrastructure, and the level of education which could impact the ability of households to modify behaviors. The links between water source and household wealth are fairly well established in literature. Dungamoro (2007) found that there was a significant association between: (1) obtaining water from a safe source and socio-economic conditions in a household including household income, type of job, and educational status of household head, and (2) household size and safety of source.

Wealth was assessed on an asset based wealth index created using principal component analysis (PCA) (described in Filmer & Pritcher, 2001; Sahn & Stifel, 2003; Booysen *et al*., 2008). In this method, wealth is represented by household assets rather than consumption expenditures or household income. While conventional measures of income such as household income work well in the developed world, consumption and expenditure data can be more difficult to collect accurately in less developed countries where many such flows are not monetized because of household self-provision with food, fuel, services, etc. Asset based wealth is simpler and less fraught with measurement error. Moreover, index based rankings generated from asset based data are strongly correlated with the index based rankings based upon household expenditures (Sahn & Stifel, 2003). Filmer & Pritcher (2001) also argue that the econometric evidence in the literature suggests that utilizing asset indexing as a proxy for economic status is at least as reliable as the more conventional expenditure measuring methods noted above.

The results of the principal component analysis are summarized in Table 4-4 (Supplementary Information 2). Wealth factors included in this analysis were: (1) status of dwelling, and (2) assets owned. Wealth was generally correlated with source water type with over 90% of the richest 20% having access to tap water.

Household Health

Factors Influencing Waterborne Disease Incidence

Utilizing the survey data collected at the household level, a bivariate analysis was conducted to compare significant risk factors that were observed to be linked to household diarrhea morbidity (Supplementary Information 3). We use the WHO definition for diarrhea: the passage of three or more loose or liquid stools per day. Household diarrheal morbidity is defined as self-reported diarrheal incidence from the interviewee in every identified member of the household during the past year. The significant factors (defined as an odds ratio of greater than 1.5) were included as input variables in the multivariate regression model. The dependent variable for the model was whether diarrheal disease had occurred at the household level over a period of one year.

The following bivariate relationships were significant: open defecation, using an unprotected water source, having a kitchen not separated from the main dwelling, utilizing an "unsafe" method to dispose of children's feces, storing water in a clay pot, and absence of a hand washing station by the latrine. These variables were defined using the descriptions provided in the WHO/UNICEF survey instrument (2004). For example, an unprotected water source

was defined as a water source that had no structure or equipment in place to avoid pollution of the source water by users, animals, or runoff. The results of the multiple logistic regression analysis are summarized in Supplementary Information 3 Table 4-7 and analysis of variance in Table 4-8.

When the multiple regression analysis results are compared to the bivariate analysis, several variables that were identified as significant in the bivariate analysis such as open defecation, using an unprotected water source, and utilizing clay pots exclusively for storage and transfer, were found to not be statistically significant (Table 4-7 in Supplementary Information 3). These variables were also related to each other and related to the socio-economic status of the household, so the variables may still be significant, but are difficult to disentangle. For example, a higher proportion of less well-off households were users of an unprotected spring, practiced open defecation, and had a kitchen that was not separated from the dwelling. In general, those less well-off had less WASH infrastructure and resources available compared to their richer counterparts.

Three multivariate models were created for the same risk factors and for the following socio-economic groups as rated by wealth index: (1) the bottom 40%, (2) the next 40%, and (3) the top 20%. The adjusted odds ratios are compared in Table 4-2 and the analysis of variance and model fit in Table 4-3. The adjusted odds ratio with a P-value less than 0.05 were considered statistically significant are in bold and italic type.

Table 4-2. Adjusted Odds Ratio Arranged by Wealth Index

Asset Index/Factor	All (n=235)	Top 20% (n =47)	Middle 40% (n= 95)	Bottom 40% (n= 94)
Proper Disposal for Child's Feces Under 5	***0.40***	***0.07***	1.05	***0.22***
Hand washing station located by the latrine	***0.57***	1.21	***0.21***	0.78
Using Unprotected Water Source	1.47	No users	1.88	1.02
Always Utilize Clay Pot for Water Storage	2.19	No users	5.97	0.82
Separate Room for Kitchen	0.71	0.41	0.87	1.22
Open Defecation	1.42	No users	***3.78***	***4.12***
Constant	1.31	9.17	1.23	0.37

Table 4-3. Analysis of Variance for Multivariate Linear Regression Model

Model	R^2	Adjusted R^2	Percentage of Correct Predictions	Mean square of regression	F-value
All	0.10	0.08	68%	1.239	4.193
Top 20%	0.32	0.22	88%	0.497	3.779
Middle 40%	0.23	0.11	76%	0.377	1.918
Bottom 40%	0.14	0.08	70%	0.361	1.423

Even the multivariate regression model for the highest wealth group, which best explained the variance in the data, could only account for 32% of the variance in the data. Nonetheless, the models created for highest and middle wealth groups better explained the data compared to the multivariate regression model that encompassed all wealth groups (which only explained 10% of the variability in the data). The multivariate model that accounted for the bottom 40% explained the variability in the data as well as the multivariate model for all wealth groups. Such results indicate that there were still key factors that were missed in this analysis that impact self-reported diarrheal disease occurrence in households.

The multivariate regression models did reveal that certain factors were more significant when associated with wealth group. Open defecation was associated with diarrheal occurrence for middle and lower wealth households, but was not a factor of consideration in the highest wealth households. Proper disposal of a child's feces under five was considered significant for both the top and bottom wealth groups, but was not significant for the middle wealth

group. The result for the middle wealth group is likely a false negative. It is likely that proper disposal is significant for middle wealth groups given that practices are very similar to lower and the highest wealth groups. Locating a hand washing station near to the latrine had the lowest adjusted odds ratio for the middle wealth group.

Only households in the middle and low wealth groups reported practicing open defecation. The adjusted odds ratio for open defecation is 3.78 for middle wealth and 4.12 for lower wealth, respectively. Open defecation adversely impacts household and community health. Open defecation is generally practiced after dark and occurs in common areas. Therefore, contamination from open defecation practiced in public locations is spread in the community environment. In this particular study, open defecation was practiced in the public market and during rain events the waste would wash down into the unprotected spring. When practiced within the confines of the homestead (i.e. whole farm area or backyard of a home), open defecation also can spread contamination to an individual household.

A latrine has several roles when properly functioning: (1) it provides a place to dispose of highly contaminated solids and liquids, (2) removes the possibility of future contact with these highly contaminated solids and liquids within the household, and (3) provides an environment for household members to privately perform necessary hygienic functions such as wiping and hand washing after use. Because of these roles, proper latrine use protects against some contamination in the household. Well-designed and maintained pour flush latrines will be superior to dry latrines because there will be little to no smell and the inside can be maintained to be more hygienic (EHP, 2003). However, pour flush latrines require 1-3

liters of water per flush (which is a significant consideration for an individual whose water consumption is 15 L/day), and can potentially be unhygienic when not well maintained. Flies and pests can become attracted to the pit storing the excrement when it is not properly covered. This implies that improperly maintained storage pits have the potential to become another exposure route for contamination (WHO, 2004).

The result for proper disposal of a child's feces was likely significant for all income groups even though the adjusted odds ratio was insignificant for the middle wealth group. Proper disposal techniques for children's feces (i.e., having the child use the latrine, throwing the waste into the latrine, or burying the feces) are critical in reducing exposure to pathogens compared to improper disposal techniques (i.e., not disposing of feces or leaving it on the ground, throwing feces outside or dwelling, or throwing feces outside of the homestead). Children are less likely to use WASH infrastructure and their feces generally has higher contaminant loading compared to adult feces (EHP, 2003). Proper disposal of children's feces (for households reporting having children) was the single most important factor (adjusted odds ratio of 0.40) for the top wealth group in reducing diarrheal disease occurrence. There was little difference in self-reported process of disposal with 69% of the highest wealth reporting proper disposal techniques compared with 60% for middle wealth and 62% for lower wealth. Pathways for contamination are complex and numerous. Reducing contamination through behavioral change or WASH infrastructure does not guarantee reduction in contamination if poor hygienic behavioral practices remain. Other hygienic practices (i.e., no open defecation) and WASH infrastructure (i.e., built latrine) were well-

established in the higher wealth group. Thus, it is possible that improper disposal was a practice that had more impact in contamination pathways in higher wealth households.

Locating a hand washing station by the latrine only had a significant adjusted odds ratio for the middle wealth group (Table 4-2). In the highest wealth group, a majority (69%) did not have hand washing stations located by the latrines, although 97% of households reported always having available soap. In the low wealth group, most (96%) did not have a hand washing station by the latrine and only 63% reported always having soap available. In the middle wealth group, a majority (82%) did not have hand washing stations located by the latrines and 78% reported having soap readily available. It is clear from these data that there is an association between soap availability and availability of more complex WASH structures for hand washing. Still, because the presence of a hand washing station is related to hand washing behavior and soap utilization, it is difficult to determine which of these factors is significantly responsible for reduction in diarrheal disease. Because utilizing soap in hand washing in the household provides an effective barrier to disease (Luby *et al*., 2009), it is possible that this association with diarrheal disease was actually related to utilization of soap in the household.

The following factors were not statistically significant in the multivariate regression model (Table 4-7 in Supplementary Information 3): using an unprotected water source, always using clay storage for transfer and storage of water, and having a separate room for the kitchen. This was surprising because based upon observational data, it was thought that these behaviors would be significant. For example, the unprotected water source had greater

contamination compared to the pipe and *bono* (public standpipe) sources (Table 4-7). Our regression results underscore, however, that contamination of water can also occur at the household level (and associated behaviors such as drawing out water using a *taza* or rinsing glasses via hands). The non-significance of always using a clay storage or transfer vessel likewise counters more casual observations that using a clay pot rather than a *jerikan* (10 or 20 L plastic storage vessel) requires the user to draw out water using a *taza* which facilitates hand contact with the water. Finally, we observed flies and other pests accumulate in the largest numbers in households' kitchens. When the kitchen is located in the household dwelling, flies and other pests can live in high concentrations in the household as well, potentially transmitting contaminants.

Hand Washing

The increase in water contamination from source to household in Agew Gimjabet, and the results from household surveys which indicate that significant factors of diarrheal disease included proper disposal of feces, open defecation, and having a hand washing station by the latrine both suggest that one source of contamination could be a result of hand contact with water. It was apparent to the researchers that hand washing could be a vital hygiene behavior to reduce water contamination in the household. Hands frequently make contact with water, food, and infants, and unclean hands can facilitate disease spread. Hand washing with soap was also identified as a potentially critical intervention step for public health after latrine use. Hands are almost exclusively utilized during food preparation and as eating utensils, thus, better hand washing practice could promote an effective barrier for spread of pathogens via food.

Consistent use of soap with hand washing can reduce the spread of waterborne disease (Luby *et al*., 2009). Soap availability was rated by households in the survey on a four point scale from "never available," "available less than three times a year or only on special occasions," "frequently available, but sometimes not present in the household," and "always available in the household." In this study, soap was reported to be available less than three times a year or only on special occasions or frequently available (grouped in Figure 4-3 as 'sometimes available') in 19% of households and always available in 67%. Soap availability was visually confirmed during visits of households reporting soap use. Availability of soap was related to the socio-economic status of the household (Figure 4-3). Wealthier households such as those that source water from a pipe were more likely to have the financial resources to always keep soap in the household. Cost was the most frequent reason (for 73% of these respondents) given for the absence of soap in households that reported not always having access to soap.

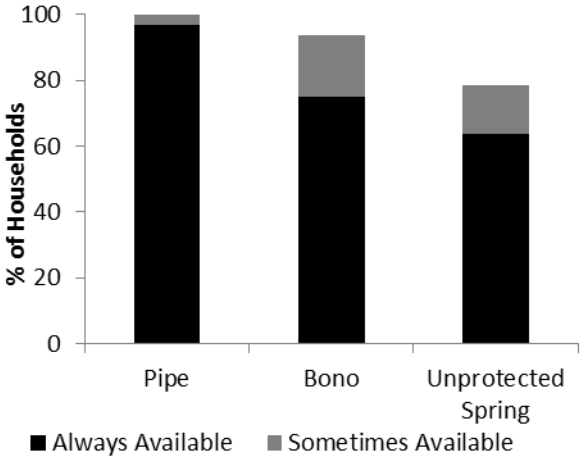

Figure 4–3. Self-reported availability of soap in households among different source users.

Availability of soap did not necessarily equate with use of soap for hand washing. Soap was viewed as a luxury item by some households that reported soap was always available. Instead of utilizing soap consistently to wash body and hands, soap was instead utilized in the following ways: (1) as a lotion after bathing and (2) for washing clothes. Soap was also predominantly used for hand washing after eating fatty foods which occurred frequently on holidays or other special occasions.

A hand rinsing study was carried out in fifteen households to measure the efficacy of hand washing with soap and washing with only water. Turbidity and microbial samples were taken from the source, hand rinsing before washing hands, and then hand rinsing after washing hands. The results presented in Figure 4-4A and 4-4B indicate that hand washing with soap is very effective in removing contamination on the surface of hands compared to using only water. Comparatively, the data indicates that turbidity removal by hand washing is less effective (Figure 4-4C).

There was no significant difference in source water quality between households that washed hands with soap (45 CFU/100 mL ±123% and 2.89 NTU ± 53%) and those not using soap (57 CFU/100 mL ±83% and 2.90 NTU ±48%) (Figures 4-4A and 4-4B). However, the contamination level after hand washing differed considerably: 53 CFU/100 mL ±110% for those that utilized soap compared with 353 CFU/100 mL ±89% for those who did not. Only among those who wash with soap was there no a significant difference in the contamination level between the hand rinsing effluent compared to the household water used for hand washing (Figure 4-4B). The implication is that significant improvements in water quality

could occur even without behavioral changes regarding transport and transfer of water. Two key elements are that: (1) the source could be cleaned up and protected with residual disinfectant such as chlorine and (2) hand washing with soap is practiced during critical hand washing times (as defined by WHO/UNICEF, 2004 and Luby *et al*., 2011).

Oswald *et al*. (2007) found that hand rinsing sample contamination level measured as CFUs/100 mL had similar contamination level to the drinking water found in glasses at the household level. It was suggested that the central mechanism for transfer of contamination was the cleaning method, which involved hand contact on the inside surface of the glass (Oswald *et al*., 2007).

The measured microbial reduction (equation 1) for hand washing was 94.2% reduction for soap users compared to 48.7% reduction for those who only washed with water (Figures 4-4A and 4-4B). The reported log reduction in turbidity was 59.3% reduction for soap users compared to 22.4 % reduction for those just using water. The reductions of microbial activity using soap were much more significant than reductions in turbidity after hand washing. This reduction suggests that soap is very effective in removing microbial contamination from the surface of hands, and that soap is also better at removing dirt compared to those just using water.

$$Reduction = \left(\frac{C_{Effluent}}{C_{Influent}} \right) 100\% \qquad (4\text{-}1)$$

Where: $C_{Effluent}$ is defined as the concentration measured (i.e., CFU/100 mL or NTU) for hand rinsing after hand washing and $C_{Influent}$ is defined as the concentration measured for hand rinsing before hand washing.

The majority (97%) of households surveyed reported knowledge that diarrhea was caused by either: (1) dirty water and dirty food or (2) dirty surroundings. A very small minority (3%) linked diarrheal disease with a spiritual affliction known as the 'evil eye.' However, in spite of this perception that dirt is a source for spread of disease, soap is not readily used in critical hand washing times such as after latrine use or before eating.

Community members practice visual inspection of hands for dirt as a way to determine when to hand wash and the completeness of their hand washing. Such a practice is a misleading diagnostic because an important factor for hand washing is the reduction of microbial contamination on hands which cannot be visually ascertained. Turbidity of water is a surrogate, but not directly correlated with microbial contamination of water. Clear water can be contaminated (Figures 4-4A, 4-4B, and 4-4C). While there is more reduction of turbidity during hand washing when using soap (Figure 4-4C), the reduction may not be readily apparent to someone washing their hands.

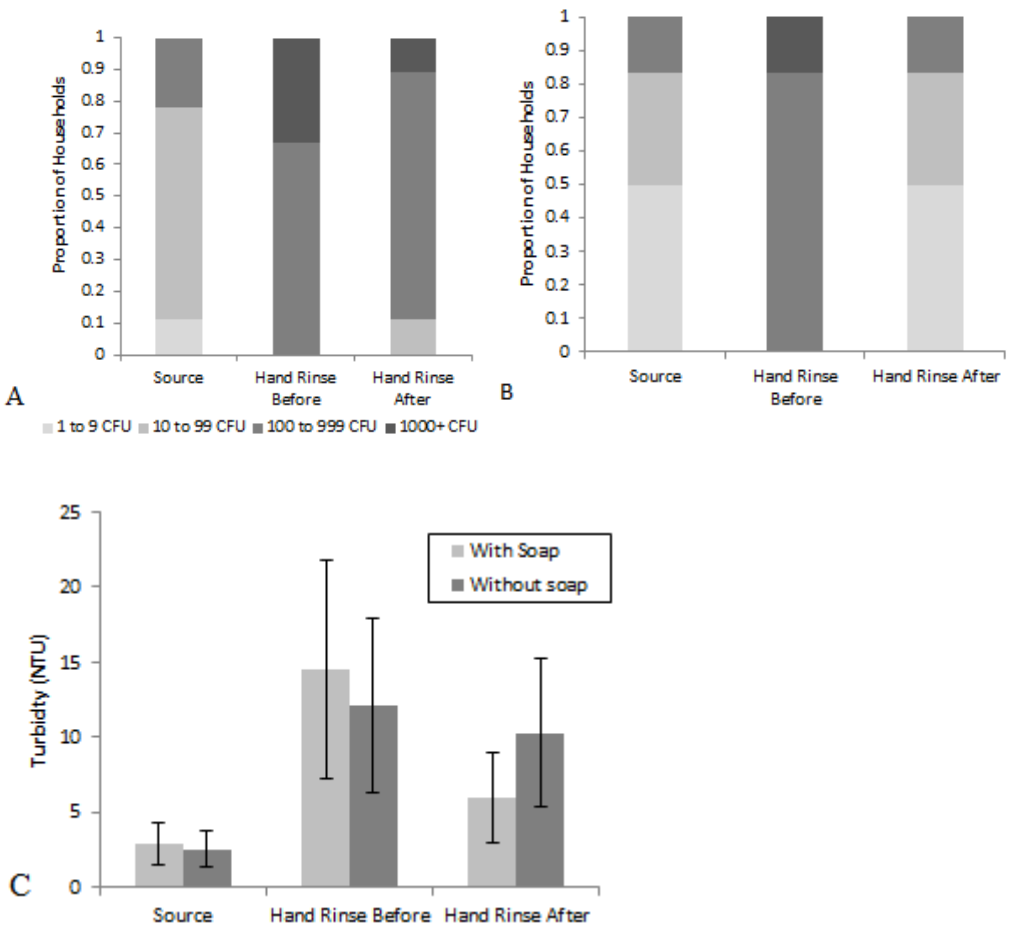

Figure 4–4. A. Hand rinsing microbial data for users washing with water and no soap (9 households). B. Hand rinsing microbial data for users washing with soap (6 households). C. Aggregate turbidity data for users washing with soap and users washing without soap.

Household Observations and Conceptual Map

Household observations aided in forming a local concept map of WASH behaviors and infrastructures that impact household health (adapted from Waddington and Snilstveit, 2009; Figure 4-1). The map was also developed by interactions with several key informants in the community. At the far left of this local concept map (Figure 4-5) are WASH behaviors and infrastructure such as storage and handling of liquid waste. Such WASH behaviors and infrastructure impact (shown in dashed lines in Figure 4-5) the sanitary conditions of transfer surfaces summarized as: source water quality, fingers, fomites, and flies. Finally these surfaces are linked with the proximate fecal-oral exposure route by which pathogenic organisms can be transmitted to human beings. The total linkage between hygienic behaviors or WASH infrastructure and health status represents a candidate pathway for transmittance of pathogens.

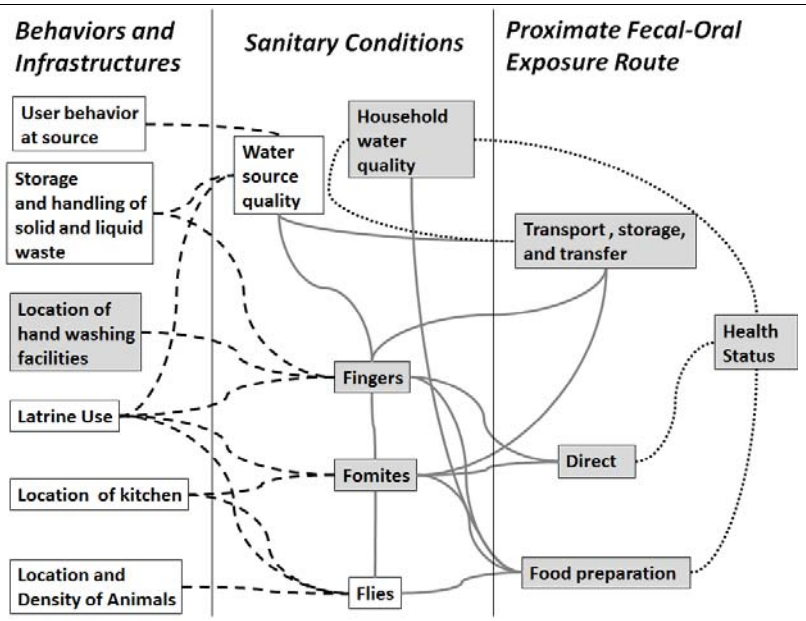

Figure 4–5. A conceptual map for Agew Gimjabet town of impacting health status based on household observations. The dashed line represents links between hygiene behaviors and WASH infrastructure and sanitary conditions. The gray line represents links between sanitary conditions and proximate fecal-oral contamination pathway. Finally, the fecal-oral contamination pathway is linked with health (represented by the dotted line).

A candidate pathway for transmission of disease illustrating the impact of the location of hand washing facilities on health status is highlighted in gray, and was observed to occur in some households. In many households, no hand washing station by the latrine exists. Under this scenario, after latrine use, household members would have to walk into the household dwelling to utilize a wash basin. One possible consequence is that members would walk into the household and wash their hands using a pour jug technique. One of the household

member's hands would touch the jug (fomite) while pouring water on their other hand and then alternating. The washed hand could be easily re-contaminated if there was sufficient contact time with the jug and future household members' hands could also now become contaminated as a result of contact with the jug. Another possible consequence is that distractions could arise during the trip from the latrine to the dwelling, and household members would forget to use the wash basin. The surfaces of their hands would remain contaminated with fecal matter. Contaminated hands transmit pathogens through direct means such as by wiping eyes, nose, eating, or more indirect means such as contact with the water supply when utilizing a *taza* (dipping cup) to draw out water.

The scenario described above led to the hypothesis that a cause of increased contamination of household water is hand contact with water, which would be consistent with the results presented in this paper that support hands contaminating water. The above scenario also underscores the need for consideration of combined intervention strategies with the explicit goal of significantly reducing potential pathogen exposure. For example, locating a hand washing station by the latrine may not be effective in removing pathogens on the surface of hands if soap is not utilized. This local conceptual map is a demonstration of the target areas of WASH infrastructure and behavioral practices at the household level that could be studied more intensively in later survey work.

Based upon our observations and analysis of water quality and household survey data, we hypothesized that household water quality is a vital factor of household health. The most direct waterborne source of transmission of pathogens is drinking water. Source water in

Agew Gimjabet is not generally chlorinated. Thus, the majority of source water could already be contaminated before it reaches the household. However, further contamination of the source water can occur in the household. Contamination was observed to occur through two mechanisms: (1) mixing of different water sources in storage or transfer vessels, and (2) unsanitary handling of transfer, storage, or drinking vessels (i.e. contact by hands). A common practice for cleaning drinking glasses is to rapidly wipe the inside surface with one's hands while rinsing the glass. If the hands are contaminated, then the rapid wiping motion facilitates in the deposition of dead skin cells (and with them pathogenic organisms) on the glass surface. Often recycled water is utilized when cleaning the glass and used washing water is poured into subsequent glasses that are cleaned. The drinking glass is also not typically dried before being utilized so that contaminated or recycled water can easily be mixed with other drinking liquids.

Conclusions

In this field study, source water quality was not strongly associated with self-reported diarrheal disease (Table 4-7). While the unprotected source water was relatively more contaminated than the protected piped source, the adjusted odds ratio was insignificant for those using unprotected source water. No significant relationship between disease incidence between the rainy and dry phases was found, even though water sources were more highly contaminated during the rainy season (Table 4-1). Instead, the results of the multivariate regression model suggest that households utilizing piped water were healthier because of better hygiene behaviors and greater access to other household-level WASH infrastructure (Table 4-7).

Significant factors of the multivariate regression model for self-reported diarrheal incidence were locating a hand washing station by a latrine and sanitary disposal of children's feces (Table 4-7). Multivariate regression models were also created to distinguish factors on the basis of socio-economic status (Table 4-2). Important factors found in these models varied by socio-economic status. These results reflect that effective intervention strategies should consider the socio-economic status of the household before health message promotion takes place.

Water quality data of transport, transfer, and drinking vessels (Figures 4-2A and 4-2B) indicated that household contamination continued to increase through subsequent transfer. The advice currently given by public health extension workers to change transfer vessels from clay pots to *jerikans* may be too limited in scope, as contamination is also recorded to occur between the transfer and drinking vessel. It would also be important for public health officials to focus on other sources of contamination at the household level now that there is an association with contamination levels in hands and final household water quality.

Another possibility to reduce contamination would be to consider the installation of centralized drip chlorine systems for the protected and unprotected sources in the community. However, more study is required to determine the required residual of chlorine that would be palatable to the community, and if this level of residual would be sufficient to protect the water against contamination at the household level, especially for water that underwent long term storage (i.e., more than four hours).

Preliminary data from this study (Figures 4-4A and 4-4B) also indicates that hand washing with soap constitutes a vital step to remove contamination from hands which is linked with contamination of both food and water. When hand washing is properly done with soap, hand washing is linked with a 48% reduction in diarrheal disease (Cairncross *et al*., 2010). However, more study is required to understand the best practices for implementing use of soap as a behavioral change. Problems in achieving sustained behavioral change through large-scale public health campaigns have been reported even under ideal conditions with available soap, water, and access to information (Chase & Do, 2012). It is also important to be cognizant that low wealth families in the community may be unable to afford soap. In addition, there is a risk that soap may be stolen or played with by children in the household (Curtis *et al*., 2007). Therefore, future interventions could focus on both the behavioral change aspect (i.e., recognition of the need to use soap, critical times to hand wash, etc.) and the physical mechanisms to improve efficiency of hand washing (i.e., best hand washing methods). Sustained behavioral change likely requires a bottom-up, participatory health campaign with households that is sensitive to the limitations of poor households. From a physical standpoint, it is important to understand the best and most correct ways to wash with soap and the most vital times to hand wash with soap (Luby *et al*., 2011).

References

Alem, G. (2012). *World Vision Ethiopia WASH Program Division*. WASH Baseline Survey Report on Banja Woreda World Vision ADP.

Black, R.E., Merson, M.H., Rahman, M.M., Yunus, M., Alim, M.A., Huq, L., Yolken, R.H., and Curlin, G.T. 1980. A Two Year Study of Bacterial, Viral, and Parasitic Agents

Associated with Diarrhea in Bangladesh. *J. Infect. Dis.* **142**(5), 660-664.

Booysen, F., Servaas van der Berg, R. B., and Von Maltitiz, M. (2008) Using an Asset Index to Assess Trends in Poverty in Seven Sub-Saharan African Countries. *World Dev.* **36**(6), 1113-1130.

British Environmental Agency (BEA). 2009. *The Microbiology of Drinking Water. Part 4 – Methods for isolation and enumeration of coliform bacteria and Escherichia coli (O157:H7).*

Cairncross, S., Hunt, C., Boisson, S., Bostoen, K., Curtis, V., Fung, I. C.-H., and Schmidt, W.-P. (2010). Water, sanitation and hygiene for the prevention of diarrhea. *Int. J. Epidemiol.* **39**(1), i193-205.

Chase, C. and Do, Q. T. (2012). Handwashing behavior change at scale: Evidence from a Randomized Evalation in Vietnam. *ERN World Bank Policy*. **8**(58), Paper 6207.

Curtis, S.B., Rabie, T., and Garbrah-Aidoo, N. (2007). Health in our hands, but not in our heads: understanding hygiene motivation in Ghana. *Health Policy Plan.* **22**, 225-233.

Devi, A. and Bostoen, K. (2009). Extending the critical aspects of water access indicator using East Africa as an example. *Int. Jnl. Env. Health Res.* **19**(5), 329-341.

Dungumaro, E.W. Economic differentials and availability of domestic water in South Africa. (2007). *Phys Chem of the Earth*. **32**, 1141-1147.

Environmental Health Programme (EHP). (2003). *Guidelines for Assessing Hygiene Improvement*.

Eisenberg, J., Scott, J. C., and Porco, T. (2007). Integrating Disease Control Strategies: Balancing Water Sanitation and Hygiene Interventions to Reduce Diarrheal Disease Burden. *Am. J. Pub. Health*. **97**(5), 846-852.

Filmer, D. and Pritchett, L.H. (2001). Estimating Wealth Effects without Expenditure Data-or Tears: An Application to Educational Enrollments in States of India. *Demography*. **38**(1), 115-132.

Jensen, P.K., Ensink, J.H., Jayasinghe, G., van der, H.W., Cairncross, S., Dalsgaard, A. (2002). Domestic transmission routes of pathogens: the problem of in-house contamination of drinking water during storage in developing countries. *Trop Med Intl Health*. **7**, 604-609.

Kremer, M., Ahuja, A., and Peterson-Zwane, A. (2010). Providing Safe Water: Effort from Randomized Trials. Discussion Paper—23, Cambridge, Mass.: Harvard Environmental Economics Program. Accessed Online: http://www.hks.harvard.edu/m-rcbg/heep/papers/KremerHEEPDP23.pdf

Lindskog, R.U. and Lindskog, P.A. (1988) Bacteriological contamination of water in rural areas: an intervention study from Malawi. *Journal of Tropical Medicine and Hygiene*. **91**(1): 1–7.

Lopez, A.D. (2006). *Global Burden of Disease and Risk Factors*. Oxford University Press: World Bacnk, Washington DC.

Luby, S.P., Halder, A.K., Tronchet, C., Akhter, S, Bhuiya, A., and Johnston, R.B. (2009). Household Characteristics Associated with Handwashing with Soap in Rural Bangladesh. *Am. J. Trop. Med. Hyg.* **81**(5), 882-887.

Luby, S.P., Halder, A.K. Huda, T., Unicomb, L., and Johnston, R.B. (2011). The Effect of Handwashing at Recommended Times with Water Alone and With Soap on Child Diarrhea in Rural Bangladesh: An Observational Study. *PloS Med.* **8**(6), e1001052.

McGuigan, J. T., Elmore-Meegan, M., and Conroy, R. M. (1996). Incidence of enteropathogens in stools of rural Maasai children under five years of age in the Maasailand region of the Kenyan Rift Valley. *East African Medical J.* **73**(1), 59-62.

Montgomery, M.A. and Elimelech, M. (2007). Water and Sanitation in Developing Countries: Including Health in the Equation. *Environ. Sci. Tech.* **41**(1), 17-24.

Oswald, W.E., Lescano, A.G., Bern, C., Calderon, M.M., Cabreara, L., and Gilman, R.H.

(2007). Fecal contamination of drinking water within peri-urban households, Lima, Peru. *Am. J. Trop Med Hyg.***77**, 699-704.

Rufener, S., Mausezahl, D., Mosler, H-J., and Weingartner, R. (2010). Quality of Drinking Water at Source and Point of Consumption – Drinking Cup as a high potential Recontaminatoin Risk: A Field Study in Bolivia. *J Health Popul Nutr.* **28**(1), 34-41.

Sahn, D. E., and Stifel, D. (2003). Exploring alternative measures of welfare in the absence of expenditure data. *Review of Income and Wealth.* **49**(4), 463-489.

Tumwine, J.K., Thompson, J., Katua-Katua, M., Mujwajuzi, M., Johnstone, N., Wood, E., and Porra, I. (2002). Diarrhoea and effects of different water sources in sanitation and hygiene behaviour in East Africa. *Trop. Med Intl. Health* **7**(9), 750-756.

USAID. 2011. *Demographic and Health Surveys Methodology*. DHS *Questionaires*: Household, Woman's, and Man's.

Waddington, H. and Snilstevit, B. (2009). Effectiveness and sustainability of water, sanitation, and hygiene interventions in combating diarrhea. *Journal of Development Effectiveness* **1**(3), 295-335.

Wallner, W.E. 1987. Factors Affecting Insect Population Dynamics: Differences between outbreak and non-outbreak species. *Ann. Rev. Entom.* **32**, 317-340.

WHO/CEHA. (2008). *Health Environment for Children Survey Instrument*. Module III: Water, Hygiene, and Sanitation.

WHO/UNICEF. (2004). *Harmonization of Major Survey Instruments WHO/UNICEF Joint Monitoring Program of Water Supply and Sanitation*.

WHO. (2004). *Fact Sheet 3.6 Pour Flush Latrines.* Obtained: October 11, 2012: http://www.who.int/water_sanitation_health/hygiene/emergencies/fs3_6.pdf

The World Bank. (2005). *The Handwashing handbook: A guide for developing hygiene promotion to increase handwashing with soap.* Washington, D.C.: The World Bank.

Wright, J., Gundry, St., and Conroy, R. (2004). Household drinking water in developing countries: a systematic review of microbiological contamination between source and point-of-use. *Trop. Med. and Int. Health.* **9**(1), 106-117.

Supplementary Information 1. Sample Size Calculation

The appropriate sample size (n) of households was found to be 93 based on equation (4-2) adapted from Alem (2012).

$$n = \frac{z^2 p(1-p)N}{e^2(N-1) + p(1-p)z^2} \qquad (4\text{-}2)$$

Where: N is the number of households in Agew Gimjabet, p is the expected proportion of people who are expected to have waterborne disease (since this unknown, a 50% value was chosen as this yields maximum sample size), e is the confidence interval (±10%) and z is a standard variate from a normal distribution (at the 95% confidence level , z = 1.96). Based on equation 1, a minimum of 186 interviews should be conducted equally divided during the dry and wet phase of the Ethiopian highlands monsoon. In actuality, we carried out 100 surveys during the long dry phase and 135 surveys were conducted during the long rainy phase.

Supplementary Information 2. Results of Principal Component Analysis for Creating an Asset Based Wealth Index

PCA produced a scoring factor for each variable (i.e., kitchen in a separate room) under the two components summarized in Table 4-4. A composite wealth index score was given for each household based on the summation of each variable score. Given the composite wealth index for each household, the households were grouped according to their composite score into three categories: poorest 40%, middle 40%, and richest 20%.

One discrepancy that was apparent in Table 4-5 was that middle and the poorest users owned more animals than richest in Agew Gimjabet. However, the richest 20% were likely to own higher market value animals such as milk cows, horses, and oxen compared to *bono* and unprotected spring users which were more likely to own lower market value animals such as chicken and sheep. A total of 79% of the richest 20% reported having a bank account compared to 17% of the middle 40% and 4% of the poorest.

Source water use was generally correlated with wealth distribution. Approximately 90% of the richest 20% from the survey data were also piped users, and only 9% of the poorest 40% were pipe users. Educational attainment was also higher for those on the piped network. A majority of household heads utilizing piped water graduated from high school (Table 4-5). For the piped users, 94% of the household heads had professions in skilled or higher paid labor areas (such as civil servants, teachers, business owners/merchants) compared to just 55% of the unprotected spring users who were more likely to earn a living in unskilled areas (such as farmer, shepherd/rancher, daily laborer). The higher skilled labor may also be

associated with the higher proportion of male headed households among pipe users compared to *bono* and unprotected spring users.

Table 4-4. Results of the Principal Component Analysis

Agew Gimjabet Town				Means		
	Scoring Factor	**Mean**	**Standard Deviation**	**Poorest 40%**	**Middle 40%**	**Richest 20%**
Component 1 – Status of Dwelling						
High Quality Dwelling	0.57	0.62	0.49	0.20	0.86	1.00
Low Quality Dwelling	-0.57	0.38	0.49	0.80	0.14	0.00
Number of Animals	-0.02	2.27	4.33	1.79	2.89	1.97
Kitchen in a Separate Room	0.04	0.75	0.43	0.61	0.89	0.82
Number of rooms	-0.03	1.19	0.57	1.12	1.16	1.36
Component 2 – Material Possessions						
Own Refrigerator	0.51	0.06	0.23	0.01	0.03	0.21
Own TV	0.42	0.20	0.40	0.01	0.13	0.69
Have Bank Account	0.33	0.24	0.43	0.04	0.17	0.79
Own Bike	0.19	0.06	0.26	0.03	0.08	0.08
Own Radio	0.18	0.65	0.53	0.42	0.68	0.95
Own Cell Phone	0.03	0.75	0.44	0.60	0.79	0.97
Own Clock	0.12	0.45	0.50	0.27	0.51	0.67
Wealth Index		0.46	0.94	-0.50	0.81	1.70

Table 4-5. Educational and Labor Measures for Water Users

Source	Average years of schooling for HH head	Average years of schooling for spouse	Proportion in those HH who are literate that are aged 18+	Proportion of HH heads with a job that is considered skilled labor
Pipe	14.1	11.6	0.82	0.94
Bono	11.0	10.0	0.71	0.63
Unprotected Spring	7.34	6.0	0.55	0.55

Supplementary Information 3. Results of the Bivariate Analysis and Multivariate Analysis for Diarrheal Disease Incidence and Water Consumption Analysis

The factors influencing diarrheal disease incidence according to the bivariate analysis are presented in Table 4-6. The following factors were not significant in this bivariate analysis: seasonality, owning animals, location of animals in the homestead, water use per capita, household having children under 5, and availability of soap in the household.

Table 4-6. Factors associated with diarrheal incidence using the Bivariate Analysis

Factor	**Odds Ratio**	**95% Confidence Interval**
No Latrine located in homestead	7.88	5.07-12.25
Using Unprotected Water Source	5.22	3.81-7.15
Kitchen Not Separated from Main Dwelling	5.03	3.62-6.98
'Unsafe" Method for Disposal of Child's Feces Under 5	2.49	1.74-3.56
Store All HH Water in Clay Pot	1.79	1.11-2.13
No Hand Washing Station by the Latrine	1.71	1.12-2.63

Significant factors as determined by the bivariate analysis were the included factors in a multivariate binary logistic regression model. The results of the multivariate model are given in Table 4-7, and the corresponding variance of the model is given in Table 4-8.

Table 4-7. Results from the Multivariate Binary Logistic Regression Model based upon Best Linear Unbiased Estimator

Factor	**Coefficient (β)**	**Standard Error**	**P-value**	**Adjusted Odds Ratio**
Proper Disposal for Child's Feces Under 5	-0.91	0.39	0.02	0.40
Hand washing station located by the latrine	-0.56	0.39	0.05	0.57
Using Unprotected Water Source	0.39	0.30	0.20	1.47
Always Utilize Clay Pot for Water Storage	0.75	0.60	0.21	2.19
Separate Room for Kitchen	-0.35	0.35	0.33	0.71
Open Defecation	0.35	0.40	0.39	1.42
Constant	0.46	0.49	0.57	1.31

Table 4-8. Analysis of Variance for Multivariate Linear Regression Model

Source of Variations	**Sum of squares**	**Degree of freedom**	**Mean square**	**F-value**	**P-value**
Regression	7.43	6	1.239	4.193	0.001
Residual	67.05	227	0.259		
Total	74.48	233			

Percentage of correct predictions 68%, standard error of the estimate = 0.54

Supplementary Information 4. Water Consumption Analysis

In a meta-study of diarrheal morbidity in Eastern Africa (Tumwine et al. 2002), there was a strong association between diarrheal disease reduction and increased per capita consumption of water for personal hygiene (i.e., hand washing and bathing) and household cleaning (i.e., washing clothes, cleaning other household items). However, in this study the reported average consumption among the pipe, *bono*, or unprotected spring source users did not vary significantly (Figure 4-6). The reported household average was not statistically significantly different (within ±1 L/person/day) for personal hygiene and household cleaning purposes.

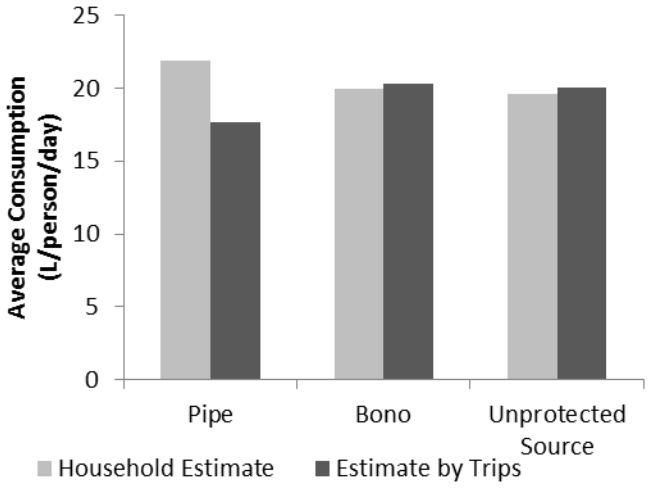

Figure 4–6. Average water consumption for daily household activities among pipe, *bono*, and unprotected spring users.

The number, type, and distribution of animals in the homestead were all variables anticipated to impact diarrheal morbidity. Animals can transmit disease to humans through a variety of mechanisms through the fecal-oral pathway. However, there was no significant difference in

diarrheal morbidity. One explanation is that 82% of households that owned animals reported keeping animals separated from the household through construction of separate animal dwellings. Households also handled animal waste products in the same way that other liquid and solid waste products were handled. Human and animal solid and liquid waste was removed from the household at least once every three days in 80% of households surveyed.

Seasonality has been linked in other studies with diarrheal disease incidence since seasonality is linked with population dynamics of parasites and their hosts (Black et al., 1980). However, pest and parasite population dynamics are a result of many factors and difficult to predict (Walner, 1987). In addition, water quality is poorer during wet seasons especially for shallow ground and surface water sources due to run-off and infiltration/deposition of sediment. Poorer water quality could be offset by more water available during the wet season for sanitary and hygienic purposes.

For this study, water quality in terms of turbidity and microbial activity was better during the dry season for the unprotected spring source, but there was no significant difference for piped and *bono* users (Table 4-1). There was also no significant difference in reported water consumption between the wet and dry season: 15.6 L/capita-day and 15.4 L/capita-day, respectively (Figure 4-7). It was observed that there were larger fly populations in households during the dry season compared to the wet season. One possible explanation is that there were more resources available to flies in the environment during the wet season so they were less likely to concentrate in dwellings. With the combination of these factors, it made sense that

there was no significant difference in diarrheal incidence between the dry and wet season for users.

CHAPTER 5: CONCLUSIONS AND FUTURE STUDIES

Conclusions

The experimental apparatus and methods of non-destructive analysis of solids concentration described in Chapters 2 and 3 provide a system for an improved understanding of floc blanket formation and behavior. The method has been validated in the following ways:

- A two component calibration for suspensions containing kaolinite clay and aluminum hydroxide was built (Figure 2-5). Light attenuation measurements were taken and converted to the corresponding suspended solids concentration at varying concentrations (500-2000 mg/L) and positions (20-75 cm) in the floc blanket reactor. The predicted concentrations from image analysis were compared with TSS grab samples (Figure 2-6) and the corresponding error for any predicted concentration measurement was less than 15%.

- Continuously sampled turbidity measurements validate image analysis as an experimental method for measuring real-time solids concentration in a floc blanket (Figure 3-6).

There are several new insights with respect to floc blanket formation and behavior provided:

- Analysis of data presented in Chapter 2 confirm prior observations that floc blanket concentration is relatively uniform with respect to height (Figure 2-11B) (Gould, 1969) and that concentration in a floc blanket is influenced by the interface upflow velocity (Figure 2-12) (Gregory, 1979; Letterman, 1999; Hurst et. al., 2010).
- Floc blanket thickening (i.e., increasing solids concentration increases over time) was observed to occur even when interface velocity remains constant (Figure 2-13B; Figure 3-7D;

Figure 3-8B). While the postulated cause is decrease in floc size over time, more study is required to fully understand what physical changes flocs undergo that cause an increase in solids concentration.

- Image analysis revealed three distinct stages of floc blanket formation: thickening (increasing suspended solids concentration) in the absence of an observable floc-water interface, thickening with an interface, and steady-state at influent turbidity of 100 NTU and alum dosages of 25 and 45 mg/L (Figure 3-7; Figure 3-8).

- Floc blanket performance (Figure 3-4), concentration (Figure 3-7B), and height (Figure 3-7D) data from an alum dosing of 45 mg/L and influent turbidity of 100 NTU suggest that solids concentration has a more direct relation to turbidity removal than does blanket height.

- Mass transfer of suspended solids from the floc blanket supernatant to the floc blanket may be an important consideration for blanket formation dynamics. As blanket solids concentration increases, floc volume fraction in the floc blanket increases and the supernatant concentration decreases. Floc blankets with higher solids concentration than the supernatant (as observed in Figure 3-9) contain flocs with higher sedimentation velocities than the interface velocity. When flocs with greater sedimentation velocities than the interface velocity are carried upward into the supernatant by turbulence, they will readily settle back to the floc blanket.

Chapter 4 investigates risk factors associated with diarrheal incidence within households in the Ethiopian highlands and results suggest that household water contamination is significant

and likely related with hand contamination. There are several important insights provided by this investigation:

- Water quality data regarding transport, transfer, and drinking vessels (Figures 4-3A and 4-3B) indicated that household contamination continued to increase through subsequent transfer.
- Source water quality was not strongly associated with self-reported diarrheal disease (Table 4-7) and instead, the results of the multivariate regression model suggest that households utilizing piped water were healthier because of better hygiene behaviors and greater access to other household-level WASH infrastructure (Table 4-7).
- Preliminary data from this study (Figures 4-5A and 4-5B) also indicate that hand washing with soap constitutes a vital step to remove contamination from hands which is linked with contamination of both food and water.

Future Studies for Floc Blanket Research

Determination of the effect of jet and bottom geometry on the ability to re-suspended particles

Flocs that settle to the bottom surfaces of the sedimentation tank are returned via an incline to the influent jet to be resuspended. Solids resuspension by the jet of influent flocculated water is critical because the floc blanket cannot form if settled flocs are not resuspended. In spite of the importance of resuspension, there does not appear to be any literature that details the hydraulic and bottom geometry conditions required for solids resuspension. The lack of attention to this topic in the literature most likely stems from a lack of ability to image

sedimentation tank systems.

The goal of future studies will be to identify solid, liquid, and bottom geometry interactions in the floc blanket that are critical components in ensuring that settled flocs are returned to the inlet jet to be re-suspended. Results of this dissertation reveal high concentration debris flow along the inclines of the reactor wall (Figure 2-7). Future research is needed to identify physical mechanisms and geometric bottom conditions required for re-suspension of settled solids. Future research with the experimental apparatus is expected to determine the effect of jet and bottom geometry on the ability to re-suspend returning debris flow.

Mechanisms of particle removal in a floc blanket

Much of the recent literature on floc blanket clarification has focused upon modeling solids flux in the floc blanket to predict floc blanket performance (Chen et al., 2003; Sung & Lee, 2005; Zhang et al., 2006). Such an empirical approach cannot generally predict floc blanket response with respect to changes in coagulant dose and turbidity just as mass flux cannot be utilized to predict residual turbidity in the effluent from a floc blanket clarifier. Prediction of performance requires a greater understanding of the mechanisms of particle removal in a floc blanket. Understanding mechanisms of particle removal in a floc blanket may allow for the optimization of design and operation of a floc blanket clarifier with lamellar sedimentation.

The goal of future studies will be to evaluate particle removal efficiency as a function of interface upflow velocity, floc blanket suspended solids concentration, floc blanket height,

and tube settler capture velocity. It is likely that if a particle has a terminal settling velocity close to the upflow velocity, that the solids residence time of that particle in the floc blanket will be controlled through physical wasting. However, for smaller sized particles that disproportionally impact effluent quality, it appears that particle-particle interactions as the particle moves upward through the floc blanket will affect particle removal in the floc blanket.

Investigation of Floc Blanket Stability

The notion that floc blankets are prone to instability (i.e. particle carry-over) has prompted a focus of prior research on mass flux with respect to blanket formation and stability (Chen *et al*., 2006, Su *et al*., 2004, and Sung, 2003). While floc blanket mass flux models have focused on the flux across the floc-water interface (Sung *et al*., 2005; Chen *et al*., 2002; Gregory, 1979), instability in the floc blanket may ultimately result from changes in inflow conditions (solids concentration, coagulant dose, volumetric flow rate, etc.) that change the equilibrium suspended solids concentration of the floc blanket. Likewise, the delayed formation of floc blankets may result in part from poor settling characteristics of incoming flocs. In addition, inflow jet conditions that fail to resuspend settling flocs may render maintenance of the fluidized bed of suspended flocs difficult.

Future study is recommended that focuses on changes in solids concentrations and vertical-upflow velocity that produce changes in blanket stability. A significant and sudden change in

vertical-upflow velocity is expected to immediately result in a change in the fluid velocity in the blanket and force significant bed expansion or contraction. A change in influent solids concentration is not expected to produce immediate instability unless influent particles and/or colloids are not sufficiently coated with aluminum hydroxide precipitate. If not sufficiently coated, it is anticipated that influent particles will not aggregate with flocs in the blanket resulting in higher effluent turbidity.

Effect of NOM and particle type on floc blanket effluent performance

An alum dosing relationship for a floc blanket was derived in Hurst *et al*., (2010) for ranges of kaolin turbidity between 10-500 NTU. The generality of this dosing relationship to other raw water compositions and other types of colloidal particles is uncertain.

Regardless of the type of natural organic matter (NOM), there is a general expectation that NOM will adsorb to the surface of aluminum hydroxide flocs and colloids effectively increasing the negative surface charge of these particles (Bose & Reckhow, 1998). If surface charge were an explanation for part of the predominant mechanism by which colloids are removed in floc blanket clarification, then the charge of NOM would be an important consideration as higher NOM content would require more coagulant dose.

Bacteria and algae have a negative surface charge but a much lower density than clay particles. It is unclear whether the upflow velocities applicable to flocs containing clay will be applicable to other particle types. Research appears warranted on the effect natural

organic matter and suspended microorganisms on removal of turbidity and NOM. Future experiments could quantify the impact of floc blanket performance with respect to NOM dose coupled with changing interface velocity, suspended solids concentration, and coagulant dose

Future Studies Related to Sanitation and Hygiene

The following presents several follow-up studies/interventions that could be of additional interest for investigators and/or public health officials.

Sources of Contamination of Water in Rural Ethiopia

Contamination in the rural environment is likely to have disparate and significant pathways of contamination. Compared to the peri-urban area, the rural area is likely to: have a significantly higher population of animals, have significantly less assets per household, and have greater access to public health campaigns sponsored by NGOs and the Ethiopian government.

A future study could investigate pathways of contamination in the household through use of household survey data and water quality data. Analysis of household survey data related with diarrheal incidence could inform risk factors associated with transmission of water-related disease. Bacterial counts could identify sources of contamination in the water that occur either at the source or household level. The results could inform future intervention strategies that may require a different outlook and analysis as compared to the results presented in the peri-urban analysis in Chapter 4.

Contamination Link Between Hands and Food

Hands are the common utensil utilized in food preparation and consumption in the Amhara

region of Ethiopia. A significant source of household contamination could result from ingestion of pathogens from food. Future research could investigate the foodborne pathway of contamination through use of household surveys and taking fecal counts on the surfaces of hands and food.

Water Contamination Sources Between Households

While the study presented in Chapter 4 presents results that suggest hand contamination is a likely significant source in household water, the study does not investigate sources of contamination between households. One possibility is that hands also are significant at spreading contamination between households. One underlying reason is that hands are exchanged very commonly in greeting, and hand washing in absence of soap is a commonly shared practice between households regardless of socio-economic status. Another possibility is that food shared between households could also facilitate spread of water-related disease.

Impact of Centralized Chlorination on Community Health

Chlorination at the source may significantly reduce water-related disease transmission by: (1) disinfecting source water, and (2) providing a residual disinfect in the source water that will protect against re-contamination in the household for a limited period of time.

A future study could require implementation of a low cost, hydraulically-driven, and operator-friendly chlorination system. Likely, the design of the hydraulically-driven chlorinator utilized will be based upon community demand and size. The rural areas likely require a system that requires discrete dosing for every *jerikan* due to the low demand, while towns could directly dose into a reservoir.

APPENDIX A: IMAGE ACQUISITION: OPENING AND USING THE MASTER PROGRAM

Program Overview amd Troubleshooting

An image acquisition program was developed to acquire sequential images and control camera properties such as rate of image acquisition and shutter speed, where a shutter speed of 20 is defined as shutter opening for 400 μs for one image. This program is opened from the LabVIEW visual instrument (VI): Master Program (Figure A-1). The camera ID is serially assigned by National Instruments (NI) Measurement and Acquisition software. In Master Program, the camera selected is "cam 0." Typically, if "cam 0" is not available in Master Program, it is likely that the driver is not compliant or incorrectly configured with LabVIEW software. A remedy is to to re-install the LabVIEW driver and then re-configure the camera to the LabVIEW driver using National Instruments Measurement and Acquisition Software.

Acquiring Images Utilizing Image Acquisition Software

In Master Program, the user selects the rate of acquisition and shutter speed. The user must also choose the location for storage of images and the metafile. The metafile folder path stores pertinent information concerning the series of images taken including the start time of image acquisition, location of images, the number of images taken, the shutter speed, and user comments made during or after acquisition.

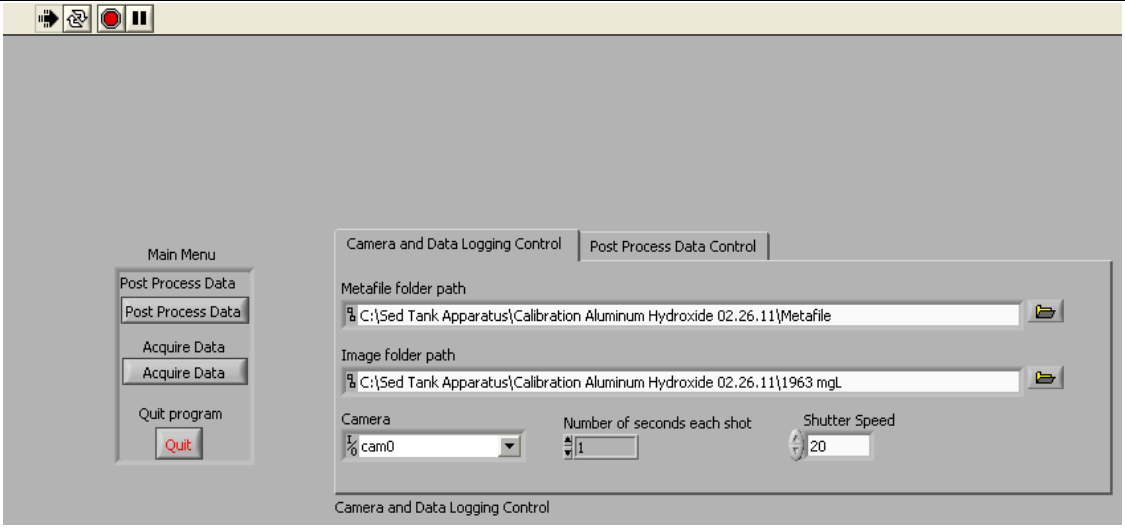

Figure A-1. The start-up screen for the master program VI in LabVIEW.

After image acquisition is initiated, the computer interfaces with the camera to automatically acquire and then store images. A screen showing the most current image taken provides immediate visual feedback and confirmation for the user of the image taken (Figure A-2). Each image is initially acquired as a 24 bit TIFF image file. Additionally, the user can follow real-time data under the tab "Real-time Data" which tracks blanket concentration and height of the floc water interface in the reactor.

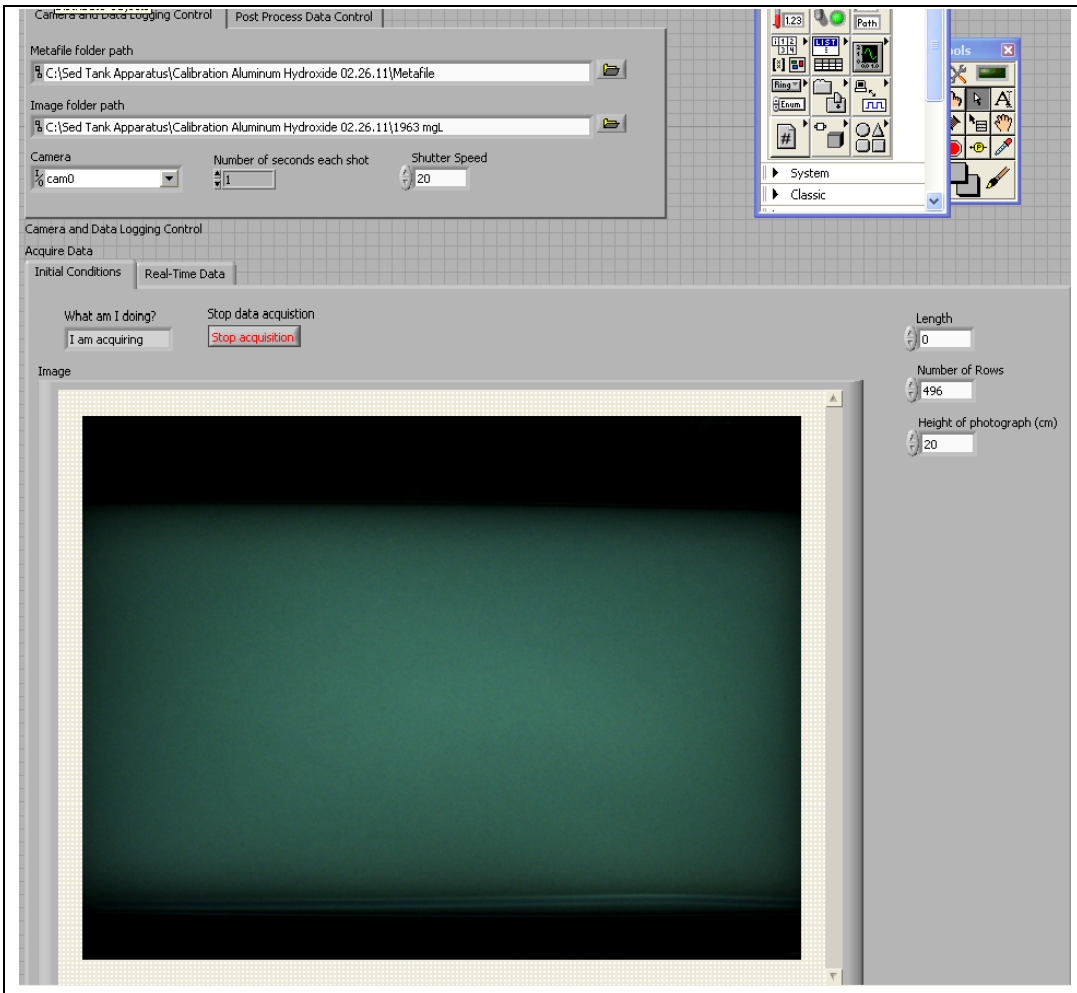

Figure A-2. Viewing screen during image acquisition.

APPENDIX B: ANALYSIS OF VARIABILITY IN INTENSITY OF LED LIGHT SHEET

Analysis of Average Intensity

The reactor was filled with a blank (aerated, tap water), and a sequential series of photographs were obtained. Visually, it was apparent that light intensity was greater in the center than at the sides of the light panel (Figure B-1A). A region of interest (ROI) was selected corresponding to the area that was analyzed by the software. One pre-programmed visual instrument (VI): **IMAQ LinearAverages** acquired the average intensity of all pixels in each column. These values were then input into a graph of the average measured intensity with respect to height Figure B-1B from the photograph shown in Figure B-1A. The results corroborated the intuitive visual feedback that higher intensity of light output existed near the center of the LED light panel.

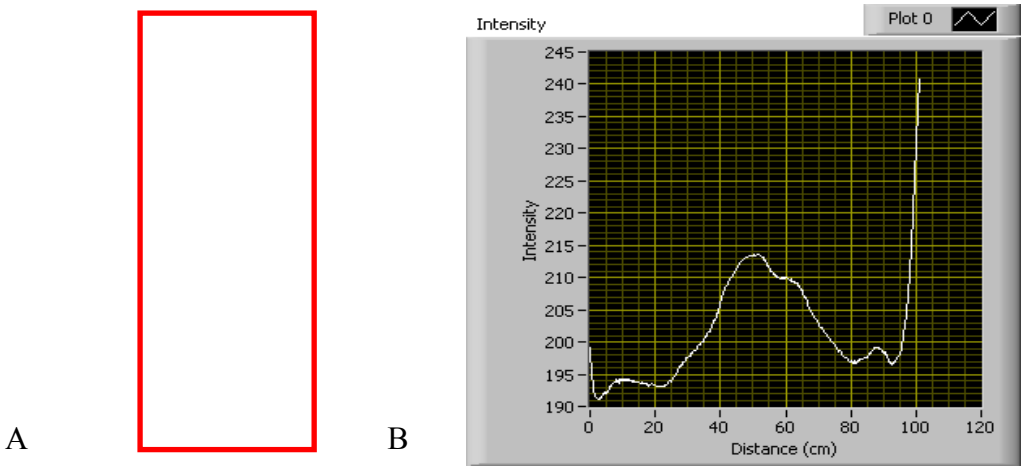

Figure B-1. A. The image of the LED light panel shot at a shutter speed of 50 (lens exposure time of 1 ms). B. A graph of the average linear intensity for each column of pixels as shown in A.

Analysis of Red, Green, and Blue Wavelengths at Specified ROIs

Another pre-programmed VI: **IMAQ ExtractSingleColorPlane** could extract the color planes of red, blue, and green and analyze each as a new separate image. The resulting input 24 bit TIFF image and output red, blue, and green 8 bit images TIFF images are shown in Figure B-2.

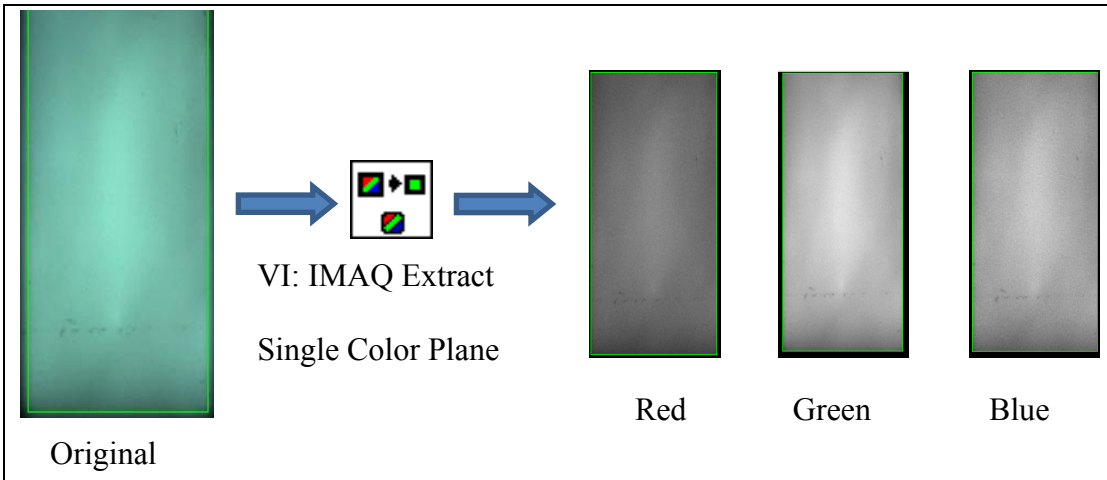

Figure B-2. Schematic of method for extraction of red, green, and blue wavelengths utilizing the VI **IMAQ ExtractSingleColorPlane** function in LabVIEW.

Subsequent analysis for various regions of interest in the red, green, and blue color planes revealed that the each wavelength revealed close to the same response for intensity variance resulting in coefficient of variations for each of approximately ± 15% (Figure B-3). Although there is variability in the light panel with respect to position in the light panel (Appendix B), each measurement is normalized with respect to transmitted light intensity, thus, the variability in light intensity will not significantly impact light attenuation readings.

A 

B 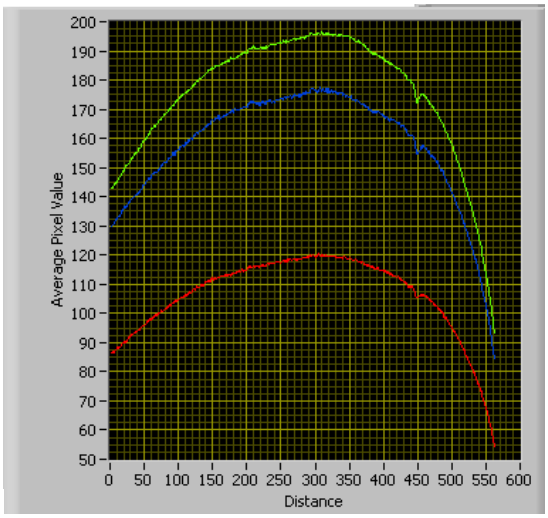

Figure B-3. A. The image of the LED light panel with ROI and laminate diffusive sheet shot at a shutter speed of 20 (lens exposure time of 400 μs). B. A graph of the average linear intensity for the ROI of the red, blue, and green planes respectively.

APPENDIX C: CALIBRATION OF EXPERIMENTAL APPARATUS WITH RED DYE

A spectra of Red Dye #40 was obtained utilizing a HP Spectrophotometer 8542A Diode Array with a path cell length of 1.3 cm and a red dye concentration of 150 mg/L (Figure C-1). The curve revealed, as anticipated, that wavelengths in the blue and green lights will be strongly absorbed by the dye, while red wavelengths will not.

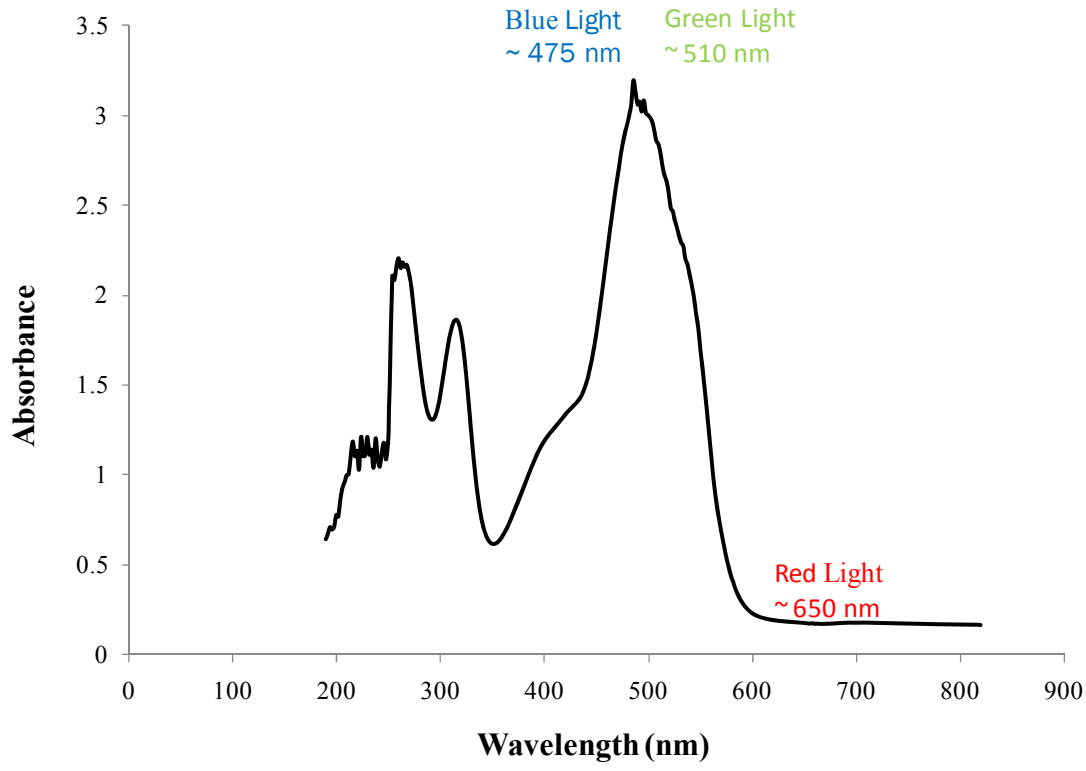

Figure C-1. Absorbance curve for red dye #40 at a concentration of 150 mg/L.

A calibration curve for Red Dye #40 (Figure C-2) was developed to: (1) examine the sensitivity of absorbance response to changes in concentration, (2) determine whether absorbance exhibited a linear response for concentrations of concern, and (3) confirm that absorbance readings were measurable for red, green, and blue wavelengths. Dye inputs were

injected into the reactor, and then vigorously mixed to create uniform dye concentrations of: 0, 10, 20, 50, and 100 mg/L. At each concentration, a series of photographs were obtained every 1 second for period of 2 minutes. Each photograph was analyzed for the absorbance of light in the red, blue, and green wavelengths, and the results were averaged for each subset concentration and wavelength.

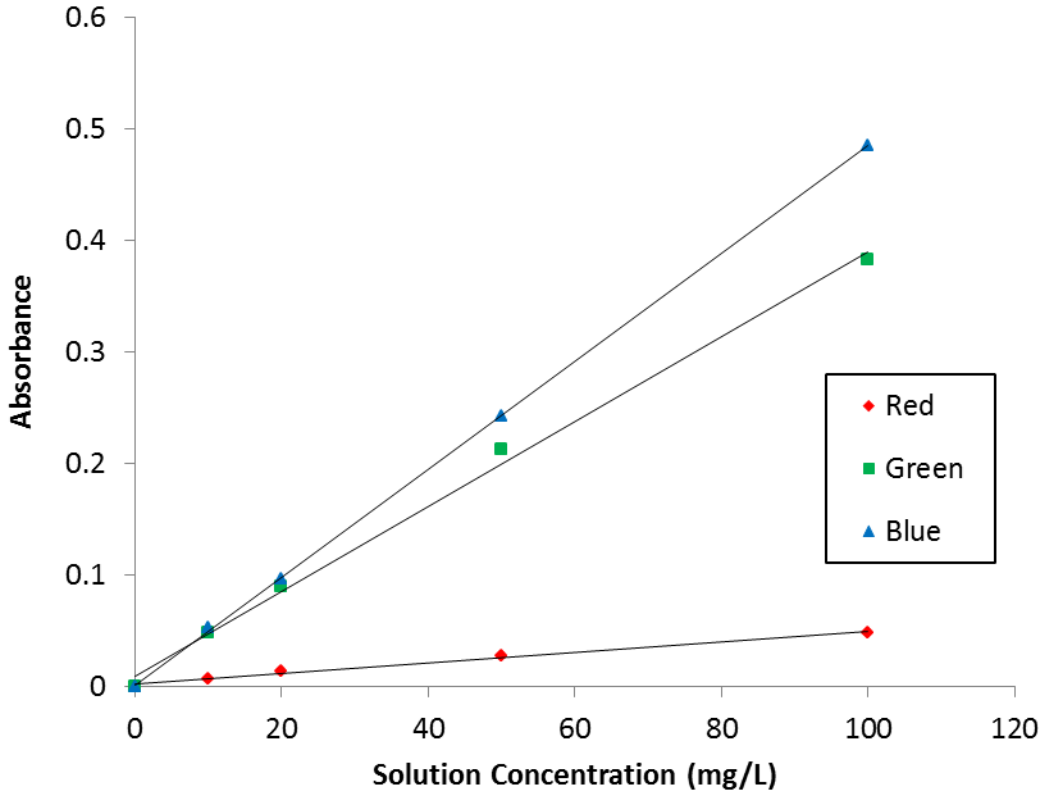

Figure C-2. Red dye curve obtained at a shutter speed of 20 (400 µs).

As expected, light in green and blue wavelengths was absorbed more strongly by the red dye than light of red wavelengths (Figure C-2). Linear regression fit the data very well ($r^2 \geq 0.985$) in the green, blue and red wavelengths.

APPENDIX D: CLAY CALIBRATION CURVE DEVELOPMENT

Kaolinite clay exists on the length scale of ~1 μm, and was used as the influent source turbidity for all laboratory experiments. The kaolinite suspension is expected to be relatively stable and uniform due to the negative surface charge of the clay particles which will inhibit kaolinite aggregation. The clay was continuously recirculated into the reactor utilizing a peristaltic pump and gently stirred between imaging to maintain a relatively uniform clay suspension. A clay calibration curve was created for suspended solids concentrations typical of a floc blanket: 200 – 8000 mg/L (Hurst *et al*., 2010) (Figure D-1). Sequential photographs at each specified concentration were taken every 1 second for 2 minutes. At each concentration point, the light attenuation measurement for red, blue, and green wavelengths were assessed using the method described in Appendix B, and averaged.

A non-linear response at higher concentrations was observed (Figure D-1). As concentration increases and separation distance between particles decreases, particles increasingly "shadow" light from reaching other particles that are in the same path of light (Weingartner *et al*., 2003). Some of the particles under more dilute concentrations that would contribute to scattering and absorption of light are now blocked out by other particles, resulting in an increase in the incident light hitting the detector. Some of the scattered light that has been scattered away from the detector can also be scattered back towards the detector by a second particle. Increasing the number of particles increases the frequency that some of the scattered light makes it to the detector, and decreases the frequency which particles contribute to light absorption, causing a slight reduction in light attenuation and a nonlinear response at high

concentrations. A second-order polynomial fit accounted for the non-linearity at higher solids concentrations (Figure D-1).

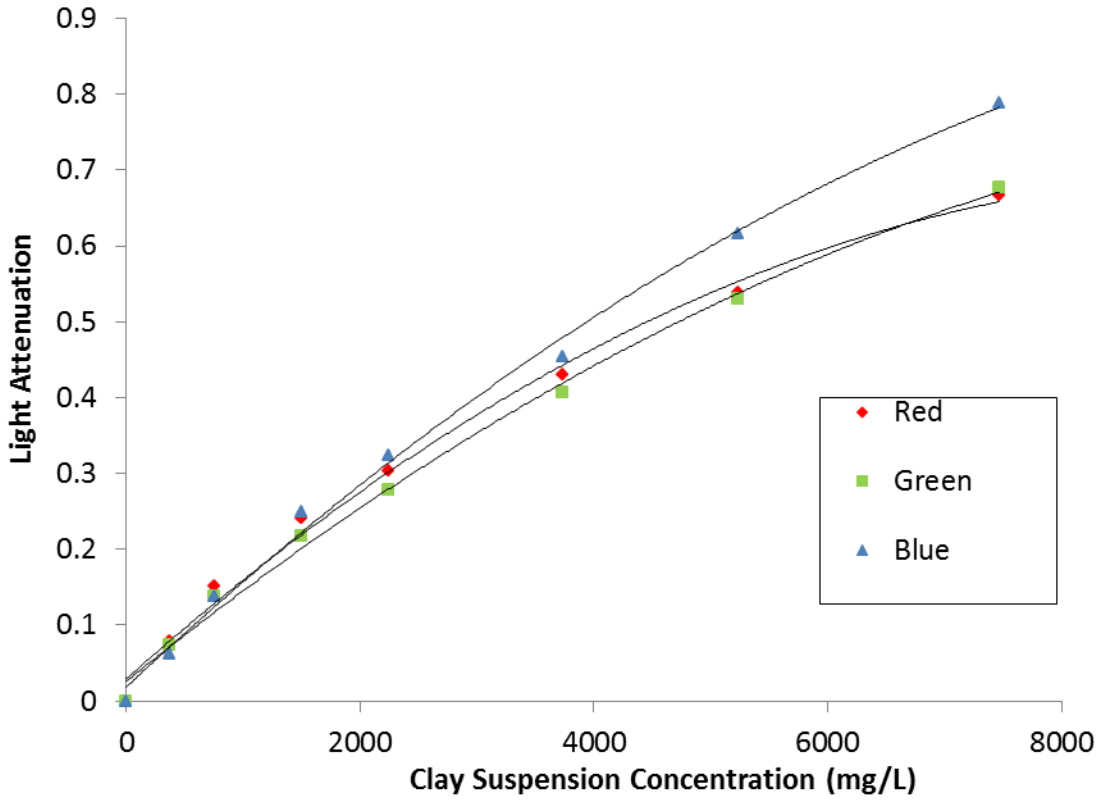

Figure D-1. Clay calibration curve obtained at a shutter speed of 20 (400 µs). The corresponding second order polynomial fits are shown as lines.

APPENDIX E: ALUMINUM HYDROXIDE CALIBRATION CURVE DEVELOPMENT

An aluminum hydroxide concentration calibration curve was developed over a range of aluminum hydroxide concentrations: 0, 100, 200, 400, 800, 1300, and 1900 mg/L. Aluminum hydroxide was precipitated out of a concentrated stock of alum using a combination of concentrated sodium hydroxide solution and sodium carbonate for buffer. The concentrated alum stock was titrated with concentrated sodium hydroxide solution until a target pH of 7.0 was achieved. Compared to a suspension of kaolinite, aluminum hydroxide precipitation results in larger, white, porous, fractal particles. The resulting suspension was kept well mixed and then injected in discrete amounts in the reactor and gently stirred using a large plywood stirrer. The resulting calibration is displayed in Figure E-1.

A non-linear response at higher suspension concentrations was observed (Figure E-1). Increasing the number of particles results in increased scattering and decreased absorption of light than would be predicted from the suspension behavior at more dilute suspension concentrations. A slight reduction in light attenuation at higher suspension concentrations results in the nonlinear response at high concentrations. A second-order polynomial also provided good fit that accounted for the non-linearity at higher solids concentrations (Figure E-1).

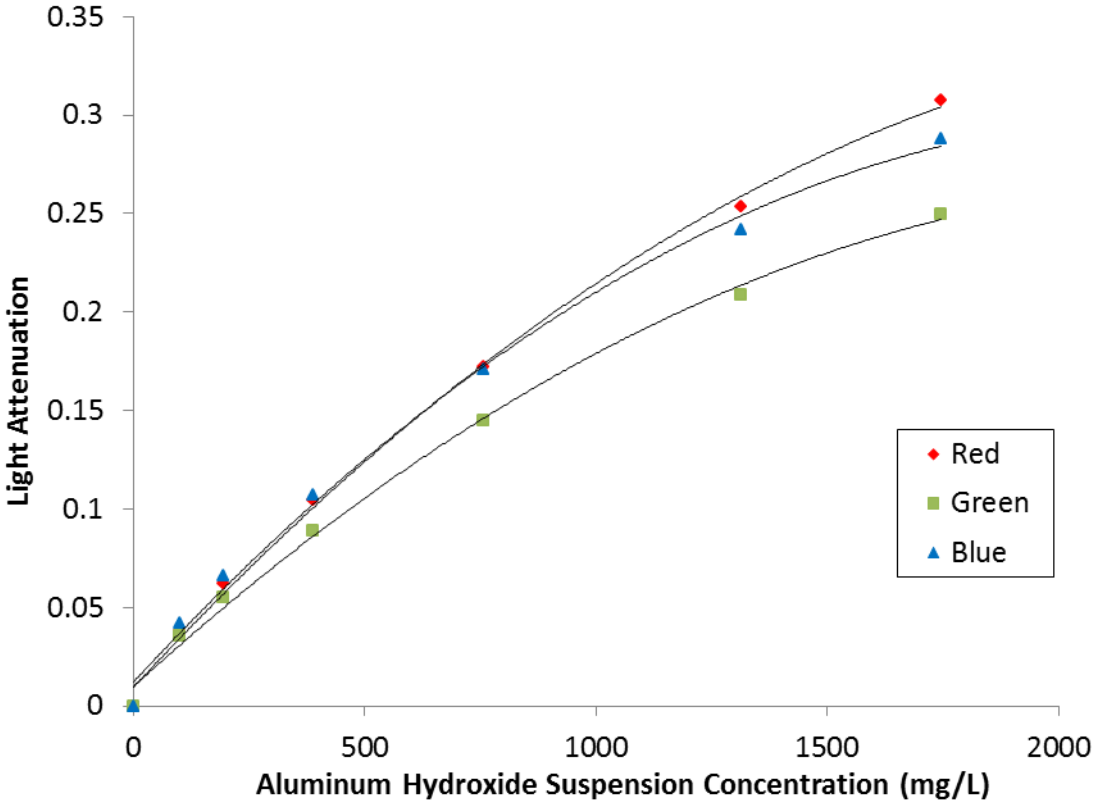

Figure E-1. Aluminum hydroxide calibration curve obtained at a shutter speed of 20 (400 µs).

APPENDIX F: TOTAL SUPSENDED SOLIDS TEST

Background

The solids concentrations analysis is adapted from Standard Methods' (1998) total solids dried at 103-105 ºC test (Clesceri *et al*., 1998). The results are representative of the mass of solids in the sample per total mass.

Apparatus

a. *Drying Oven* set at 105 ºC

b. Dessicator

c. *Gooch crucible*: 25 mL capacity

Procedure

A Gooch crucible that has been oven dried at 105 ºC is desiccated for at least 30 minutes. The dry mass is taken and then a sample of at least 25 mL taken from the floc blanket with a peristaltic pump at a specified floc blanket height is carefully poured into the Gooch crucible and the mass is taken again. The Gooch crucible is carefully loaded into a drying oven at 105 ºC. After the sample is evaporated and dried, the sample is put into a dessicator to cool and then weighed. The sample is then put back into the oven and dried. The procedure is repeated until the dried sample is a constant mass. The solids concentrations can then be ascertained from this procedure utilizing equations (F-1) and (F-2).

$$m_{sample=crucible} = m_{liquid+crucible} - m_{crucible} \qquad \text{(F-11)}$$

$$C_s = \frac{m_{drymass}}{m_{liquidmass}} \qquad \text{(F-2)}$$

Where: $m_{crucible}$ is the dry mass of the crucible, $m_{liquid+crucible}$ is the total mass of the crucible and liquid, $m_{sample=crucible}$ is the mass of the sample in the crucible, $m_{drymass}$ is the dry mass of the crucible, and C_s is solids concentration of the sample taken.

APPENDIX G: MEASUREMENT OF SUSPENDED SOLIDS BY IMAGE ANALYSIS

Suspended solids concentration measurements for each image pixel were determined from light attenuation measurements which were calibrated to a combined, two-component calibration curve for known concentrated suspensions of kaolinite-aluminum hydroxide flocs. The advantage of utilizing a two-component calibration curve method is that the method is applicable for an infinite number of possible aluminum hydroxide and clay concentration combinations as long as the initial clay and aluminum hydroxide concentrations are known.

User Instructions for "Standalone program for Concentration ROI – multiple images"

This program gives the average concentration of a region of interest (ROI) for a series of images in the red, blue, and green calibrated concentration ranges from ~200 mg/L up to ~10,000 mg/L. A typical program screenshot with all pertinent information entered is given in Figure G-1. Depending on the number of images, the program can take up to ten minutes to process the data. The sequential steps to run the program are detailed as follows:

1. Open the program located at: C:\Documents and Settings\mwh65\Desktop\Post-Analyze Programs\Concentration for ROI for Multiple Images
2. Choose the appropriate file path for post analysis of images.
3. Choose the appropriate file path to load the region of interest (ROI) for the image. This ROI should be in the form of an MS excel document (i.e., ".xls") to load correctly. The average or ROI descriptor may be blank if no previous data analysis has been done, but will still load.
4. Choose the file path for the blank images.
5. Set the number of pixels/cm. This should be calibrated with respect to camera distance from the reactor wall.

6. Select the number of seconds per shot that was specified when the series of images was taken.

7. Select the average raw water influent turbidity during the experiment.

8. Select the alum dosing utilized for the experiment. If different, alum doses were utilized it may be helpful to break up the image directory into separate images where changes in alum dose occurred.

9. Smoothing is optional but is not recommended for this program.

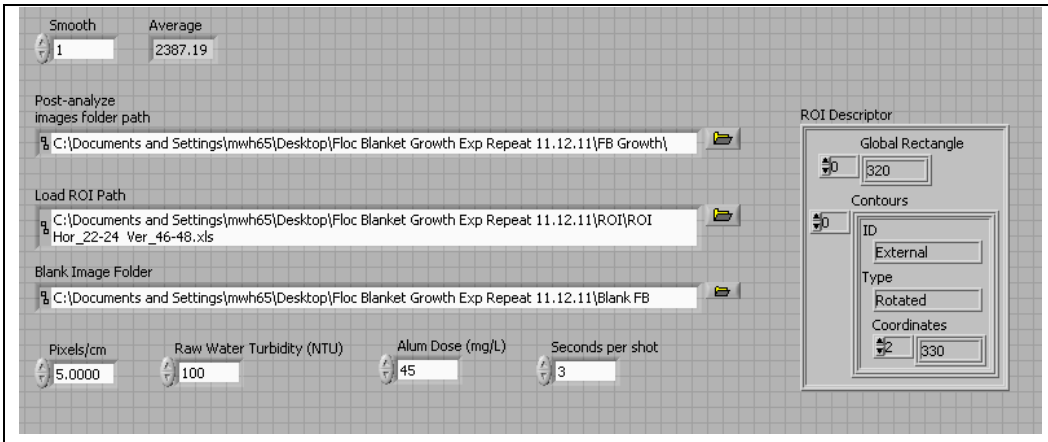

Figure G-1. Screenshot of what the initial program screen should look like when all of the necessary information has been filled out by the user.

The following steps exist for subsequent data analysis:

1. Scroll to the right and one should see a concentration plot against time for the ROI of interest shown in Figure G-2.

2. Right clicking on the concentration plot and selecting export>export to excel will open the data in an excel workbook shown in Figure G-3.

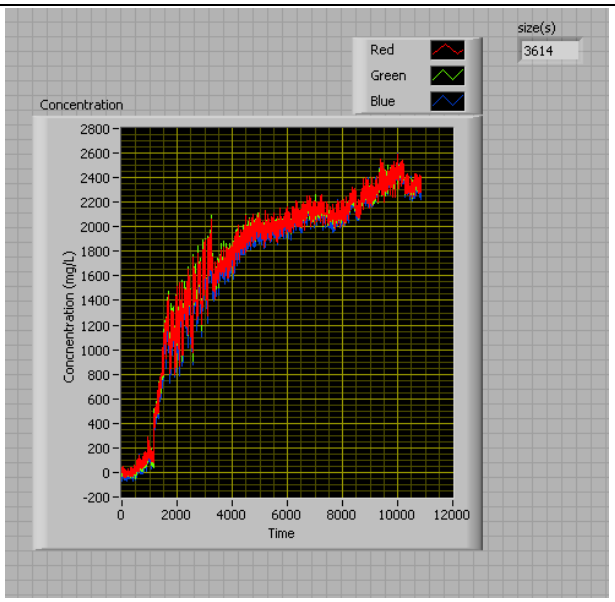

Figure G-2. The resulting data of average concentration over time in the ROI.

	A	B	C	D	E	F
1	Time - Red	Concnentration (mg/L) - Red	Time - Green	Concnentration (mg/L) - Green	Time - Blue	Concnentration (mg/L) - Blue
2	0	-4.21472	0	-15.6505	0	-66.4865
3	3	11.6565	3	-19.5592	3	-11.0769
4	6	6.76363	6	11.1931	6	-36.742
5	9	7.8826	9	-27.9512	9	-10.0039
6	12	1.86425	12	-6.21509	12	1.05244
7	15	43.8963	15	22.799	15	-13.4244
8	18	10.5833	18	-6.03462	18	-14.3287
9	21	35.0902	21	28.7479	21	-8.0146
10	24	21.8292	24	25.6313	24	7.66288
11	27	33.4828	27	26.3002	27	35.3557
12	30	37.624	30	5.68069	30	-12.9918
13	33	33.136	33	50.0981	33	17.8106
14	36	44.9601	36	18.4825	36	0.601393
15	39	12.8719	39	-15.4399	39	1.04972
16	42	39.3288	42	-13.2681	42	12.4306
17	45	17.5908	45	-9.96454	45	-29.7722
18	48	-23.0909	48	-6.65032	48	-25.8398
19	51	32.9103	51	-6.39445	51	-31.5156
20	54	46.6553	54	-24.6177	54	3.51229
21	57	22.745	57	-8.67679	57	-27.8752
22	60	26.5053	60	-6.47142	60	-2.64222
23	63	-34.7074	63	-16.5595	63	-26.6214
24	66	7.45495	66	-27.5063	66	-45.1951
25	69	20.2435	69	-23.4959	69	-49.9032
26	72	2.29595	72	-37.73	72	-13.0803
27	75	14.5992	75	-18.334	75	-52.1242
28	78	27.0958	78	-15.8665	78	-23.9455

Figure G-3. Typical suspended solids concentration data displayed from image analysis.

If the concentration readings drop below -100 mg/L for preliminary concentration measurements, it is likely that either: (1) light background light intensity between the sample and blank has changed significantly or (2) the blanket had suspended solids present that were not present when the test began. The easiest remedy is to take another set of blank images after cleaning the reactor, and then running the post analysis process again with these new blanks.

User Instructions for "Save ROI" Program

This program saves information to load a ROI in an excel file for later use in future analyses. A typical program screenshot with all pertinent information entered is given in Figure G-3. The sequential steps to run the program are detailed as follows:

1. Open program : C:\Documents and Settings\mwh65\Desktop\Post-Analyze Programs\Save ROI
2. Select the path to which you wish to save the ROI
3. Set the number of pixels/cm.

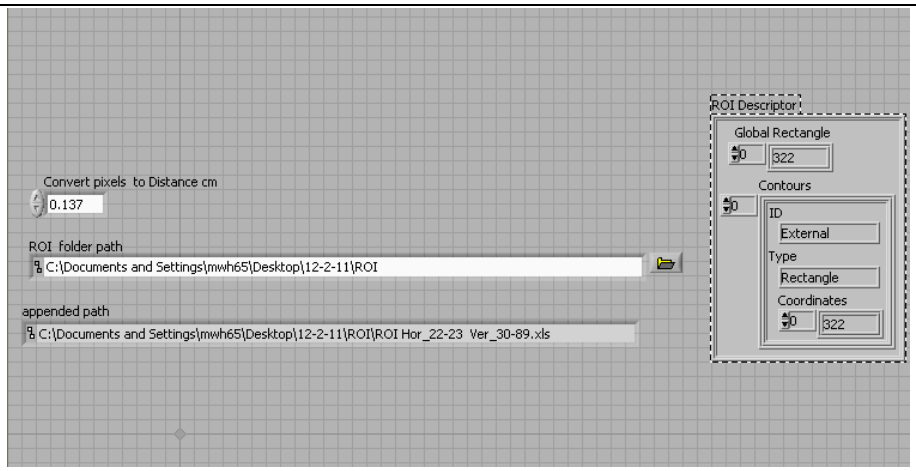

Figure G-3. Screenshot of what the initial program screen should look like with all the information filled out.

4. Hit the run button, and a dialogue box should prompt you asking you for the image in question.

5. Using the tool bar on the left (Figure G-4), select a drawing tool, then click and drag to form the appropriate ROI to be later used in image analysis

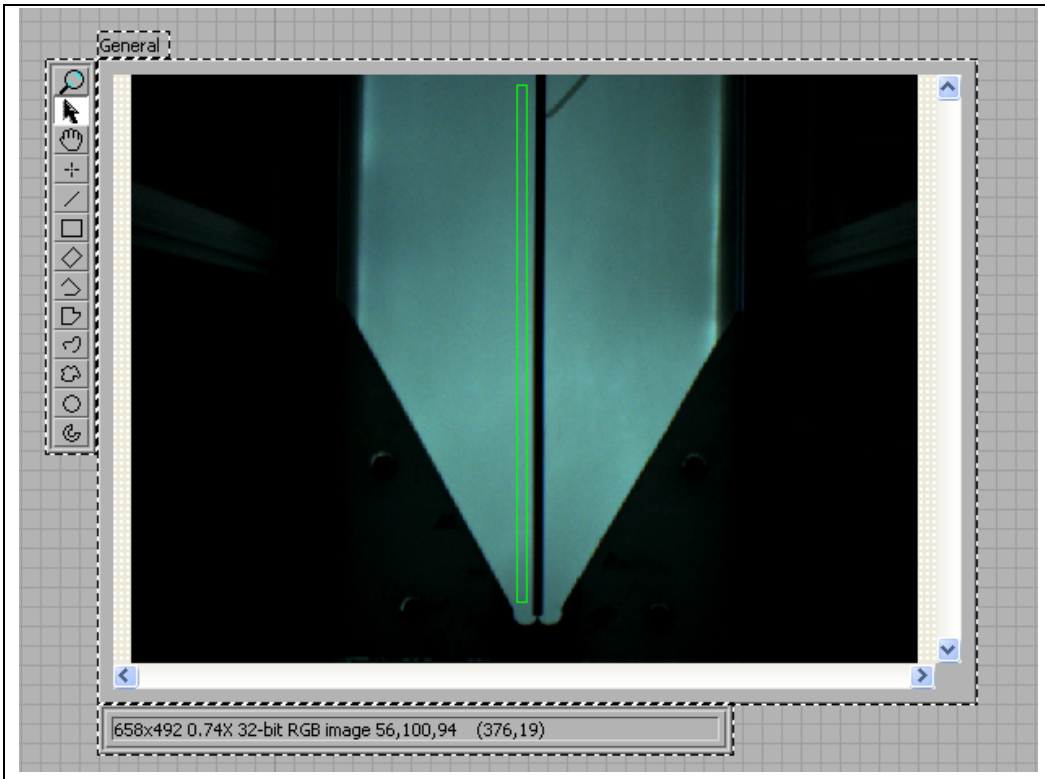

Figure G-4. Screenshot of the resulting data ROI.

APPENDIX H: MEASUREMENT OF FLOC-WATER INTERFACE POSITION BY IMAGE ANALYSIS

The zero point between the greatest difference in positive and negative values of the second derivative of light attenuation with respect to height was used to determine the position of the floc-water interface. Below describes the methodology utilized to locate the floc-water interface and user instructions for the floc-water interface program.

Method for Measuring Floc-Water Interface Utilizing Intensity Values

A sub VI was created to conduct floc-water interface analysis. In the subVI, a series of images were loaded from a called file path, and each image was individually analyzed for the floc-water interface in the area from a pre-loaded ROI (Figure H-1Figure).

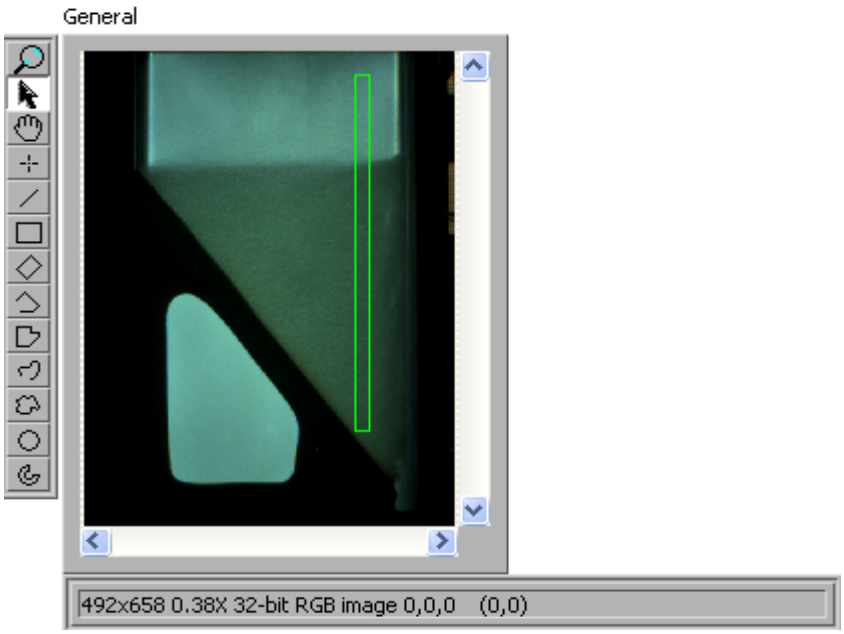

Figure H-1. Analyzed image with pre-loaded ROI (shown in neon green).

Next, linear row averaging is conducted for the image for red, blue, and green wavelength attenuation values that are obtained. At this point, it is even apparent from the linear average

of intensity that an interface exists (Figure H-2).

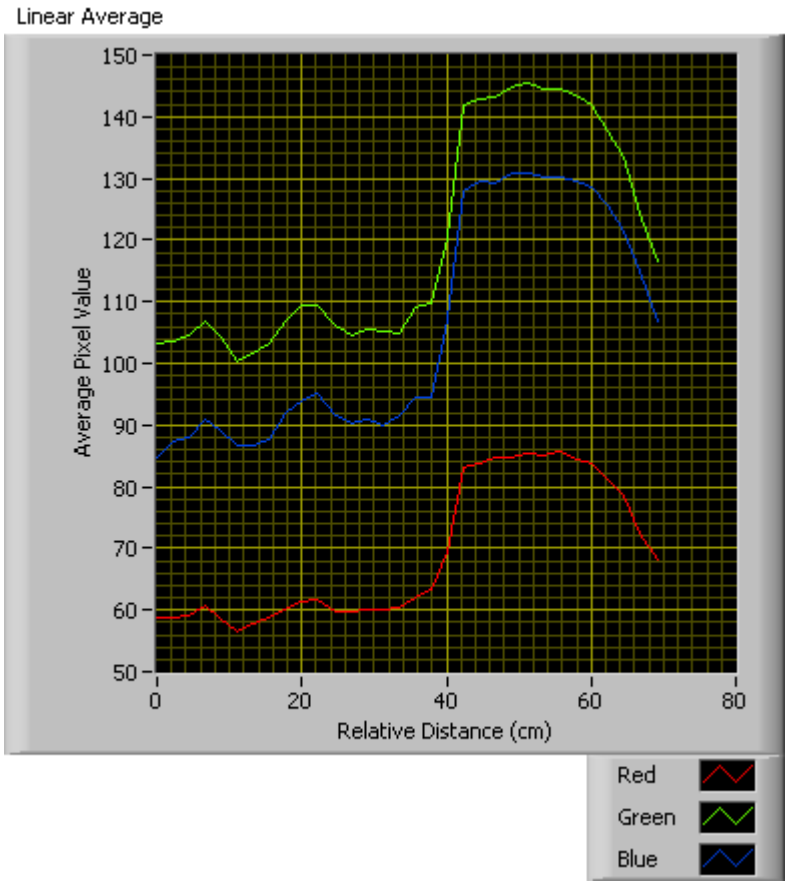

Figure H-2. The response of the image in the selected ROI with respect to the linear average of intensity.

The first and second derivatives of the intensity data with respect to distance are obtained and smoothed over a 15 point interval. The first derivative graph reveals a sharp negative change in slope occurring ~40 cm (Figure H-3A) while the second derivative reveals a zero intercept which is an inflection point around ~40 cm (Figure H-3B). While there are many zero intercepts, there is only one with such a large magnitude of change in slopes which also corresponds with the position of the interface. This zero point corresponds with the position of the floc-water interface.

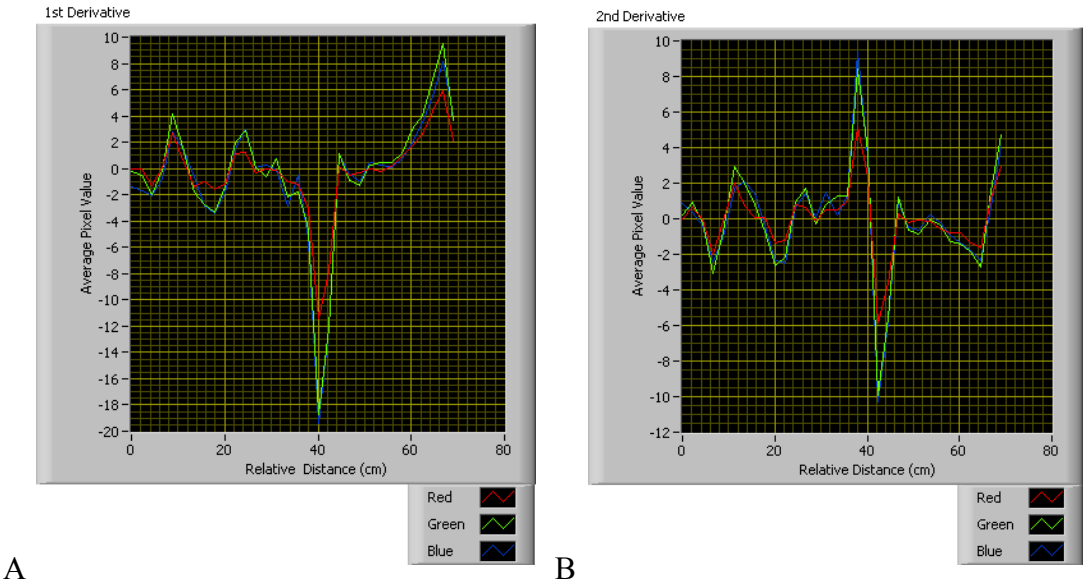

A B

Figure H-3. A. The first derivative response of the image in the selected ROI with respect to the linear average of intensity. B. The second derivative response of the image in the selected ROI with respect to the linear average of intensity.

User Instructions for "Standalone program for Floc-Water Interface"

This program takes a series of images for a floc blanket and computes the resulting floc-water interface for the series of images. An exemplary screenshot before computation of floc-water interface height values is given in Figure H-4. The relevant steps to run the program are:

1. Open the program located at: C:\Documents and Settings\mwh65\Desktop\Post-Analyze Programs\Final Code for Floc-Water Interface (constant calibration values).

2. Select the raw water turbidity and alum dosing conditions for the experimental run.

3. Select the appropriate smoothing value. Based upon experience, a value of 10 is appropriate for analysis of a floc-water interface. First, a linear average of all pixel values across a row is taken. This value is then "smoothed" to reveal an average of the linear

average values previously obtained. For example, a smoothing of 10 corresponds to the corresponding average pixel value representing the average of 10 linear averages.

4. Select the ROI that you wish to use. If you have not already created a ROI for this analysis, you can do so in the **"Save ROI"** program and then load the ROI here.

5. Select the series of blank images that you wish to have included. Note that these blank images should have been taken before this experiment and after the reactor was thoroughly cleaned so that very little residual suspended solids remained in the reactor upon running the experiment.

6. Select the series of images which you wish to analyze.

7. Select the pixels/cm. This value can be calculated knowing the distance between the camera and the reactor wall, and given this information, calculating the number of pixels per that image in the image. One available method is to measure the number of pixels for a 10 cm height of the black PVC "jet reverser" insert.

8. The parameter bounds will set the minimum value required by the program to accept the floc-water interface value, otherwise a zero value will be returned. It is highly recommended going through a run first with no values selected. If there is noisy data, then you can look at the graph of the second derivative and choose the minimum and maximum values necessary to distinguish the location of the floc-water interface from the background "noise."

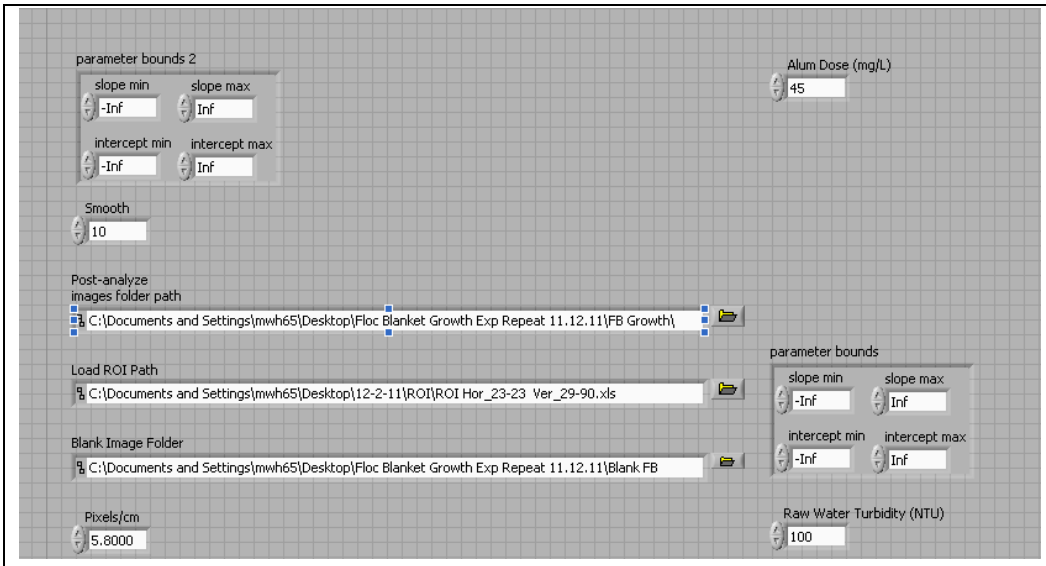

Figure H-4. Screenshot of what the initial program screen should look like with all the information filled out.

The relevant steps for data-analysis are:

1. Scroll to the right and one should see several different possible plots. The time it takes to provide the floc-water interface data will depend on the number of images you wish to analyze. As a general rule of thumb, 1000 images should take between 2-3 minutes to analyze.

2. When the computer is analyzing images, one should see all but the floc-water interface graphs changing with each passing image. The floc-water interface graph will remain blank until all images have been processed (Figure H-5). Do not panic until the end if you see no data on the floc water interface graph.

3. Right click on any graph and then export the data to excel for further analysis.

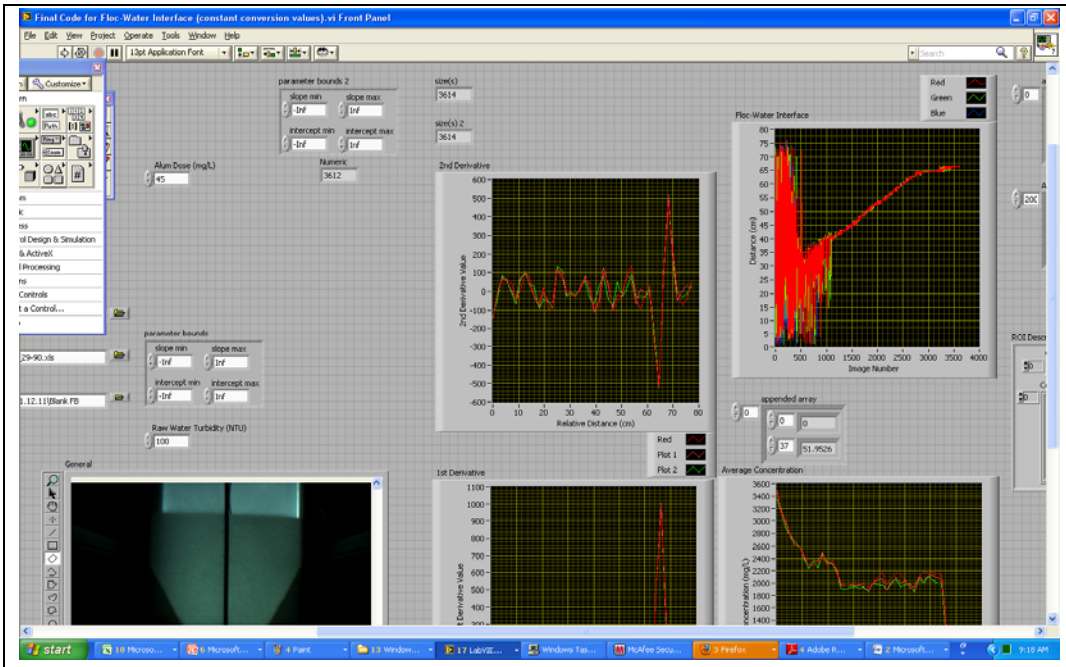

Figure H-5. Screenshot of the resulting floc-water interface analysis.

The excel file should appear like the screenshot of data shown in Figure H-6. The first part of the data may be usable even if a strenuous data filter is applied. This is because the floc-water interface is calculated based upon the location of the zero value for the greatest difference of the second derivative values. At the beginning of floc blanket formation, the difference in concentration between the background and floc blanket is less, so it is more difficult to distinguish the floc-water interface from background noise using this method (and even visually for that matter). Once there is a distinct floc-water interface, the values should remain relatively consistent and somewhat increasing over time until the blanket has reached the level of the floc wasting tube.

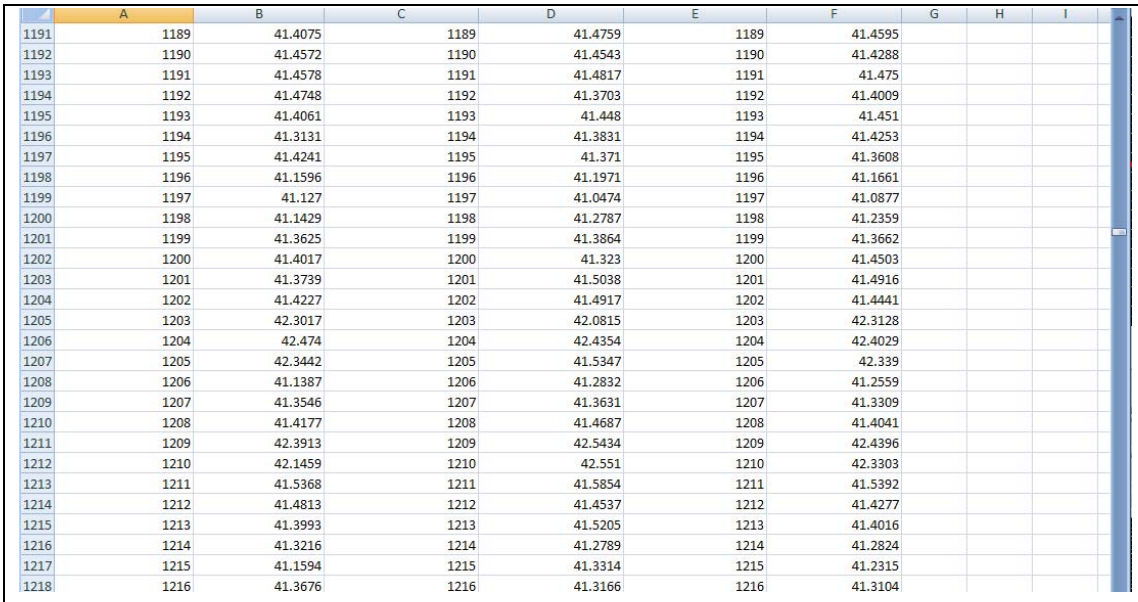

	A	B	C	D	E	F	G	H	I
1191	1189	41.4075	1189	41.4759	1189	41.4595			
1192	1190	41.4572	1190	41.4543	1190	41.4288			
1193	1191	41.4578	1191	41.4817	1191	41.475			
1194	1192	41.4748	1192	41.3703	1192	41.4009			
1195	1193	41.4061	1193	41.448	1193	41.451			
1196	1194	41.3131	1194	41.3831	1194	41.4253			
1197	1195	41.4241	1195	41.371	1195	41.3608			
1198	1196	41.1596	1196	41.1971	1196	41.1661			
1199	1197	41.127	1197	41.0474	1197	41.0877			
1200	1198	41.1429	1198	41.2787	1198	41.2359			
1201	1199	41.3625	1199	41.3864	1199	41.3662			
1202	1200	41.4017	1200	41.323	1200	41.4503			
1203	1201	41.3739	1201	41.5038	1201	41.4916			
1204	1202	41.4227	1202	41.4917	1202	41.4441			
1205	1203	42.3017	1203	42.0815	1203	42.3128			
1206	1204	42.474	1204	42.4354	1204	42.4029			
1207	1205	42.3442	1205	41.5347	1205	42.339			
1208	1206	41.1387	1206	41.2832	1206	41.2559			
1209	1207	41.3546	1207	41.3631	1207	41.3309			
1210	1208	41.4177	1208	41.4687	1208	41.4041			
1211	1209	42.3913	1209	42.5434	1209	42.4396			
1212	1210	42.1459	1210	42.551	1210	42.3303			
1213	1211	41.5368	1211	41.5854	1211	41.5392			
1214	1212	41.4813	1212	41.4537	1212	41.4277			
1215	1213	41.3993	1213	41.5205	1213	41.4016			
1216	1214	41.3216	1214	41.2789	1214	41.2824			
1217	1215	41.1594	1215	41.3314	1215	41.2315			
1218	1216	41.3676	1216	41.3166	1216	41.3104			

Figure H-6. Typical floc-water interface data displayed in excel.

APPENDIX I: CONCENTRATION PLOTTING WITH IMAGE ANALYSIS

User Instructions for "Standalone program for Concentration Plot Program for Single Image"

Concentration plotting provides high spatial resolution of suspended solids concentrations in the floc blanket. This program requires two images: a blank image and an experimental image. The average attenuation readings at each pixel are converted to suspended solids concentration readings and then a resulting concentration plot for each pixel value is plotted. The user steps to run the program are as follows:

1. Open program the program located at: C:\Documents and Settings\mwh65\Desktop\Post-Analyze Programs\Concentration Plot Program
2. Select the raw water turbidity and alum coagulant dosing that were run during the experiment.
3. Select the "concentration-pixel conversion value." This value is a conversion of light attenuation values to suspended solids concentration, and then re-plotted back into an image as pixels. For example, a value of 50 indicates that 1 pixel intensity corresponds to 50 mg/L, thus, a reading of 150 intensity in a given pixel would correspond to a concentration of 7500 mg/L. The concentration-pixel conversion value may have to be adjusted depending on the concentration resolution that you want to be displayed.
4. Select a path to save the image. This will create a new image plot of concentration that you can later access if needed.
5. When you run the program, you will be prompted to select a blank image and the experimental image.

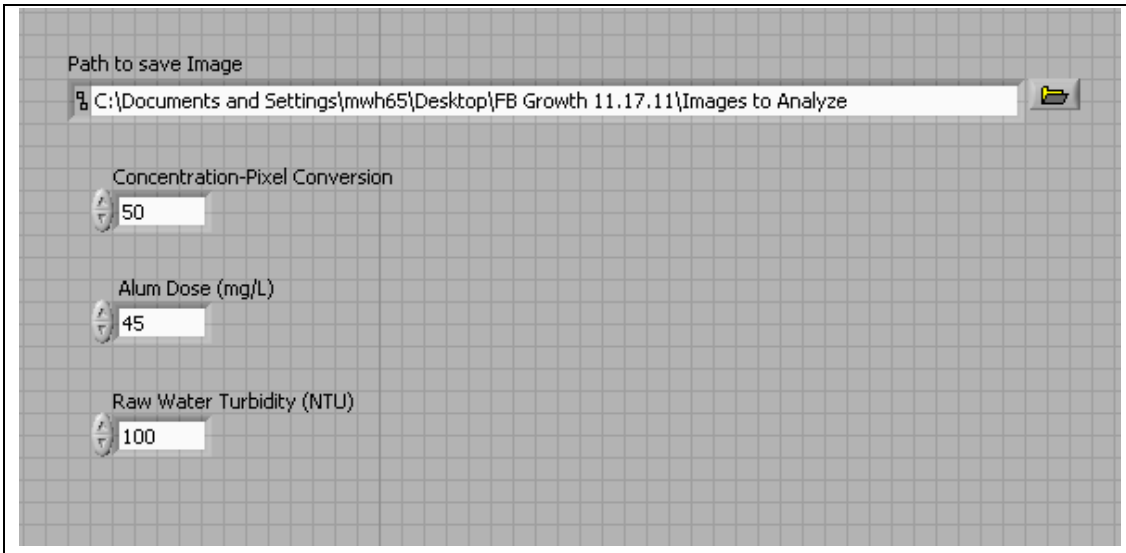

Figure I-1. Exemplary screenshot before concentration plotting commences.

When the program completes the concentration plot, the user may scroll to the right. There will be a concentration plot against distance for the ROI of interest. The user can right clicking on the concentration plot and selecting export>export to excel to open the data in an excel workbook.

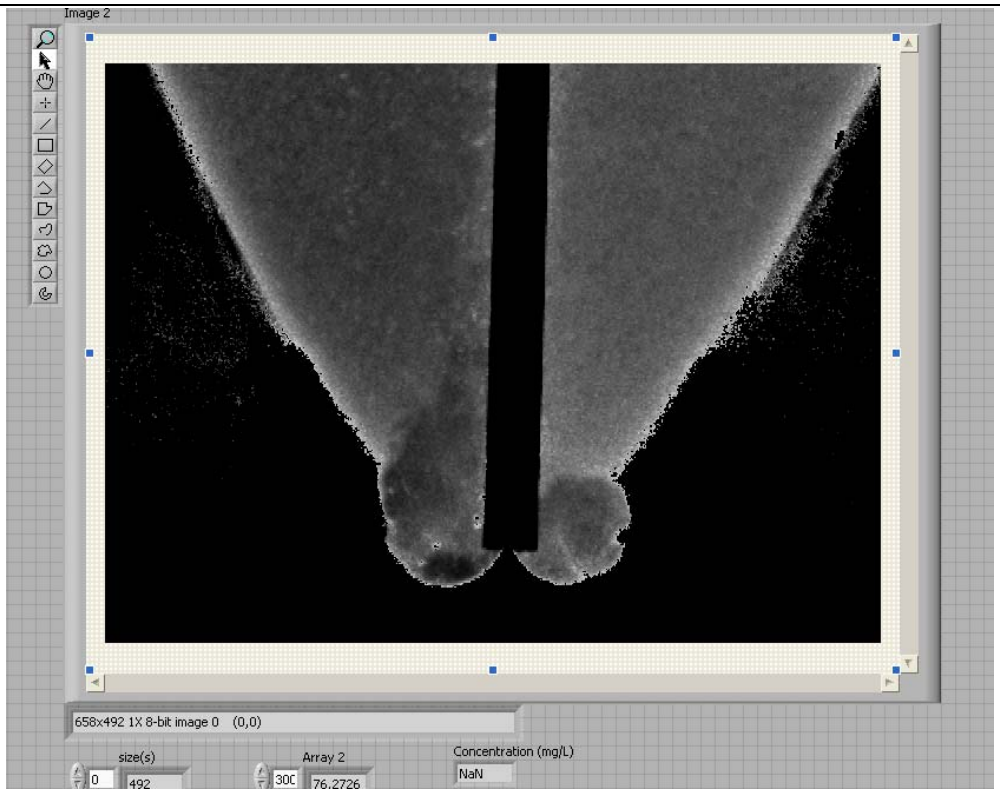

Figure I-2. Screenshot of the resulting data of average concentration over distance in the ROI.

An exemplary excel file is displayed in Figure I-3.

	A	B	C	D	E	F
1	Distance (cm) - Red	Concnentration (mg/L) - Red	Distance (cm) - Green	Concnentration (mg/L) - Green	Distance (cm) - Blue	Concnentration (mg/L) - Blue
2	2.98507	300.076	2.98507	284.976	2.98507	269.525
3	2.81924	331.302	2.81924	297.662	2.81924	272.429
4	2.6534	308.258	2.6534	290.51	2.6534	283.583
5	2.48756	302.091	2.48756	277.266	2.48756	299.101
6	2.32172	282.431	2.32172	303.87	2.32172	256.401
7	2.15589	405.794	2.15589	292.862	2.15589	260.77
8	1.99005	390.772	1.99005	310.788	1.99005	262.453
9	1.82421	297.7	1.82421	331.399	1.82421	279.903
10	1.65837	290.361	1.65837	324.763	1.65837	298.612
11	1.49254	414.905	1.49254	370.877	1.49254	296.648
12	1.3267	440.838	1.3267	469.453	1.3267	486.51
13	1.16086	697.117	1.16086	662.675	1.16086	486.016
14	0.995025	687.22	0.995025	963.829	0.995025	1077.31
15	0.829187	1452.94	0.829187	1311.87	0.829187	1082.2
16	0.66335	1462.37	0.66335	1864.15	0.66335	2058.5
17	0.497512	2819.85	0.497512	2533.22	0.497512	2105.78
18	0.331675	2811.95	0.331675	3140.03	0.331675	3109.57
19	0.165837	3338.19	0.165837	3505.07	0.165837	3107.38
20	0	3323.54	0	3607.32	0	3416.93

Figure I-3. Typical concentration plot data displayed in excel.

REFERENCES

Alem, G. 2012. World Vision Ethiopia WASH Program Division. *WASH Baseline Survey Report on Banja Woreda World Vision ADP*.

AWWA/ASCE. (1990). *Water Treatment Plant Design*. McGraw-Hill, New York.

Baldyga, J., Bourne, J.R., and Gholap, R.V. (1995). The Influence of Viscosity on Mixing in Jet Reactors. *Chemical Engineering Science.* **50**(12), 1877-1880.

Black, R.E., Merson, M.H., Rahman, M.M., Yunus, M., Alim, M.A., Huq, L., Yolken, R.H., and Curlin, G.T. (1980). A Two Year Study of Bacterial, Viral, and Parasitic Agents Associated with Diarrhea in Bangladesh. *J. Infect. Dis.* **142**(5), 660-664.

Booysen, F., Servaas van der Berg, R. B., and Von Maltitiz, M. (2008). Using an Asset Index to Assess Trends in Poverty in Seven Sub-Saharan African Countries. *World Dev.* **36**(6), 1113-1130.

British Environmental Agency (BEA). (2009). *The Microbiology of Drinking Water. Part 4 – Methods for isolation and enumeration of coliform bacteria and Escherichia coli (O157:H7)*.

Cairncross, S., Hunt, C., Boisson, S., Bostoen, K., Curtis, V., Fung, I. C.-H., and Schmidt, W.-P. (2010). Water, sanitation and hygiene for the prevention of diarrhea. *Int. J. Epidemiol.* **39**(1), i193-205.

Chase, C. and Do, Q. T. (2012). Handwashing behavior change at scale: Evidence from a Randomized Evalation in Vietnam. *ERN World Bank Policy*. **8**(58), Paper 6207.

City of Ithaca. (2011). *Drinking Water Quality Report.* City of Ithaca: Ithaca, NY.

Chen, L., Lee, D.-J., and Chou, S.-S. (2006). Charge reversal effect on blanket in full-scale floc blanket clarifier. *J. Env. Eng. ASCE.* **132**(11), 1523-1526.

Chen, L., Sung, S., Lin, W., Lee, D.-J., Huang, C., Juang, R., et al. (2002). Observations of blanket characteristics in full-scale floc blanket clarifiers. *Water Sci. and Tech.* **47**(1), 197-204.

Clesceri, L, Greenberg, A.E., & Eaton, A.D. (1998). *Standard Methods for the Examination of Water and Wastewater.* American Public Health Association, Baltimore.

Curtis, S.B., Rabie, T., and Garbrah-Aidoo, N. (2007). Health in our hands, but not in our heads: understanding hygiene motivation in Ghana. *Health Policy Plan.* **22**, 225-233.

Devi, A. and Bostoen, K. (2009). Extending the critical aspects of water access indicator using East Africa as an example. *Int. Jnl. Env. Health Res.* **19**(5), 329-341.

Dungumaro, E.W. Economic differentials and availability of domestic water in South Africa. (2007). *Phys Chem of the Earth*. **32**, 1141-1147.

Edzwald, J.K., Ives, K.J., Janssens, J. G., McEwen, J.B., and Wiesner, M. R. (1999). *Treatment process selection for particle removal,* Chapter 5, AWWRF/IWSA, New York.

Eisenberg, J., Scott, J. C., Porco, T. (2007). Integrating Disease Control Strategies: Balancing Water Sanitation and Hygiene Interventions to Reduce Diarrheal Disease Burden. *Am. J. Pub. Health*. **97**(5), 846-852.

Environmental Health Programme (EHP). (2003). *Guidelines for Assessing Hygiene Improvement.*

Filmer, D. and Pritchett, L.H. (2001). Estimating Wealth Effects without Expenditure Data-or Tears: An Application to Educational Enrollments in States of India. *Demography*. **38**(1), 115-132.

Gould, B. (1969). Sediment Distribution in Upflow. *Australian Civ. Eng.* **10**(9), 27-29.

Gregory, R. (1979). *Floc Blanket Clarification*. Water Research Centre TR 111, Swindon, U.K.

Gregory, J. (1985). Turbidity Fluctuations in Flowing Suspensions. *J. Col. Inter. Sci.* **105**, 676-684.

Head, R., Hart, J., and Graham, N. (1997). Simulating the effect of blanket characteristics on the floc blanket clarification process. *Water Sci. and Tech.* **36**(4), 77-82.

Hurst, M., Weber-Shirk, M.L., Lion, LW. (2010). Parameters affecting steady-state floc blanket performance. *J. of Water Supply Res. Technol. Aqua.* **59**(5), 312-323.

Hurst, M.W., Weber-Shirk, M.L., Charles, P., and Lion, L.W. (2013). An Apparatus for Observation and Analysis of Floc Blanket Formation and Performance. Submitted: *J. Env. Eng. ASCE.*

Jarvis, P., Jefferson, B. and Parsons, S.A. (2005). Measuring floc structural characteristics. *Rev in Env. Sci. & Bio. Tech.* **4**, 1-18.

Jensen, P.K., Ensink, J.H., Jayasinghe, G., van der, H.W., Cairncross, S., Dalsgaard, A. (2002). Domestic transmission routes of pathogens: the problem of in-house contamination of drinking water during storage in developing countries. *Trop Med Intl Health*. **7**, 604-609.

Kawamura, S. (2000). *Integrated design and operation of water treatment facilities,* Chapter 3, John Wiley and Sons, New York.

Kelly, M. L (ed). (1998). *Optimizing Water Treatment Plant Performance Using the Composite Correction Program Handbook*. USEPA, Cincinnati, Ohio.

Kremer, M., Ahuja, A., and Peterson-Zwane, A. (2010). Providing Safe Water: Effort from Randomized Trials. Discussion Paper—23, Cambridge, Mass.: Harvard Environmental Economics Program. Accessed Online: http://www.hks.harvard.edu/m-rcbg/heep/papers/KremerHEEPDP23.pdf

Letterman, R. (1999). *Water Quality and Treatment: A Handbook of Community Water Supplies.* McGraw-Hill, New York.

Lin, W., Sung, S., Chen, L., Chung, H., Wang, C., Wu, R., et al. (2004). Treating high-turbidity water using full-scale floc blanket clarifiers. *J. Env. Eng. ASCE.* **130**(12), 1481-1487.

Lindskog, R.U. and Lindskog, P.A. (1988). Bacteriological contamination of water in rural areas: an intervention study from Malawi. *Journal of Tropical Medicine and Hygiene*. **91**(1), 1–7.

Lopez, A.D. (2006). Global Burden of Disease and Risk Factors. Oxford University Press: World Bacnk, Washington DC.

Luby, S.P., Halder, A.K., Tronchet, C., Akhter, S, Bhuiya, A., and Johnston, R.B. (2009). Household Characteristics Associated with Handwashing with Soap in Rural Bangladesh. *Am. J. Trop. Med. Hyg.* **81**(5), 882-887.

Luby, S.P., Halder, A.K. Huda, T., Unicomb, L., Johnston, R.B. (2011). The Effect of Handwashing at Recommended Times with Water Alone and With Soap on Child Diarrhea in Rural Bangladesh: An Observational Study. *PloS Med.* **8**(6), e1001052.

McGuigan, J. T., Elmore-Meegan, M., and Conroy, R. M. (1996). Incidence of enteropathogens in stools of rural Maasai children under five years of age in the Maasailand region of the Kenyan Rift Valley. *East African Medical J.* **73**(1), 59-62.

Miller, D.G., and West, J.T. Pilot Plant Studies of Floc Blanket Clarification. (1968). *AWWA Journ.* **60**(2), 154-164.

Mohammadi, M.S. (2002). A Generalized Refractive Index Equation for Estimating the Average Particle Size in Colloidal Suspensions. *J. Dispersion Sci. and Tech.* **23**(5), 689-697.

Montgomery, M.A. and Elimelech, M. (2007). Water and Sanitation in Developing Countries: Including Health in the Equation. *Environ. Sci. Tech.* **41**(1), 17-24.

Oswald, W.E., Lescano, A.G., Bern, C., Calderon, M.M., Cabreara, L., and Gilman, R.H. 2007. Fecal contamination of drinking water within peri-urban households, Lima, Peru. *Am. J. Trop Med Hyg.***77**, 699-704.

Purushothaman, M. and Damodara, T. (1986). Defluoridation for rural areas-alum floc sludge blanket technique. *J. of Indian Water Works Assoc.* **18**(1), 91-97.

Rufener, S., Mausezahl, D., Mosler, H-J., Weingartner, R. (2010). Quality of Drinking Water at Source and Point of Consumption – Drinking Cup as a high potential Recontaminatoin Risk: A Field Study in Bolivia. *J Health Popul Nutr.* **28**(1), 34-41.

Sahn, D. E., and Stifel, D. (2003). Exploring alternative measures of welfare in the absence of expenditure data. *Review of Income and Wealth.* **49**(4), 463-489.

Schulz, C.R., and Okun, D.A. (1984). *Surface Water Treatment for Communities in Developing Countries.* John Wiley and Sons, New York.

Su, S., Wu, R., and Lee, D. (2004). Blanket dynamics in upflow suspended bed. *Water Res.* **38**(1), 89-96.

Sung, S., Lee, J., and Wu, R. (2005). Steady-state Solid Flux Plot of Blanket in Upflow Suspended Bed. *J Chinese Inst. Chem. Eng.* **36**(4), 385-391.

Tchobanoglous, G., Burton, F. L., and Stensel, D. H. (2003). *Wastewater Engineering Treatment and Reuse.* McGraw-Hill, New York.

Tse, I.C., Swetland, K., Weber-Shirk, M.L., and Lion, L.W. (2011) Fluid shear influences on the performance of hydraulic flocculation systems. *Water Res.* **45**(17), 5412-5418.

Tumwine, J.K., Thompson, J., Katua-Katua, M., Mujwajuzi, M., Johnstone, N., Wood, E., and Porra, I. (2002). Diarrhoea and effects of different water sources in sanitation and hygiene behaviour in East Africa. *Trop. Med Intl. Health* **7**(9), 750-756.

USAID. 2011. Demographic and Health Surveys Methodology. DHS *Questionaires*: Household, Woman's, and Man's.

Weber-Shirk, M. L. (2008). *An Automated Method for Testing Process Parameters.* Retrieved April 5, 2009, from AguaClara Wiki: http://confluence.cornell.edu/display/AGUACLARA/Process+Controller+Background

Weber-Shirk, M. L., Lion, L. W. (2010). Flocculation model and collision potential for reactors with flows characterized by high Peclet numbers. *Water Res.* **44**(18), 5180-5187.

Waddington, H. and Snilstevit, B. (2009). Effectiveness and sustainability of water, sanitation, and hygiene interventions in combating diarrhea. *Journal of Development Effectiveness* **1**(3), 295-335.

Wallner, W.E. (1987). Factors Affecting Insect Population Dynamics: Differences between outbreak and non-outbreak species. *Ann. Rev. Entom.* **32**, 317-340.

WHO/CEHA. (2008). *Health Environment for Children Survey Instrument. Module III: Water, Hygiene, and Sanitation*.

WHO/UNICEF. (2004). *Harmonization of Major Survey Instruments WHO/UNICEF Joint Monitoring Program of Water Supply and Sanitation*.

WHO. (2004). *Fact Sheet 3.6 Pour Flush Latrines*. Obtained: October 11, 2012: http://www.who.int/water_sanitation_health/hygiene/emergencies/fs3_6.pdf

The World Bank. (2005). *The Handwashing handbook: A guide for developing hygiene promotion to increase handwashing with soap.* Washington, D.C.: The World Bank.

Wright, J., Gundry, St., and Conroy, R. (2004). Household drinking water in developing countries: a systematic review of microbiological contamination between source and point-of-use. *Trop. Med. and Int. Health.* **9**(1), 106-117.

Zhang, Z., Chen, Z., Li, Y., Fan, J., Fan, B., Luan, Z., and Lu, D. (2006). Performance of a novel vertical-flow settler: a comparative study. *J. Enviro. Sci*. **18**(5), 858-863.